Design of an Implantable Ulnar Collateral Ligament Repair System

GXP-2021

A Major Qualifying Project Report Submitted to the Faculty
of Worcester Polytechnic Institute

In partial fulfillment of the requirements for the Degree of Bachelor of Science by

Paul Bonarrigo

_____

Logan Gaudette

_____

Carolyn Heighton

_____

Camden Holm

_____

Gregory Kaleshian

_____

Approved by:

Professor George Pins, Advisor

_____

Dr. David Magit, Advisor

_____

Table of Contents

Abstract

UCL tears are a serious injury in throwing sports that can hinder athletes from maximizing their potential due to lengthy and invasive rehabilitation procedures. Current standard treatment methods are invasive and have a long recovery time. Our goal was to create a minimally invasive alternative to the current treatment method. In collaboration with Dr. David Magit and BioSurfaces, Inc., we developed a novel biodegradable electrospun scaffold into which we can inject PRP. The scaffold would then be placed on the UCL in a minimally invasive insertion procedure. We hypothesized this device would sustain local delivery or PRP at the injury site, decreasing UCL repair time. We evaluated the physical and cytotoxic properties of the pouch and its ability to release an orthobiologic over time.

Authorship

Section	Primary Writer	Final Editor
Acknowledgements	Paul	ALL
Introduction	Camden	ALL
Literature Review	Logan	ALL
Anatomy of the UCL	Greg	ALL
Biomechanical Properties of the UCL	Paul	ALL
The Baseball Pitch	Paul	ALL
Biomechanical Analysis of the Baseball Pitch	Paul	ALL
Properties of a UCL Scaffold	Paul	ALL
Necessary Biomechanical Properties of a UCL Scaffold	Paul	ALL
Scaffold Anchoring Techniques	Paul	ALL
Hydrogels	Carolyn	ALL
Biocompatible Scaffold Properties	Logan/ Camden	ALL
Scaffold Creation through Electrospinning	Paul	ALL
Biological Additives	Logan	ALL
Comparison of Current Treatments	Paul	ALL
Prior Art	Carolyn	ALL
Design	Logan	ALL
Initial Client Statement	Greg	ALL
Stakeholders	Paul	ALL
Specifications	Logan	ALL
Objectives	Carolyn/Camden	ALL
Objectives Analysis	Camden	ALL
Constraints	Paul	ALL
Design Alternatives	ALL	ALL
Revised Client Statement	Greg	ALL
Project Approach	Carolyn	ALL
Design Process	Greg	ALL
Needs Analysis	Logan	ALL
Design Needs	Logan	ALL

Design Wants	Logan	ALL
Needs and Wants Design Matrix	Logan	ALL
Functions and Specifications	Camden	ALL
Size	Logan	ALL
Degradation Rate	Logan	ALL
Elution Rate	Logan	ALL
Brainstorming Session	Paul	ALL
Preliminary Designs and Concepts	Paul	ALL
Analysis of Preliminary Designs and Concepts	Paul	ALL
Analysis of Materials	ALL	ALL
Conceptual Designs	Paul	ALL
Ravioli	Paul	ALL
Cleat	Paul	ALL
Ridged Ravioli	Paul	ALL
Growth Factor Insertion Method Concepts	Paul	ALL
Final Design and Verification	Greg	ALL
Final Design	Carolyn	ALL
Implantation Procedure	Camden	ALL
Validation Testing	Paul	ALL
Mechanical Tests	Paul	ALL
Elution Testing	Logan	ALL
Elution Testing Results	Logan	ALL
Cytotoxicity Testing	Carolyn	ALL
Cytotoxicity Testing Results	Carolyn	ALL
PRP Validation Testing	Logan	ALL
PRP Bioactivity Testing	Greg	ALL
PRP Bioactivity Testing Results	Greg	ALL
Mechanical Testing Discussion	Paul	ALL
Drug Elution Testing Discussion	Camden	ALL

Cytotoxicity Testing Discussion	Carolyn	ALL
PRP Bioactivity Testing Discussion	Greg	ALL
Impact Analysis	Camden	ALL
Impact Analysis	Camden	ALL
Economics	Camden	ALL
Environmental Impact	Camden	ALL
Societal Influence	Camden	ALL
Political Ramifications	Camden	ALL
Ethical Concerns	Camden	ALL
Health and Safety Issues	Camden	ALL
Manufacturability	Camden	ALL
Sustainability	Camden	ALL
Conclusions and Recommendations	Paul	ALL
Recommendations	Paul	ALL
Further Mechanical Testing	Paul	ALL
Evaluate PLGA Degradation	Logan	ALL
Further Orthobiological Testing	Greg	ALL
Evaluate Internal Volume of the Scaffold	Paul	ALL
Advance to Animal Testing	Paul	ALL
Expand Applications of the Device	Paul	ALL
Conclusion	ALL	ALL

Acknowledgements

Special thanks to Professor Pins and Doctor Magit for guiding the team throughout the entire design and testing process. We would also like to acknowledge the various WPI faculty members that guided us through the year. Lisa Wall for helping the team with any and all questions they had about WPI facilities. Professor Coburn for helping the team use the spectrometer in Gateway. Professor Ambady for providing the team with cells for their tests that required them and assisting the team with helpful advice. Anthony Heng for training the team on the use of the Instron in Gateway. Finally, our partners at Biosurfaces, Matthew Phaneuf, Nate Long, and Rayan Kassab, for their insight during their design process, and all the scaffold they created for the team's validation testing.

Table of Figures

Table of Tables

1. Introduction

Ulnar collateral ligament (UCL) injuries have been a growing epidemic in the baseball world. A survey performed in 2012-2013 found that nearly 25% of MLB pitchers had undergone Tommy John surgery during their career (Zaremski, et. al., 2017). Outside of the MLB, 31.3% of the top youth pitchers elected to undergo Tommy John surgery in 2010 which is especially interesting since the long return to play time of Tommy John surgery has an even greater impact on their career as it is just starting (Zaremski, et. al., 2017). The UCL runs along the medial side of the elbow and attaches the humerus to the ulna. The ligament is responsible for providing stability in the elbow during overhead throwing motions. During such motions, the UCL undergoes valgus and varus loads which can cause injury to the ligament. These injuries can occur acutely or chronically overtime. It has been shown that over 50% of MLB players experience elbow pain from some form of strain to their UCL (Oyama, 2012). The reason some players experience pain but do not require surgery is because there are three grades of UCL tears. A grade I tear may indicate strain, stretching, and small tears or perforations throughout the UCL. Grade II indicates a larger tear across most of the UCL partially compromising the ligaments structural integrity. Lastly, a grade III tear is a complete rupture of the UCL, which is characterized by a loss of function of the arm (Magit, 2020).

Grade II tears can be difficult to heal because they typically do not require total reconstructive surgery, known as Tommy John surgery. On the other hand, they are extremely difficult to heal utilizing exclusively noninvasive methods such as physical therapy. Currently, few effective products exist that are specifically designed to aid in the repair of grade II UCL tears. Physical therapy can work in some cases, but it cannot heal a large percentage of grade II tears enough to return the patient to at least a pre-injury level of function. UCL reconstruction is extremely invasive and undesirable for those who want to return quickly to their previous level of activity.

This project was specifically aimed to help players who are experiencing grade II tears which can lead to more severe grade III tears. The goal of this project was to create a product that can aid in the healing process of grade II UCL tears and decrease the total recovery time from the injury. The product designed is a supportive scaffold that can be fixed in place on the UCL or

other ligaments using current surgical techniques that will aid in healing by providing a slow and constant release of PRP or other growth factors or biological additives.

We designed and tested a prototype biodegradable scaffold made from PLGA with an internal chamber containing a piece of zein and filled with PRP. The zein serves to regulate the release of PRP and extend the duration of its release. We showed that our design may achieve its intended goal through testing its mechanical properties, drug release properties, and biocompatibility. We showed that the scaffold is biocompatible and can withstand the forces be subjected to and will release PRP into the surrounding tissue, which was shown to have a positive effect on cell growth. Our results and the designed scaffold require further validation to determine actual effectiveness, including confirmation of our results and further testing of the devices mechanical properties. The results obtained show that the design is a viable option for UCL repair in the future.

2. Literature Review

To gain an understanding of UCL injuries and the treatment methods for them, the project team conducted a thorough literature review. The sections below contain the major findings from this research.

2.1 Anatomy of the UCL

The ulnar collateral ligament (UCL), shown in Figure 1, is a ligament located in the elbow that runs from the humerus to the ulna. This ligament complex is comprised of three bundles: the anterior, posterior, and transverse bundle. The anterior bundle of the UCL is the largest ligament and contains an anterior and posterior band. The anterior band is a single-layered ligament that runs organized longitudinal collagen fibers from the medial epicondyle to the sublime tubercle. This ligament activates during extension (30-90 degrees). The posterior band is a thicker ligament comprised of less organized collagen fibers that attaches from the humeral epicondyle to the medial ulna and is activated in flexion (90-120 degrees) of the elbow (Labott, 2018). The ligament complex works to provide stability to the elbow during valgus and varus loading with most of the load being placed on the anterior bundle.

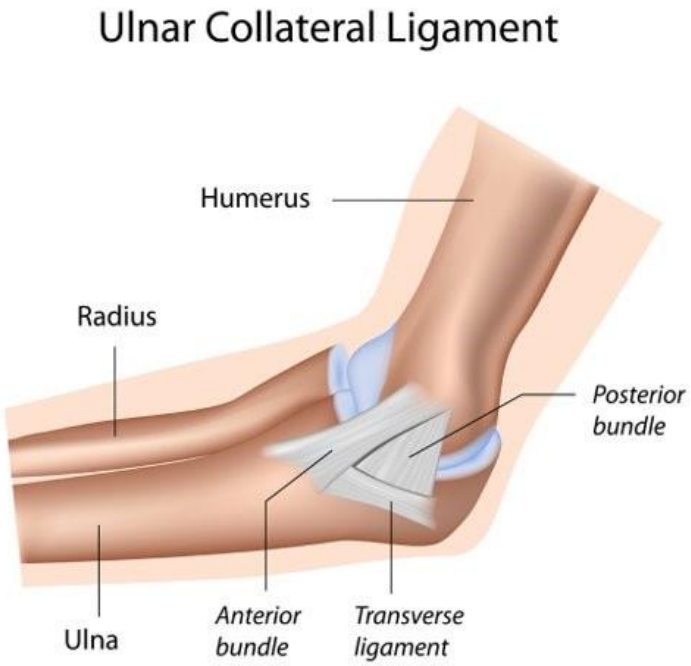

Figure 1: Schematic of Ulnar Collateral Ligament, adapted from Labott, 2018

Blood flows into the UCL from the superior ulnar collateral artery. This artery stems from the brachial artery of the medial upper arm and runs through the elbow joint (Dell, 2019). Smaller arteries such as the superior ulnar collateral artery and the anterior ulnar recurrent run behind the elbow. These arteries provide the ligament with nutrients and growth factors that facilitate the maintenance and regeneration of the UCL. A study that researched the vascularity of the ligament showed that there was a denser blood supply at the proximal end of the ligament compared to the distal end (Buckley, 2019). According to the study, the proximal end of the UCL was shown to have 68% vascular penetration compare to the 39% at the distal end. The difference in blood flow along the UCL directly effects the healing process (Buckley, 2019).

Injuries in this ligament are extremely prevalent in overhead throwing athletes. The valgus and varus loads placed on the ligament cause the UCL to be extremely vulnerable. Valgus and varus loading occur when the midline of a desired body part moves laterally or medially with respect to the midline of the body (Sharma, 2010). In the overhead throwing motion, especially in professional sports, the ligament is exposed to large torsional forces that are generated by the lower body and exerted through the elbow. These injuries can occur acutely or chronically overtime. Acute injuries happen during the throwing motion and are distinguished by a "pop" heard or felt in the elbow. Chronic injury happens over time were stress is constantly applied to the ligament causing microtears that increase the risk of a much more devastating injury.

UCL injuries are classified into three grades. Grade I tears are sprains of the UCL where the ligament is over extended and small microtears propagate. Grade II tears occur when the ligament is partially torn. Grade III is the most devastating injury, a complete tear of the ligament. These tears can occur anywhere on the ligament depending on the angle of the elbow and force applied. Usually acute grade II and grade III injuries are observed in the midsection of the ligament. Chronic injuries are determined by the tear occurring at the proximal or distal end of the ligament. Distal ligament tears are more detrimental considering the lack of blood flow compared to the proximal end (Magit, 2020).

2.2 Biomechanics of the UCL

To create a treatment for damaged UCLs, the biomechanics of the UCL and the forces it experiences during failure must be analyzed. This analysis allows for a greater understanding of the problem and can directly dictate the necessary specifications of final treatment method decided upon.

2.2.1 The Baseball Pitch

Before conducting a biomechanical analysis of the forces, a baseball player's UCL would undergo during a pitch, it is best to review the baseball pitch itself. The purpose of a fastball pitch, the baseball pitch we will be analyzing, is for a pitcher to throw a baseball as fast as possible to impede a batter's ability to react to and hit the oncoming ball. It has become a full body motion that requires years of training and skill to optimize to possibly reach a fast ball speed of up to 100 mph (Statcast, 2019). Every part of the pitch works towards creating the maximum amount of force in the shortest amount of time. This creates a large impulse which applies an extreme amount of stress to the elbow and consequently the UCL as it is the main ligament supporting the elbow throughout the pitch (Bhandari, 2011).

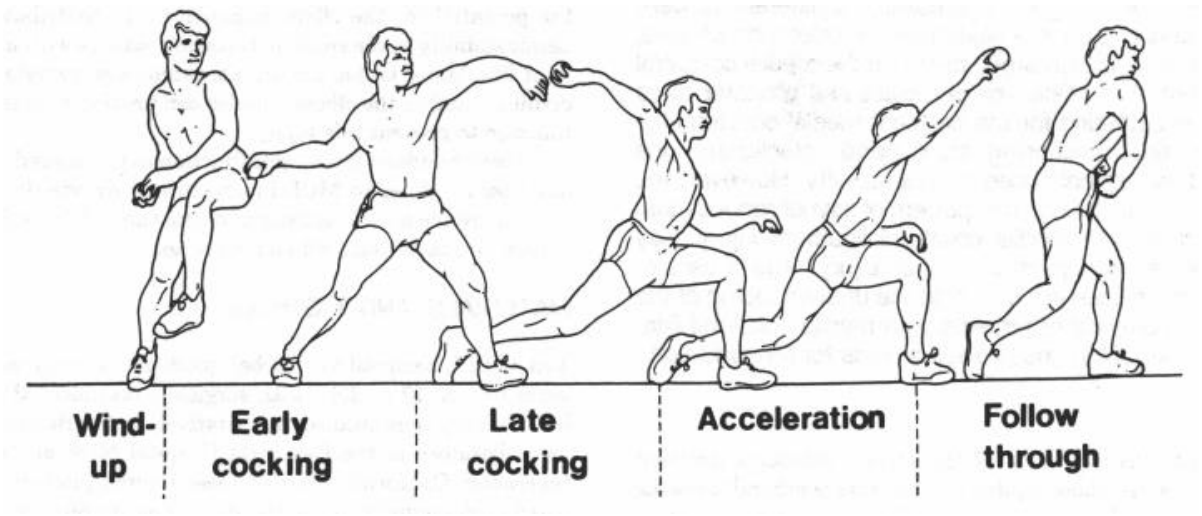

Figure 2: The Baseball Swing, adapted from Magit, 2018

The baseball pitch itself has five main phases as seen in Figure 2 (Magit, 2018). The wind-up phase entails the pitcher preparing for the pitch by cocking their throwing arm back, lifting their stride foot to prepare to step forward, and rotating their upper torso 90 degrees as shown in Figure 2. This is all done to build up potential energy in their body which will later be transferred into the baseball. In the early cocking phase, the player pushes their stride foot forward and throws their shoulder backwards to prepare for the pitch. This phase is once again about building up potential energy, but it is important to note that the stance leg, the one firmly planted behind the player, bends in this phase to give the pitcher a lower center of gravity to stabilize them for the arm swing which will begin in the next phase: late cocking. In this phase, the player rotates their shoulders and torso forward while raising their hand backwards to prepare for the translation of their potential energy to the ball. This is phase is known as the acceleration phase, where the pitcher finally leans forward into the pitch and releases the ball with the force, they have built up throughout the throwing motion. Once the ball is released, the deceleration, or follow through phase, begins. This is where the pitcher continues the swing of their arm until they can bring it to a gradual stop, and they return their shoulders to a horizontal position. This phase is necessary to reduce injury as these two motions together allow the forces generated by the arm to be dissipated over a longer range of motion. The forces applied on the UCL are greatest during the acceleration phase. The elbow undergoes extreme valgus forces during this phase as nearly all the previous forces built up during the swing are transferred to the UCL (Oyama, 2012). As previously stated, the UCL is not designed to handle these levels of forces, making it clear why so many baseball players experience UCL injuries during their career. With this understanding of the pitch, a biomechanical analysis of the pitch can be performed.

2.2.2 Biomechanical Analysis of the Baseball Pitch

Through an analysis of the UCL we will be able to understand the impact the baseball pitch has on the UCL as well as the necessary mechanical properties of a UCL scaffold. Before the analysis can proceed, it should be stated that the UCL has a failure load of 260 N when being pulled in tension (Dustin, 2015). Also, the UCL can withstand torques of 32.1 ± 9.6 Nm before failure (Magit, 2018). The variation of the failure torque is necessary to note but will be explained later. The UCL also has an average elastic modulus of 13.77 MPa in the linear region

(Smith, 2018). This failure load information will be essential in understanding when the average UCL will tear during our analysis of the pitch.

An analysis was performed on the forces applied to the UCL during a baseball throw. This study was conducted by applying external forces to a cadaver elbow and observing the force at which it failed. It was recorded that the UCL was able to receive 54% of torque applied to the system when 64 Nm was applied to the elbow mimicking a baseball pitch. Therefore, the force applied to the UCL during the throw was 34.6 Nm which caused it to fail (Magit, 2018). This means that during the average baseball pitch the UCL experiences near failure forces. This begs the question why the UCL does not break during most every pitch as this force is greater than the average failure torque, and it requires a deeper dive into the factors that are present beneath the surface. This led people to question the recent increase in baseball pitcher's UCL injuries in recent years. It was discovered that the increase in average pitching speed from 90 mph to 92.5 mph, a less than 3% increase, in recent years has influenced the amount of UCL injuries (Doran, 2015). This slight increase in speed requires a far larger amount of force to be delivered to the baseball over a shorter period which puts a larger impulse of the UCL. Since the UCL was already close to breaking during each pitch, this slight increase has been enough to lead to far more UCL tears than before. Additionally, it has been analyzed that imperfections in a pitcher's form, especially the angle of release, can drastically change the distribution of the forces in the elbow. Either a drastic error or the combination of many small errors in one's form can alter the force on the UCL enough to cause it to fail (Oyama, 2012). The combination of this increased impulse and negative impact of incorrect form both breakdown the UCL overtime. It has also been shown that if pitchers play consistently for more than 8 months per year their chance of requiring surgery increases fivefold (Fleisig, 2012).

While the research would suggest that the easiest way to avoid UCL injuries would be to refrain from putting as much force into the baseball, this goes against the fundamental ideas of competition for many athletes and for those in a higher level of play it is not an option. With the high level of competition in baseball it seems likely that the amount of UCL injuries present today are more likely to increase rather than decrease in the coming years. It truly is an epidemic that must be reviewed, and engineering solutions must be created to support these players that simply want to give it their all.

2.3 Properties of a UCL Scaffold

To create an effective UCL graft it is necessary to understand the properties it must have to be effective. In this section, the necessary biomechanical, anchoring method, and biocompatible properties of a UCL scaffold will be examined to better understand which properties make scaffolds functional.

2.3.1 Necessary Biomechanical Properties of a UCL Scaffold

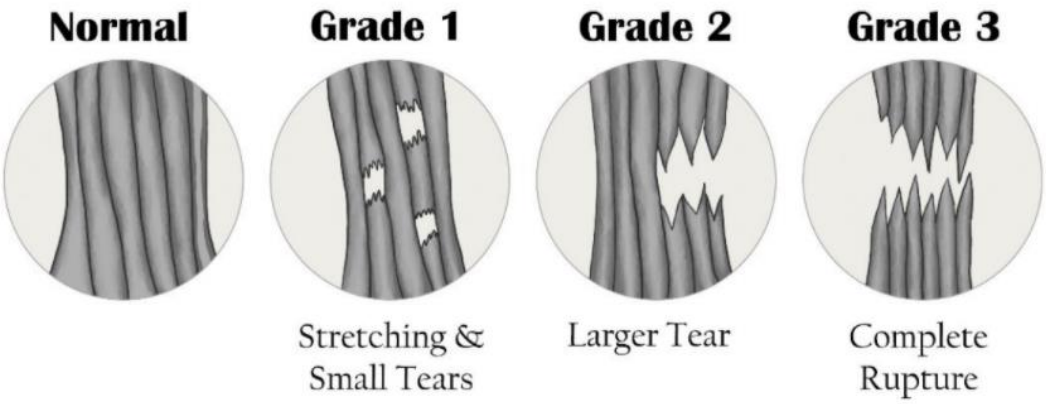

Figure 3: UCL Tear Graduation Illustration, adapted from "Sprained Ankle - Treatment, Rehabilitation & Exercises," 2019

Before this section can begin, it is important to review the concept of ligament injury graduation, see Section 2.1 for more information. Ligament injury graduation is a procedure used to grade the severity of a UCL tear. There are grades ranging from 1 to 3: 1 being minor imperfections in the ligament whereas a grade 3 tear is the complete and debilitating tear of the ligament. The different grades are depicted in **Error! Reference source not found.**. This project i s concerned with assisting in the healing process of Grade 2 tears meaning that any scaffold created should be able to withstand the same forces as the UCL as since it will be covering exposed sections of the UCL and will need to assist in preventing it from tearing more.

Degree of Flexion	Experimental		Theoretical
	Articular Contact Area $(mm)^2$	Overall Force (N)	Overall Force (N)
30°	98.0	79.3	12.9
60°	152.0	137.3	47.1
90°	171.0	160.4	132.5
Average	89.8	125.7	64.2

Table 1: Average UCL Force, adapted from Dustin, Geer, and Hulburt, 2015

To review, the mechanical properties of the UCL are a failure load of 260 N (Magit, 2018), and a failure torque of 32.1 ± 9.6 Nm N (Dustin, 2015). Knowing this information is useful, but it should be noted that the recipients of the scaffold most likely will not be pushing their UCL to its upper limits before the scaffold has completed its mission. Therefore, a more realistic study should be analyzed to understand the forces our patients will be placing on the UCL. A dynamic flexion simulation was conducted on the elbow by using a realistic model with force sensors, and it was found that a simple and slow flexion and extension cycle of the elbow loaded 125.7 N on the UCL as seen in Table 1. It should also be stated that the UCL undergoes approximately 1,400 flexion and extension cycles per day meaning that the scaffold generated will need to keep its structure after it has been loaded thousands of times (Johnson, 2000). We can assume that our patients most likely will not be pushing their UCL to its upper limits before the scaffold has completed its mission, so a failure load of 200 N, giving clearance from the 125.7 N average force, could be sufficient for the scaffold's use cases although the team should work towards creating a scaffold that can withstand the failure load of the UCL.

Figure 4: Tommy John Surgery, adopted from John, 2018

Another important aspect of the scaffold is the strength of its anchoring joints. The device most similar to the device the team is setting out to make is the UCL Internal Brace by Arthrex, See Section 2.3.2 for more information, so its anchoring methods will be used as a gold standard. This device uses two patented Swivel Lock

anchoring device which have been shown to withstand 50,000 flexure cycles cycling from 15 N to 150N, and each one has a maximum pull out force of 300N (Arthrex, 2018). Also, the actual size of the scaffold will be dependent on the anchoring method, but it must be implantable in a 4 to 6 cm incision window and be no thicker than 2mm to meet our client's specifications (Magit, 2020). Therefore, the minimum specifications for a scaffold should be that it can withstand a pulling force of 200 N over thousands of cycles and be implantable in 4 to 6 cm incision window.

2.3.2 Scaffold Anchoring Techniques

UCL tears are complicated injuries leading there to many different methods to heal them. The most common is adding some form of graft to the elbow joint to reinforce it, but even with this being the most common solution, there are many ways accomplish it. Two extremely prevalent anchoring methods are Tommy John surgery and the docking technique. Both methods involve harvesting material from the body to act as a replacement for the UCL. The two main body parts used are hamstring tendons and the palmaris longus. The palmaris longus is beneficial since it is simply a supporting muscle in the already in the arm, but only 14% of people have this muscle leading hamstring tendons to be the secondary option (Thompson, 2001). In Tommy John surgery, this material is threaded through the distal epicondyle of the humerus, and proximal epicondyle of the ulna as depicted in Figure 3 (John, 2018). This surgical method was revolutionary when it was created in 1974, but over the years, other methods such as the docking technique have surfaced that improve upon the innovation of the Tommy John technique. It has a boasted a 14% lower complication rate, at only 4%, over Tommy John surgery simply due to a few modifications to the procedure (Watson, 2014). These differences being that only a single hole is threaded into the humerus, and the material selected is then tied over a bone bridge on Figure 54. This procedure provides a lower complication rate, requires less destruction of the bones due to there only being a single incision, and gives greater stability to the elbow joint compared to Tommy John surgery. Both methods are very effective at repairing the damage created by a UCL tear, but neither help repair the UCL. Other solutions must be researched to understand the anchoring methods of a product which aims to heal the UCL instead of replacing it.

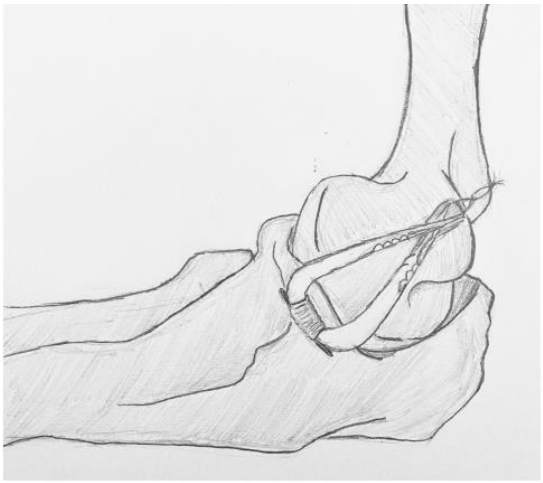

Figure 5: Docking Technique, adopted from McCarthy, Cataldo, & Cannata, 2020

The only non-surgical method that shows any potential in assisting in the UCL repair process is Arthrex: a UCL internal brace. It is a new product, which began research in 2016, which uses only two anchor points and a collagen-coated tape to assist in the healing process of the UCL (Arthrex, 2020). This method is extremely promising due to its lack of need for external material as well as its minimal invasiveness. The surgery is known as primary repair surgery, and it entails using collagen tape scaffold to support and heal the UCL at the same time. The surgery begins by creating 3.5 mm incisions in the sublime tubercle at the origin of the UCL for a suturing anchor. Then the tape is wrapped around the UCL and sutured into the UCL along with the anchor. Next, the isometric point of the UCL is found, and an incision is made in the medial epicondyle next to the isometric point where the second anchor will be placed. Finally, the suture holding the scaffold is completed with this anchor (Trofa, 2017). The player can even begin rehabilitation as quickly as a few days after the procedure and can begin throwing rehabilitation programs in half the amount of time compared if they received reconstructive surgery, the industry standard (Haley, 2017). The downside is that the primary repair surgery cannot be completed on Grade III UCL tears as there is no UCL present to repair. However, it is a fantastic option for those that do still contain their UCL as one study showed the procedure allowed 96% of the players analyzed to return to the same or greater level of play after the surgery which is on par with the 90% success rate surgical procedures have (Trofa, 2017), and it takes an average of 6.1 months to recover from the surgery which is one third of the time it generally takes for those with reconstructive procedures (Jones, 2018). Although it has yet to stand the test of time, it

seems to be a very promising new technology that the team wishes to innovate on in their final project.

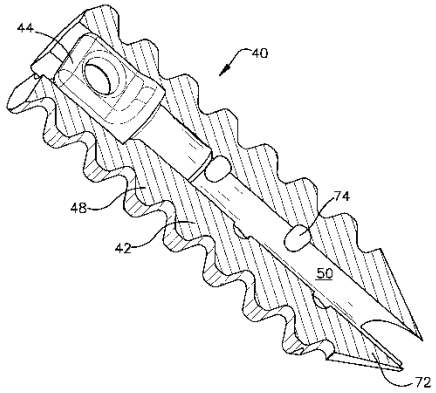

Figure 6: Anchoring Method Example, adopted from Papay and Breyman, 2001

With these methods of anchoring the UCL itself explained. It is necessary to learn about the process of creating the anchors that support the scaffold or graft themselves. To create an effective biological anchor, the anchor must be able to secure a scaffold effectively and securely, be easily implantable, allow for easy scaffold insertion, and not cause long-term issues to the patient (Pedowitz, 2016). To prevent long-term issues, most scaffolds are created by mixing two different materials, one conventional polymer and one calcium salt. For example, two commonly paired materials are PLGA and β-TCP. They are combined in a mixture of 70% PLGA and 30% β-TCP. This allows the PLGA to be the base which will decay overtime, and the β-TCP will push the bone to fill the hole the anchor occurred after it has completed its work (Pedowitz, 2016). The rest of the properties are achieved in the design which can be done in many different manners. An example anchor is shown in Figure 5. Due to the design's pointed end, it is able to be easily implanted into a large enough hole created in bone. With the anchoring location being located at the very end of the anchor, the scaffold can be easily inserted into the anchor after implanting it. Finally, as shown by the designs many ridges, it is necessary for the hold itself securing into the bone generally by applying pressure and creating friction between the length of the anchor and the bone. It will be far easier for the team to create an effective anchoring solution with these necessary design specifications and through learning from examples such as Figure 5.

2.3.3 Biocompatible Scaffold Properties

Certain properties are necessary for proper function of a biological scaffold. In addition to being biocompatible, most biological scaffolds should be bioabsorbable so as to not negatively affect the long-term function of the ligament or tendon. Biological scaffolds should degrade at a similar rate to the rate at which the body naturally produces new tissue in the location of scaffold implantation. This will protect the cells that grow into the scaffold from the environment while they are healing, but then allow the cells to be exposed to the environment once they have matured. If the scaffold degrades at the same rate as tissue ingrowth it will also help to prevent the stress shielding in the tendon or ligament (Doroski, 2006).

The success of a scaffold is often based on its resemblance to the natural properties and composition of the body. Cell viability and extracellular matrix production for biological scaffolds need to be determined to compare their function to that of the natural ligament. Cell viability must be tested to determine if the scaffold allows cells to grow into the scaffold and continue to function normally.

One way this can be determined for scaffolds with required cell ingrowth is with histological preparation and staining or immunohistochemistry. In addition to histology and immunohistochemistry, techniques such as colorimetric assays, ion exchange chromatography and reverse transcriptase-polymerase chain reaction are used to determine cell viability. Colorimetric assays can be used to determine the amount of a specific substance found in a sample using either spectrophotometry or fluorometry by finding the absorbance or concentration of a material in the sample (Doroski, 2006).

Ion exchange chromatography is a technique where the sample is dissolved in a buffer solution and percolated so that proteins separate out based on affinity for a chosen charged material. This technique can aid in determining cell viability by filtering out proteins that would only be present in certain quantities if cell viability is high enough. Reverse transcriptase-polymerase chain reaction is similar except that it detects the amount of a specific RNA transcript for the same purpose of finding certain proteins that would only be present in certain levels of cell viability (Doroski, 2006).

The extracellular matrix composes close to 80% of ligaments so a proper extracellular matrix is necessary for a successful scaffold. Close to 70% of the extracellular matrix is composed of water. Of the 30% of the extracellular matrix composed by dry components,

collagen is the primary component and accounts for 70-80% of the material (Sensini, 2018). For this reason, many techniques done to determine the integrity of the extracellular matrix focus mainly on the collagen composition of the tissue surrounding the scaffold. These techniques involve HP assays, assays for collagen cross linking and radiolabeling.

2.3.4 Scaffold Creation Methods

Scaffolds such as the one aimed to be created throughout this project are created through a few general methods these being 3D printing, phase separation, and electrospinning. 3D printing is the process of heating and extruding layers of plastic material into a finalized design. These layers will then cool and solidify creating the final product. It is a scaffold creation method since it is extremely quick and reproducible, but it falls short when it comes to prototyping freedom since the design is restricted to the abilities of the 3D printer (Do, et al., 2015). Phase separation on the other hand is a process of heating and cooling homogeneous polymers to create a multi-phase system through a solution of the polymers. This creates multiple layers, polymer rich layers, which are essentially entirely filled with polymer, and polymer poor layers which have excess space for the addition of other materials into the design. This process is still quick as 3D printing is, but its final products can be fragile leading it to not be unfavorable for certain scaffolds (Lu et al., 2013).

This section will mostly focus on electrospinning since its customizability and its extremely quick prototyping time make it more desirable than the other options. One of the most common methods for creating scaffolds is electrospinning. This process is beneficial for scaffold creation since it can create extremely small and accurate products (Bosworth, 2011). Generally, the process begins with a syringe connected to a spinneret which will consistently supplies a solution of the material bring used and a solvent to the system with the use of a syringe pump. As the material travels through the spinneret and then capillary tube, a high voltage source charges the droplet of solution. Slowly the charge accumulates near the bottom of the droplet. This charge is then attracted to the charge of an electrically charged baseplate which creates an extremely thin fiber of material. This is then extruded onto the baseplate, and as the solvent dissipates due to the electrical heat, the material solidifies into a solid state finalizing the process (Bosworth, 2011).

Electrospinning is such a common method for scaffold creation due to a variety of factors. The process is extremely customizable and allows for changes to specifications such as the pore size and thickness of the scaffold, and since scaffolds can be electrospun extremely quickly, it is ideal for prototyping. Electrospinning allows different components of a design to be embedded into the scaffold itself, such as growth factors, which is beneficial considering the size of the scaffold. The process can also be performed with a large variety of materials allowing for another level of customizability. Finally, electrospun scaffolds can mimic the extracellular matrix allowing them to more easily integrate into the body and promote cell ingrowth (Boudrioit, 2006).

2.3.5 Hydrogel Fabrication and Testing

To design an implantable healing device, a manipulable material that can handle the natural movements of the body and be loaded with additives needed to be selected. Hydrogels were studied for this device as they can be loaded with a desired growth factor and allow for controlled release over time. Also, the mechanical properties of a hydrogel make them favorable for cell growth and healing, as they can conform with the natural movements of the body. A hydrogel is made up of a network of hydrophilic polymers. These polymers combine to form water-swollen, three-dimensional structures. Hydrogels are a beneficial option as they do not alter the behavior of cells within the matrix. In the past problems have risen when scaffolds are generated on flat and stiff materials. This is because the material does not appropriately mimic in vivo conditions, causing a change in the way that cells behave on it. The stiff materials cause flattening of the cells as well as abnormal polarization. This can lead to altered reactions to pharmaceutical additives as well as a loss of differentiated phenotypes. Hydrogels are beneficial as they mimic the native extracellular matrices in the body and promote cell proliferation (Caliari, 2016).

Hydrogel mechanics mimic that of soft tissues found in the body and can support cell adhesion as well as protein sequestration. Hydrogels can be made into a 2D or 3D structure. Two-dimensional hydrogels are flat films with which cells sit on top. In three-dimensional hydrogels, cells are embedded inside of the hydrogel. When testing hydrogels, it is important to understand the mechanical properties. It is essential to define properties such as tension,

compression and shear. Hydrogels are nonlinear viscoelastic materials, meaning that their mechanical properties are dependent on both time and strain (Caliari, 2016).

Hydrogels can be characterized by mechanics, swelling, mesh size and degradation. Swelling will determine the size of the scaffold in the body as well as how much the hydrogel can hold. Swelling is measured by finding both wet and dry weight of the hydrogel. This gives the mass-swelling ratio. It is also important to know the mesh size of the hydrogel. Mesh size influences nutrient flux in the body. A high modulus value and low swelling ratio indicates a smaller mesh size. Scanning electron microscopy is used to study hydrogel microstructure. The structure of the hydrogel is defined by the mean fiber diameter, fiber density, pore size and degree of crosslinking. Degradation rate of the scaffold is important to understand to determine how the hydrogel will act in the body. Hydrogels can be placed in buffer and take samples at set time points to evaluate degradation (Caliari, 2016).

Alginate hydrogels are biocompatible hydrogels commonly used for tissue engineering applications. Alginates are composed of regions of repeating M units (b-D-man-nuronic acid) and G units (a-L-guluronic acid). When alginates are exposed to solutions containing Ca2+ the G units of adjactent chains are cooperatively bonded causing the aqueous solution to gel. An additional advantage of alginates is their ability to be gelled in situ. The major concern of alginate hydrogels for biological applications is the inability of mammalian cells to interact to them, preventing cell adhesion. In this application the hydrogel is expected to be contained within a scaffold which should negate this problem (Rowley, 1999).

2.4 Biological Additives

In the case of some UCL injuries, a full reconstructive surgery may not be the ideal form of treatment. For athletes with partial UCL tears or athletes who do not want to go through the extensive recovery process associated with Tommy John surgery, non-operative treatments may present a preferable alternative.

The current standard for non-operative treatment is physical therapy. While there is currently limited data concerning the effectiveness of physical therapy for UCL tears, some studies have found methods that may add effectiveness of physical therapy as a non-operative treatment (Rebolledo, 2017). A study conducted by Reggit et al. attempted to determine the likelihood of athletes with UCL injuries returning to their sports without operative treatment. The authors found that with three months or more of rest and physical therapy, only 42% of their

patients were able to return to their previous level of play. The authors looked at the age, duration of symptoms and whether the injury was acute or chronic to attempt to determine if any factors could help predict which athletes would be able to recover without operative treatments and which athletes would need to undergo a form of surgery. The results of the study did not suggest any difference in what athletes rest and physical therapy worked as a means of return to play (Reggit, 2001).

2.4.1 Platelet Rich Plasma (PRP)

Physical therapy is sometimes aided by biological additives intended to increase healing around the ligament, thereby decreasing recovery time. One of these biological additives is platelet rich plasma. Platelet rich plasma (PRP) consists of high concentrations of growth factors in a small amount of plasma derived from whole blood. It is believed that the use of PRP will encourage healing of the ligament through increased cell growth and blood vessel development (Rebolledo, 2017). Despite the promising theory behind PRP injections, the methods of stimulation and delivery of PRP are currently unclear. The ideal levels of PRP composition as well as mechanical and environmental properties to promote healing are widely disputed. A predominant example of this is the debate between leukocyte-rich platelet rich plasma (LR-PRP) and leukocyte-poor platelet rich plasma (LP-PRP). Leukocyte-rich PRP produces an inflammatory response when injected which could create negative consequences for the patient. It has been theorized that leukocyte-poor PRP injections may not create this response. However, a study conducted in 2017 by Hurwit et al. found that there is currently no clear consensus when it comes to the concentration of leukocytes recommended to patients. The authors of the study found that of the 36% of participants in their study who opted to undergo PRP injections, 43.9% opted for leukocyte-poor PRP, 16.6% opted for leukocyte-rich PRP, and 39.4% had no preference of what concentration of leukocytes they were given (Hurwit, 2017). This highlights the issues associated with a lack of knowledge about what type of PRP would be most effective in UCL treatment. In 2019, there were over 16 types of PRP available to UCL injury patients. All 16 types had differences in their method of collection and composition. The effectiveness of each of these 16 different types was still unknown in a clinical setting. To further complicate the PRP decision process, PRP can have different effects on each patient who is injected with it due to differences in platelet and cell concentrations even when the same collection protocol is utilized

(Apostolakos, 2020). Not surprisingly, studies have reported varying degrees of success using PRP to treat UCL injuries.

A study was conducted by Podesta et al. where athletes who had suffered a UCL injury were given an injection of LR-PRP then asked to follow a prescribed physical therapy plan. The participants who were selected had already undergone at least two months of physical therapy without return to play. Of the 34 participants who had partaken in the study, 30 of them returned to the same level of play. The participants on average had statistically significant increased scores on the Kerlan-Jobe Orthopaedic Clinic Shoulder and Elbow (KJOC) and Disabilities of the Arm, Shoulder and Hand (DASH) tests, which are questionnaires designed to determine the function of the elbow. The study did not contain a control group to indicate if the increase in elbow function was due to the combination of PRP and physical therapy or the prescribed physical therapy routine alone (Podesta, 2013).

In 2016 a study conducted by Dines et al. looked at 44 baseball players who had suffered a UCL injury and underwent 1 to 3 PRP injections in addition to physical therapy. The authors of the study followed up with the patients at an average of 11 months and determined the condition of their elbow using the Conway Scale. The Conway Scale consists of four outcomes: excellent, good, fair, and poor. A report of excellent indicated that the patient was able to return to the same level of play that they exhibited before their injury, good indicated that the patient was able to return to play at a lower level of competition than they were able to perform at before the injury, fair indicated that the patient was able to play recreationally, and poor indicated that the patient was unable to return to play at any level of the sport. The authors reported that 34% of patients reported excellent outcomes, 39% reported good outcomes, 4.5% reported fair outcomes and 23% reported poor outcomes. The study did not conduct an MRI to determine the physical healing of the UCL. Additionally, the number of PRP injections, the type of PRP used, and the physical therapy routine prescribed differed between patients in the study (Dines, 2016).

Deal et al. examined PRP injections in patients using MRIs in 2017. The patients selected for the study had undergone MRIs that confirmed a grade II UCL tear. For the study patients were given two PRP injections separated by 2 weeks. The injections were coupled with physical therapy, restricted movement, and external bracing. Two weeks after the 2nd PRP injection, MRIs were taken again. The MRIs showed full UCL repair in 91% of the patients and partial

repair in the other 9%. The authors reported that 96% of the patients returned to their previous level of play (Deal, 2017).

In 2019, a study by Chauhan et al. looked at over 500 UCL injuries in professional baseball players. Over 100 of these players received PRP injections. The authors of the study matched those who had received PRP injections with those who hadn't based on age, position, throwing side and whether they were in the major or minor league. The authors found that players who received PRP injections had a statistically significant longer time before return to play with no difference in survival rate over time (Chauhan, 2019).

2.4.2 Human Mesenchymal Stem Cells (hMSCs)

To determine if PRP injections improve healing in patients with UCL tears, studies with large control groups assigned the same physical therapy routine are necessary. A greater understanding of the effects of PRP injections on a cellular level is also necessary before it can serve as a reliable additive for UCL healing (Apostolakos, 2020).

Another biological additive that has been investigated for ligament and tendon healing is mesenchymal stem cells (MSCs). MSCs create interest as a biological additive because of their ability to differentiate into specific lineages and their ability to secrete factors that promote healing. MSCs also provide a variety of choices for its user. MSCs can be either pluripotent or multipotent, de-differentiated or pre-differentiated, embryonic, or adult, pure STEM cells or bone marrow concentrate, connective tissue or mesenchymal cells and can differ in their site of harvest (Apostolakos). MSCs have been shown to promote healing when used as a treatment for avascular necrosis, a condition where the death of blood vessels leads to a lack of blood flow to bone tissue. Despite the success of MSCs as a healing factor in other areas of the body, no studies have yet investigated its function when applied to the UCL.

2.4.3 Growth Factors

The body naturally produces certain growth factors in response to tendon or ligament injuries such as platelet derived growth factors (PDGF), transforming growth factor B (TGFB), insulin-like growth factors I and II (IGF), vascular endothelial growth factors (VEGF) and fibroblast growth factor (FGF). These growth factors assist in different phases of the healing process and have varying effects including increased cell proliferation, angiogenesis, collagen production and inflammation reduction (Molloy, 2003).

Insulin-like growth factor 1 is present in the first two phases of tendon and ligament healing, the inflammatory and proliferative phases. The main primary observed function of IGF-1 is to increase the cell proliferation and cell migration of cells at the site of the injury. IGF-1 also boosts the collagen deposition of the cells which is used to create and repair the ECM. IGF-1 has been found to work best when in the presence of certain other growth factors such as select PDGF isomers. In a study by Kurtz et al. 25 ug of recombinant IGF-1was delivered to a rat Achilles tendon using a methylcellulose gel. The authors observed an increase in healing and decrease in inflammation as early as 24 hours after the injection and as late as 15 days after the injection (Kurtz, 1999).

Transforming growth factor is believed to be active in nearly all phases of tendon healing with an added importance in the initial inflammatory phase. TGFB has a wide variety of effects on tendon and ligament healing such as stimulation of cell migration, collagen production, regulation of proteinases, termination of cell proliferation and guiding fibronectin binding. Studies have shown an increase of cell proliferation and collagen production after the introduction of TGFB. Despite the advantages of TGFB, high doses of TGFB can also lead to an increase in tendon adhesion which may decrease the tendon range of motion (Molloy, 2003). A study conducted by Chang et al. found that animals with wounds treated with TGFB1 antibodies had a greater range of motion after healing than the control group. This suggests that decreasing the bioactivity of the TGFB1 present in the healing process allowed for a more complete range of motion recovery. The same study found no difference in range of motion between the group injected with just TGFB1 antibodies and the group injected with TGFB1 and TGFB2 antibodies which suggests that TGFB2 may not have the same tendon adhesion properties as TGFB1 (Chang, 2000).

Vascular endothelial growth factor contributes to the proliferative and remodeling phases of tendon healing. VEGF has particular importance in the remodeling phase where it has been shown to promote angiogenesis. Expression of the VEGF gene can be increased through many known biological and mechanical stimuli such as other growth factors, interleukins, hypoxia and bone osteogenesis (Molloy, 2003).

Platelet derived growth factor is believed to have a role in the production of additional growth factors during the initial phases of tendon healing. A study conducted by Letson and Danhers (Letson, 1993) found that treating injured tendons with injections of PDGF lead to an

increased ligament strength and stiffness. PDGF injections were also given with IGF1 and FGF with similar results. The authors hypothesized that had the trial continued longer the groups treated with combination PDGF and either IGF1 or FGF would have shown increased healing due to the effects of IGF1 and FGF on later phases of healing.

Fibroblast growth factor has been shown to lead to an increase in cell proliferation and cell migration as well as stimulate angiogenesis. A study conducted by Chan et al. found that increasing doses of bFGF on rat patellar tendon was correlated with increased collagen production and cell proliferation (Chan, 2000). When Kobayashi et al. tested the effect of bFGF on healing in the ACL they found results that aligned closely with the study conducted by Chan et al. The authors found that the bFGF injections increased the rate of healing in the initial stage of healing which in turn led to greater healing in the later stages (Kobayashi, 1997).

2.5 Comparison of Current Treatments

There are four main treatments for UCL Injuries. These are reconstructive surgeries, unassisted physical therapy, platelet rich plasma (PRP), and Arthrex's Internal Brace. The positive and negatives of each method must be compared to better understand the beneficial parts of each previous design. Unassisted physical therapy can be effective for those with minor UCL injuries since this can be identified through MRI scans of the elbow. However, when the injuries become more egregious, physical therapy can take up to two years to fully heal the UCL, and it is even possible that the UCL will not fully heal without some form of intervention (Clark et al., 2018). It should be noted that all the methods from this point forward are used in combination with physical therapy to ensure the most effective healing of the UCL. Reconstructive surgeries are the industry standard for UCL repair procedures. This is because they have the most research and results backing them compared to the other methods, and since they have been around so much longer than the other methods. They are effective at healing the UCL, and the player can expect to return to play after an average of 18 months (Clark, 2018). They are fantastic options for those that need their UCL replaced, especially since they are the only method that will repair complete tears of the UCL, but their long return to play time has led baseball players to search out innovative methods that will get them back to play quicker (Clark). The two most prominent innovative methods are Arthrex's Internal Brace and PRP. Both are promising since their average return to playtime is approximately 6 months and they can heal up to grade II UCL tears. However, they each have limitations. The Internal Brace is limited by its inability to treat grade

III UCL tears along with it having limited and inconclusive evidence to support it even if the current studies say it has a success rate of 96% (Clark, 2018). It is interesting to note however that scaffolds have been shown to have lower gap formation than normalized reconstruction surgeries and they fail at essentially the same rate making them seem like a fantastic option for those players with average to below average grade II UCL tears although more research will be needed to confirm this claim (Trofa, 2017). PRP is limited by its extreme novelty leading even insurance companies to not cover the treatment (Magit, 2020), and its drop from an 88% success rate to a 73% success rate when the tear on the UCL spans over 50% of the ligament shows that it is only truly effective at less aggressive tears (Clark, 2018). Learning from these current devices allows the team to understand the current state of the market and learn from the past successes of the engineers before them. **Error! Reference source not found.** shows a synthesis o f the information explained in this section as well as provides more statistics on each treatment methods. It should be mentioned that the data in rows 3 and 4 of the table come from limited trials and may not be representative of their actual effectiveness.

Current Treatment	Return to Play Time	Limitations
Unassisted Physical Therapy	Dependent on Severity of Injury	Far less effective on more intense injuries
Reconstructive Surgeries	Approximately 18 Months	Long return to play time
Arthrex - Internal Brace	Average 6 Months	Unable to heal grade III tears
Plasma Rich Proteins (PRP)	Average 6 Months	New experimental treatment

Table 2: Comparison of Current Treatment Methods

2.6 Prior Art

A grade two sprain of the UCL ligament indicates the presence of a partial tear or stretch along the ligament. Treatment for this injury spans from rest and physical therapy to surgery.

The treatment is dependent on numerous factors such as the extent of the UCL tear, the location of the tear and the individual's personal health goals. There is a gap in the current technology regarding the treatment of a grade two tear. Physicians stay on the more conservative side of treatment with activity restrictions, orthotics, ice compressions, medications, physical therapy and pulse ultrasounds. These treatments often take a greater amount of time and run a high risk of reinjury due to incomplete healing. On the other end of treatment options, surgery is a very intense option, with serious risks and implications. Some of these risks include temporary or permanent neuropathy, chronic pain when throwing or losing the ability to fully extend one's arm. Even after surgery there is a risk of stretching or rupturing the new tendon which would result in additional surgeries. This project aims to address the current gap and design a scaffold to aid in the repair of grade two tears (Gomber, n.d.).

To address this gap an in-depth review of the current market and the patents that have been previously filled relating to this field was performed. This search was split into three areas to address the different aspects of this project. These topic areas include current scaffolds, treatments for other areas of the body, and electrospinning. There are numerous different patents in each topic areas that relate to the development of this project.

There are numerous patents regarding the shape, mechanical loads, biological additives and methods of forming scaffolds. Many of these patents are not meant to limit the use of scaffolds but instead outline and provide knowledge for the generation of future scaffolds. Biologic scaffolds are commonly used in biomedical engineering and have a wide variety of applications and fabrication techniques. Scaffolds vary in material composition, structural requirements and biological aspects depending on where the scaffold is being applied in the body. The purpose of a biological scaffold is to repair and renew damaged cells and tissue within the body. Scaffolds should be biocompatible, meaning as the area heals the scaffold degrades into the body (Abdalla, 2019). These scaffolds can also deliver cells and drugs to a targeted area to promote healing. There are currently various scaffolds that address hard versus soft tissues, such as bone versus ligaments. These scaffolds will vary in mechanical strength, the amount of time it takes to degrade in the body and surface chemistry. Each scaffold is specific to the area of the body for which it is being applied. This is because each area of the body requires different mechanical strengths and withstands different stresses (O'Brien, 2011).

Scaffolds are sometimes made from different parts of the body and utilized for treatment. Utilizing autografts is associated with numerous complications. It is very expensive and painful to harvest the graft itself. The process also runs a high risk of infection and hematoma which could result in a failed repair. There is also a high risk of rejection with these grafts due to an immune response and a risk of introducing infection from the donor to the patient receiving the graft (O'Brien, 2011). It is for these reasons that many have turned to the development of tissue engineered scaffolds which aim to regenerate damaged tissue instead of replacing them. Current scaffolds are composed of unique material compositions. They utilize natural polymers, synthetic polymers, or a combination of both. Natural polymers are beneficial as they are biocompatible and are unlikely to initiate an immune response. They do however have lower mechanical strengths and are difficult to control the degradation rates. Synthetic polymers have controlled degradation rates and can be formed into complex shapes. Synthetic polymers are also lower in cost and typically have a longer shelf life (Karaman, 2020).

Current scaffold fabrication techniques fall into two categories, conventional and modern techniques. Some conventional methods include freeze-drying, gas foaming, electrospinning and thermal-induced phase separation. Some modern techniques that have been used include, stereolithography, selective laser sintering, solvent-based extrusion freeforming, bioprinting and fused deposition modeling. Each one of these methods has its advantages and disadvantages for scaffold fabrication (Abdalla, 2019).

There are currently numerous patents regarding scaffold generation and the applications for which they are used inside the body. These patents cover different fabrication techniques as well as applications. An example of this is a patent with a unique design that uses braided fibers in the fabrication of the scaffold. The design braids collagen derived fiber together to create a woven scaffold. The properties of this design are suitable for repairing a tendon or ligament. This design showed high tensile strength as well as flexibility which is ideal for the loads that the UCL ligament encounters. This design was made to address full tears of the UCL in the thumb and be absorbed into the body as the ligament heals (Koob, 2012).

While there is currently no available option for the UCL specifically, similar treatment options have been made for different areas of the body. One of these inventions is the use of biostaples. This patent addresses the use of dry or partially hydrated biocompatible biostaples. These resemble a standard staple but are made from biodegradable materials such as collagen

fibers. These are usually applied to ligament repairs and replacements in the hand or wrist. This can be applied to the UCL to anchor the scaffold to the target area. The fixation needs to be strong enough to withstand loads within the body as well as the stress put on it during the post-operative and rehabilitation period (Wiedrich, 2017).

Scaffolds have been developed that aid in the healing process of completely or partially ruptured Achilles' tendons. The scaffold is attached to the injured area and used to promote cell growth and repair over time. This has a similar end goal to our project, just applied to a different area of the body (Saltzman, 2010).

A patent for a cardiovascular graft has a similar design and aspects that can be applied to our project. The patent is for both the scaffold itself and the process for making it. This patent breaks the fabrication process into five steps. It defines the materials used in the fibrous layer and the graft construction. With this design the way in which the fibrous layers were laid was also unique. For some patents the fibers are put down parallel to one another and seeded with cells to promote growth. In this case at least one layer of the electrospun fibers needs to be intertangled. One layer of this scaffold is also adhered through an adhesive free chemical bond. This is a unique combination of graft and fibrous sublayer that allows for optimal blood flow and mechanical properties in the heart (Laksin, 2012).

Another patent that is interesting for this project is the design of a self-fixating scaffold. The patent for a self-fixating scaffold combines a scaffold used for repair with a fixation element which allows the scaffold to be anchored into the tissue. This is essential because if a scaffold is not properly anchored in place, it can become dislodged. In this case the therapeutic materials embedded in the scaffold would no longer be reaching the targeted areas, rendering the scaffold useless. The patent for the fixation element can be applied to any of the scaffold fabrication techniques. The scaffold is then combined with a fixation element which can be made of either biodegradable or non-biodegradable polymers. This is applicable to our design as we need to determine the best way to attach the scaffold to the ligament (Sigg, 2007).

Electrospinning is a common technique used in scaffold fabrication. Electrospun fibers mimic the extracellular matrix of the natural tissue. These scaffolds also allow for cell adhesion and proliferation, meaning that the ligament can repair itself as the scaffold degrades (Karaman, 2020). These scaffolds also have appropriate porosity to allow for blood to flow through them. There are numerous patents regarding using electrospinning to create scaffolds. These cover the

way in which the fibers are laid, the materials used, and the applications of the design (Lelkes, 2011). After conducting a patent search, it was clear to the team that even though there are not many patents related to the UCL specifically, there are many areas that the team needs to keep in mind. During the design process the team needs to ensure that the design does not infringe on current patents. This is especially important when fabricating the scaffold itself as there are many patents that cover the fabrication parameters of tissue engineered scaffolds.

Zreiqat et al. designed a synthetic polymer scaffold composed of a hydrogel forming polymer and a biocompatible ceramic material in a bundle of fibers forming a braided scaffold. This scaffold is designed mostly to be a synthetic ligament or tendon to allow to body to rebuild the ligament. It is designed so that it can be modified for a wide variety of ligaments and tendons in the body (Zreiqat, 2017).

Hwang et al. designed a bioresorbable connective tissue scaffold composed of polymeric fibers to replace the need for tissue grafts. It is designed with anchoring segments on either side, with a central segment composed of more bioresorbable polymeric fibers with void spaces and binding regions to encourage tissue ingrowth. This central region can be designed differently depending on the difficulty or type of tissue ingrowth desired. It can be composed of fibers running parallel and not interconnecting, to fully braided, and any amount of these two combined. This central region, as well as the anchoring regions, can also be coated with a biological material that encourages cell proliferation, such as a natural extracellular matrix material (Hwang, 2012).

Rocco et al. designed a composite scaffold for repair and regeneration of ligaments. This scaffold has a porous interior, increasing the surface area and void volume for cell proliferation, which is all surrounded by a flexible support structure so it can maintain its shape and withstand tension. It is designed to stabilize soft tissue injuries while facilitating tissue regeneration. The porous interior is designed to facilitate cell proliferation by allowing ingrowth, but it can also be filled with a hydrogel or PRP or other biological fluids (Rocco, 2020).

Another method for repairing bone-soft tissue damage was designed by Johnson et al. This design uses electrospun polymer fibers. In a surgical procedure using this device, the ligament would be attached to the bone using surgical hardware, and the damaged portion in need of regrowth is covered with a patch consisting of electrospun polymer fibers which are

lined up with the ligament to encourage alignment during cell proliferation. It aims to decrease the healing time for ligament detachment injuries (Johnson, 2018).

A multi-phased scaffold for soft tissue repair was designed. It consists of fully synthetic nanofiber materials that are biomimetic and biodegradable. It is composed of several layers of polymeric nanofibers and biocompatible ceramic oriented to mimic the native tissue anatomy to encourage aligned growth and proliferation (Lu, 2009).

Martha M. Murray created a ligament repair technique using a collagen composition that could be formed into a scaffold or incorporated into a scaffold comprised of other materials or traditional ligament repair device. The material is designed to quicken the healing process by encouraging incorporation of the material into the healing process (Murray, 2017). She also devised a method of repairing a torn or ruptured anterior cruciate ligament by bridging the gap between ligament stumps with a scaffold. This method was designed fo the ACL, but could be applied to other torn or ruptured ligaments (Murray, 2020).

Laurencin et al. Designed a braided scaffold to be used as a graft material in ligament and tendon repair. It is designed out of biodegradable polymer fibers and has distinct attachment ends on either side, with a midsection that facilitates cellular integration and proliferation. The scaffold can be seeded with cells to encourage ingrowth (Laurencin, 2015).

2.7 Background Conclusions

Currently, UCL repair techniques lack the ability to heal the UCL in a short amount of time. Multiple solutions exist, but few are effective enough to be commonly used, and even fewer achieve rapid healing of the ligament. There is a need for a minimally invasive repair technique that consistently improves the outcome and decreases the healing time of UCL repair procedures. The market this product will enter is professional and amateur athletics, specifically sports with a large emphasis on throwing mechanics.

3. Project Strategy

The design portion of the project began by creating an initial client statement based on the information that had been received from the client. The client identified the need for a device that can aid in the healing of Grade II UCL tears. This device should be less invasive than reconstructive surgery while also more effective than current conservative treatment options such as physical therapy. To address this need, the team identified a set of specifications, objectives and constraints for our project. After narrowing down and ordering the project's objectives, the team produced a revised client statement and formulate a project approach for the remainder of the year.

3.1 Initial Client Statement

With the client statement, the team attempted to convey what the client was looking for in the final product. The three focuses of the client statement were the ease of use of the product by surgeons, the ability of the scaffold to support the injured UCL and the ability of the scaffold to aid in the UCL healing process. It is necessary that the product be easily manipulated by surgeons to increase efficiency during the operation. Mechanical support of the device is key in preventing further injury to the patient during the recovery process. It is also essential that the device assist in healing or it would have no advantage compared to products currently on the market.

3.1.1 Client Statement

Design, develop, and characterize an implantable scaffold which consistently improves the outcome of Grade II UCL repair surgeries. The scaffold must be highly compatible with current surgical practices, and the scaffold should provide mechanical support for the ligament while assisting in the healing process.

3.2 Stakeholders

To better inform the design process, a stakeholder analysis was conducted to ensure the final product would be take everyone's desires into account. The major stakeholders are the patients receiving the surgery, biomedical companies who can produce the product, the surgeons performing the surgery, WPI, along with our advisor, Professor Pins, and finally the MQP team

themselves. The patients that will be receiving the surgery are some of the most important stakeholders in this scenario. Their acceptance of the surgery is paramount since if they do not believe in the effectiveness of the procedure, they will not attempt the procedure. This means that part of the project's success is based upon player's abilities to accept and trust the UCL repair method the team produces. Player's main concerns are that the procedure returns them to an equivalent or better level of play, and that it has a quicker return to play time and lower complication rate compared to their other options. Also, for the players that are not at a professional level, the affordability of this device is likely to have a significant impact on the audience it is able to reach. Amateur and youth players are less likely to have the funds that a major league player has for this device. If no one were to receive the surgery, it would have no use and ultimately be abandoned by the medical field, so ensuring it is effective and attractive for possible candidates must be at the forefront of the team's mind during design.

Possibly the most important stakeholders are biomedical engineering companies since without their acceptance of the product cannot be manufactured, distributed, or marketed to those that need it. They are mainly interested in an effective and safe product for their patients, but they are also very interested in the product's marketability and IP. The product we create must show a clear benefit over the other products currently on the market to make it marketable, and it must be distinct enough from those products and other IP to ensure the company is not risking infringement if they invest in the product.

Surgeons' abilities to accept the surgery will also affect the outcome of the product since without anyone willing to give the surgery no player could receive the surgery. For the product to gain traction in the market, it will need the acceptance and help of surgeons to do so. Their concerns include those of the players, that the surgery is affordable, has a lower return to play time and complication rate compared to alternatives, as they want the best option for their patients. However, they are also interested in the procedure being easy to complete to prevent complications as well as for the procedure to be effective at promoting cell ingrowth to heal the UCL as quick as possible. Along with the criteria stated before, the team must also be aware of the difficulty level of the procedure created through the project to ensure physicians will adopt the procedure.

The advisor, Professor Pins, and WPI are both excited to see the innovative solution the team can create through the project. They have emphasized the importance of the device not only

being beneficial to the healing of the UCL but also as a novel idea that is patentable. The school desires to license our team completes and wants to ensure that the product the team created is a novel design. The institution wants the team to expand their knowledge and practice their engineering skills, while at the same time ensuring they are not liable to possible plagiarism or that the device created is not patentable leading the school and students to possibly not get credit for the intense amount of work put into the project. Finally, the team's goal throughout the project is to learn as much as they can while also receiving credit for the work they are doing. Although they most likely care about the product, they develop at the most surface level they must complete the project for a grade to graduate. The project will be a learning experience for them, and they are really excited about the project, but their time constrains and the understanding that this project is only a part of their total course load should be understood throughout the project. Through this analysis, many key factors and opinions have been examined which will need to be remembered throughout the course of the project.

3.3 Specifications

1. Easily implantable in 4-6 cm incision window
2. Dimensions of 1x2 cm with a maximum thickness of 0.5 mm
3. Attach to the ligament and bone for secure anchoring
4. The scaffold should degrade after 4 to 6 weeks
5. Can withstand cyclic loading in the elbow
6. Can adequately support to the UCL during the healing process
7. Does not affect the throwing mechanics of the patient
8. Promote healing of the UCL
9. Biocompatible
10. Low cost
11. Long shelf life
12. Easy reproducible

Through background research and conversation with our sponsor the group came up with the 12 specifications listed above for our product. The first two specifications were that the device should ideally be implantable in a 4cm to 6cm window and have dimensions of 1x2 cm

with a maximum thickness of 0.5 mm. The third specification is that the device must be attachable to the ligament or bone. This is necessary to ensure that the device stays in place in the elbow once implanted. The fourth specification is that the scaffold should degrade and be replaced by native tissue in a 4-6 week time frame. The fifth specification is that the device can withstand cyclic loading. This is important as the device will undergo cyclic loading while the patient performs day to day activities during the recovery process. Certain strengthening or stretching exercise may cause additional loading of the device. The sixth specification is that the device can provide enough mechanical support to the UCL to lower the chance of reinjury during the recovery process and hold up to manipulation by the surgeon during implantation. The seventh specification is that the device should not affect the throwing mechanics of the patient. Our target demographic are athletes who hope to continue some form of athletic activity at any level in their future. If they are unable to return to their previous throwing mechanics with our product, they will likely opt to undergo a complete UCL reconstruction surgery or forgo surgery entirely. The eighth specification is that the device should promote healing of the UCL. Promoting healing of the UCL would give our device an advantage over other products currently on the market. The ninth specification is that the device must be biocompatible. If our device triggers an adverse immune or fibrotic response from the body, it will cause more complications for the patient's attempt at return to play rather than assist it. The tenth specification is that the device should be low cost. If we can keep the price of the device low, we would remove an important obstacle for medical device companies and hospitals to purchase our device. The eleventh specification of our device is that it is easily reproducible. If our device is to be commercialized, we will need to prove that it can be produced within certain parameters every time. These specifications were created to help in the design process but would ultimately need to be expanded upon to consider the complexity of the final device.

3.4 Objectives

The team then identified six objectives based on the project specifications outlined above. To rank the significance of each objective in relation to the project, a pairwise comparison chart was generated. This chart was used to compare the project objectives against one another. Each comparison was given a score of 0, 0.5 or 1. A score of "0" indicates that the objective in the left-hand column is less important than the objective it is being compared to. A score of "0.5"

indicates that the objectives have equal importance. Lastly, a score of "1" indicates that the objective in the left-hand column is more important than the objective it is being compared to. The completion of this chart allowed for the objectives to be ranked for importance. The weight value found for each objective will also be used later in a Pugh analysis to compare possible design solutions.

	Provide Mechanical Strength	Low Cost	Short Return to Play Time	Easily Implantable	Reproducible	Promotes Healing of the UCL	Total
Provides Mechanical Strength	X	1	0	1	0.5	0	2.5
Low Cost	0	X	0	0.5	0	0	0.5
Short Return to Play Time	1	1	X	1	1	0	4
Easily Implantable	0	0.5	0	X	0	0	0.5
Reproducible	0.5	1	0	1	X	0	2.5
Promotes Healing of the UCL	1	1	1	1	1	X	5

Table 3: Pairwise Comparison Chart of Objectives

Rank	Objective	Description
1	Promotes Healing of the UCL	Must be biocompatible, promote cell ingrowth, be able to be seeded with growth factors to fully heal the tear and restore native tissue biomechanics
2	Short Return to Play Time	Must decrease the total recovery time while still bringing the ligament back to its pre-injury strength
3	Reproducible	Design must be easily reproducible to become commonplace in UCL repair
4	Mechanical Strength	Must be able to support the UCL during the healing process
5	Easily Implantable	Surgeon must be able to manipulate scaffold easily without fear of damaging it and it should fit within a small window
6	Low Cost	Must be affordable to both professional athletes and the public

Table 4: Ranked Objectives

The scaffold's ability to promote healing was found to be more important than any other design objective. Ultimately, if the device does not aid in the healing process, then it is not a valuable option and would not be worth the risk of surgery.

It was determined that mechanical strength was not as important as promoting healing of the UCL. Promoting healing in the UCL would result in mechanical support after the tear has healed. We determined that being easily implantable and inexpensive was less important than mechanical strength. This is because after surgery, the patient's elbow would be immobilized for several weeks, with no loading being placed on the UCL or the implanted device. After a few weeks, the patient would begin physical therapy and would be instructed to avoid placing heavy loads on their UCL, reducing the need for the device to withhold large loads but requiring a small amount of loading capability.

Reproducibility was determined to be equally as important as mechanical strength. Without reproducibility, the device cannot be manufactured and produced in the quantities required to be a common and effective product. If the device cannot be accurately reproduced, it's effectiveness in implantation is questionable at best.

Another objective that was examined was the ease of implanting the scaffold. We determined that the scaffold being easy to implant was not as important as the scaffold

promoting the healing of the UCL since there would be no reason to implant the scaffold if it did not promote healing of the UCL. We determined that the scaffold being easily implantable was only slightly more important than cost. If the device is not easily implantable it would be difficult to convince surgeons of its value. A device that is difficult to implant could lead to complications during surgery. If the surgeon is unable or unwilling to implant the device, then the cost does not matter. A surgeon would likely be willing to work with a material that is slightly harder to implant if it meant that their patient was more likely to have a shorter return to play time.

On the other hand, the device being low cost was said to be less important than the other objectives as many players would be willing to pay the extra money for the surgery if it would significantly aid in the healing of their UCL. Low cost was also ranked at the bottom equal to ease of implantation because the functionality of the device is ultimately a more important consideration than how much time the surgeon is required to spend implanting the device or how inexpensively it can be manufactured. If the device improves the healing process better than its competition, surgeons will likely be willing to put more effort into the procedure and patients will likely be more willing to pay more for the procedure to achieve a better outcome than an alternative method.

3.4.1 Objectives Analysis

The team then identified more specific objectives that fell into the categories of the main objectives. These secondary and tertiary objectives are described in the infographic below followed by a more detailed description in the subsequent tables.

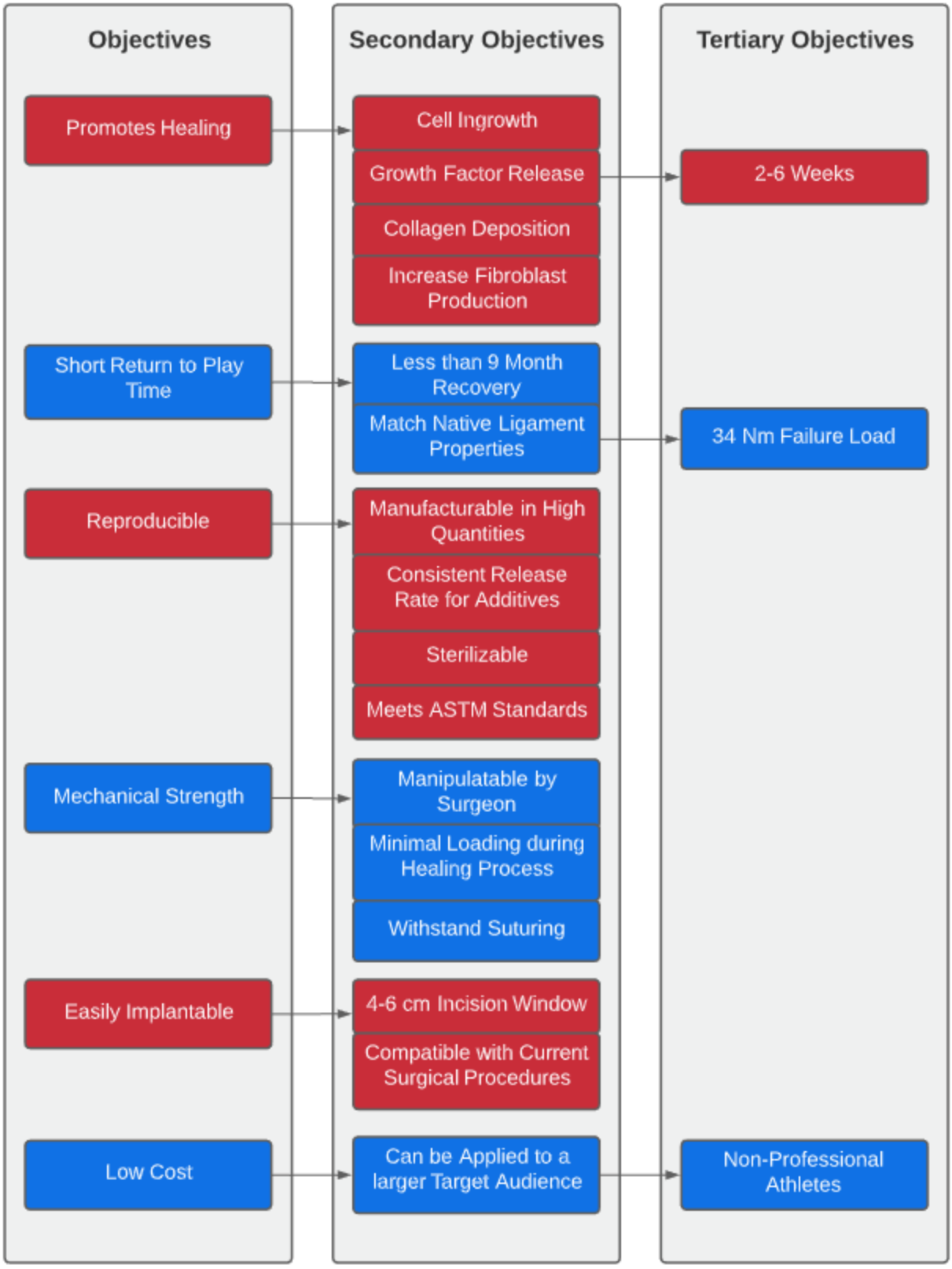

Figure 7: Objectives Tree

Promotes Healing	
Secondary Objective	**Description**
Cell Ingrowth	Implanted device has properties that allow for cell regeneration in tissue and ingrowth into the device
Growth Factor Release	Implanted device has properties that allow for controlled release of growth factors for the duration of healing
Collagen Deposition	Implanted device has properties that increase collagen deposition in the damaged tissue
Increase Fibroblast Production	Implanted device has properties that increase the production of fibroblasts

Table 5: Objective 1 Secondary Objectives

Short Return to Play	
Secondary Objective	**Description**
Less than 9 Month Recovery	Implanted device decreases healing time to approximately 9 months as opposed to the current 12-18 months
Match Native Ligament Properties	Restored tissue must match original ligament properties fully

Table 6: Objective 2 Secondary Objectives

Reproducible	
Secondary Objective	**Description**
Manufacturable in High Quantities	Device must be able to be manufactured on a large enough scale to be readily available to surgeons
Consistent Release Rate for Additives	Manufactured devices must have consistent additive release rates matching the desired amount
Sterilizable	Devices must be sterilizable after production and be stored in sterile packaging
Meets ASTM Standards	Device must meet ASTM standards for biocompatibility, mechanical strength, and release rate

Table 7: Objective 3 Secondary Objectives

Mechanical Strength	
Secondary Objective	**Description**
Manipulatable by the Surgeon	Device must withstand manipulation during implantation without compromising structural integrity or premature growth factor release
Withstand Minimal Loading During healing	Device must be able to withstand incrementally larger amounts of loading during the healing process
Withstand Suturing	Device must be able to withstand suturing and not tear out

Table 8: Objective 4 Secondary Objectives

Easily Implantable	
Secondary Objective	**Description**
4-6 cm incision	Device must be implantable within a 4-6 cm incision to be large enough to cover ligament while minimizing incision size and potential scarring
Compatible with Current Surgical Procedures	Device must be able to be implanted by any orthopedic surgeon similarly to how similar devices are implanted

Table 9: Objective 5 Secondary Objectives

Low Cost	
Secondary Objective	**Description**
Can be Available to a Larger Target Audience	Device must be inexpensive enough to manufacture so that it can be made available to non-professional athletes

Table 10: Objective 6 Secondary Objectives

3.5 Constraints

There are major constrains for both the product and the team that will influence the course of the project. The product has constraints since without certain features it will never be a viable solution for our sponsor or any biomedical engineering company. It must not elicit an immune response from the body and must be sterilizable since if the product does not contain these characteristics, it could not be used in a surgery. The scaffold must be implantable through a 6cm incision window since that is the standard incision window for these procedures and the product

must not stray too far from current practice. Finally, the product cannot fall under any current patents to prevent patent infringement. These constraints will have a large impact on the product produced, but the product will also be affected by constraints the team has throughout the course of the project.

The two main constraints for the team are time and money since the team only had a singular year to complete the project while needing to spend time on their other classes, and the team was only allocated $150 per person after lab costs meaning with five people the project had a budget of $750. Although these are the biggest constrains the team also must also understand the limitations created by the current pandemic. This does not affect the team's workflow or ability to meet since many things can be done online, but it severely hinders their access to lab space especially as an entire team. This means that each member must relay any information they learn during lab time to the other teammates which takes up time and could lead to lose of information. All these constraints, listed below, will need to be considered to create a viable final product and to inform the team's timeline and budget.

1. The scaffold cannot elicit an adverse immune response from the body
2. The scaffold must be sterilizable
3. The scaffold must be implantable through a limited incision window created by the surgeon
4. Our method of producing the scaffold cannot fall within any currently existing patents
5. The scaffold must be completed by the end of the academic year with a budget of $750

3.6 Client Statement

After meeting with our client and advisor over the course of the term and creating our project specifications and objectives, the client statement was revised to fully encompass the criteria described by our client. The addition of degradation time was discussed in a meeting with Dr. Magit. In this meeting the team received specifications that Dr. Magit specifically asked for with degradation rate and return to play time having a large emphasis. The second revision in the client statement included the need for bulk manufacturing. In a joint meeting with Professor Pins and Dr. Magit it was discussed that to make this product commercially available and competitive that the device would have to be easily produced. A third addition was made to the statement after a meeting with Dr. Magit that included the finalization of the dimensions for the scaffold.

3.6.1 Revised Client Statement

Design, develop, and characterize an implantable scaffold which consistently improves outcome and decreases return to play time of UCL repair surgeries. The scaffold must be 1cm in width, 2cm in length, and 0.5mm in thickness to be compatible with current surgical practices. The materials chosen for the scaffold should pass biocompatibility tests based on ISO standards. It must be able to store at least 3 mL of a therapeutic agent and release the chosen therapeutic agent for a duration of at least 7 days in order to restore native elbow biomechanics within 9 months. The scaffold must promote cell growth by increasing cell proliferation 10% or more compared to control. As for its mechanical properties, the scaffold must be able to withstand 10N/mm per suture, and the ultimate tensile strength of the scaffold should not alter with three-point bending manipulation. Finally, the scaffold should degrade within four to six weeks and be reproducible.

3.7 Project Approach

3.7.1 Management Approach

To remain on track throughout the year the team created a Gantt chart. The Gantt chart outlined all tasks that needed to be completed along with a general time frame for each. This chart was updated weekly as the team progressed. The chart can be found on the main page of the team's OneDrive.

To ensure the team stayed on track, team and client meetings were conducted on a regular basis. Weekly meetings were held with the client and advisor. These meetings were used to provide updates on the progress made as well as plans for the upcoming week. Meetings with the client were held to discuss project specifications and clarify points of confusion. Lastly, team meetings were held a few times each week to discuss the project and divide up areas of research.

3.7.2 Design Approach

Throughout the term, the team compiled extensive background research in areas that could contribute to a final design selection. A set of project specifications as well as design objectives were identified based on research and client input. The team conducted a brainstorming session in the first week of B-term to conceptualize the information found and present possible design solutions. After choosing a few viable solutions, SolidWorks CAD

drawings were generated to better visualize the design. These drawing helped to define the specific shape and size of the device. Before final testing was conducted, the team performed a set of preliminary experiments to ensure the protocols properly provided the team with the needed data. The preliminary tests included testing on the use of hydrogels, determining optimal testing strategies for degradation rate, and electrospinning prototype scaffolds. Once preliminary testing had been completed, the team ran experiments on their final materials and scaffolds. The results were analyzed and compared to the desired functions and specifications found through literature analysis and discussion with an orthopedic surgeon.

3.7.3 Financial Approach

Each member of the team was allotted $250 from Worcester Polytechnic Institute to be used towards the completion of the project. The team completed research in Goddard and Salisbury Laboratories so $100 was taken from each member for the use of the lab and lab equipment. This left the team with a budget of $750. The team evaluated what materials were available and what needed to be purchased. Research on possible materials helped ensure that only viable material options were purchased. After brainstorming and design selection, the team compiled a list of all materials needed and ran a cost analysis to ensure that the project fell within the appropriate budget.

4. Design Process

The design process for this project started in the beginning of B term by collecting all the project specifications, objectives and constraints put together in A term. The team then analyzed these parameters by ranking primary objectives and creating secondary objectives. After having a clear understanding of the objectives, the team held a brainstorming session which included Dr. Magit and Prof. Pins. This brainstorming session was integral in the preliminary design process as topics such as conceptual designs, potential materials, anchoring methods, manufacturing methods, and controlled release mechanisms were discussed. Following the brainstorming session, the team reconvened to organize all the information presented in the brainstorming session. The ideas from that session were then collected and analyzed using pairwise comparison charts. The results of this analysis led to the develop three main design concepts, determining the correct materials, and the creation of preliminary testing protocols.

4.1 Needs Analysis

To ensure that the focus of the project was kept in the right direction, different aspects associated with the desired product were grouped into two categories: "Needs" and "Wants." The "Needs" category consisted of aspects of the product that were necessary for it to function. Without these aspects, the device either would not work, or would provide no value to our target audience. The "Wants" category consisted of aspects of the product that could improve the function of the product without being necessary. Aspects of the product in this category may increase its value to the consumer or likelihood of being utilized by surgeons but are not required for the product to function.

There is a need for a minimally invasive ulnar collateral ligament (UCL) repair technique that consistently improves the outcome of UCL repair procedures. It needs to be biocompatible, promote healing, decrease the overall recovery time, not impede natural biomechanics, be easy to manipulate by the surgeon, and include a controlled release of biological additives. The market this product will be for is professional and amateur athletics, specifically sports with a large emphasis on throwing mechanics such as Major League Baseball.

4.1.1 Design Needs

Biocompatibility: It is necessary that the proposed scaffold be biocompatible, or not trigger an adverse immune response when implanted into the body. If the scaffold were to trigger an

adverse immune response it would negatively affect the healing of the UCL rather than promote healing of the UCL in accordance with the previously laid out objectives. A negative immune response additionally has the potential to endanger the overall health of the patient.

Healing promotion: To create value compared to the existing solutions for UCL tears, the proposed scaffold must promote the healing of the UCL. Procedures that allow patients to regain elbow function already exist, but they rely on the natural healing of the body. If the proposed scaffold can improve upon the healing process already present in the elbow, it would give reason for surgeons to switch from their current options.

Does not impede natural throwing biomechanics: Since the proposed product is intended for athletes who wish to return to play, it is necessary that the device does not prevent patients from returning to their pre-injury biomechanics. If the scaffold did not allow patients to return to their previous level of play, patients looking to return to their sport would likely avoid the proposed scaffold. Surgeons would additionally be unlikely to use this product for the same reason.

Manipulated by surgeons safely: The scaffold must be able to be safely manipulated by surgeons so that it is not damaged during the implantation procedure. If the scaffold is damaged before it is implanted, it may release biological additives at an improper rate. This means that the scaffold must have a minimum yield strength so that it is not torn while being handled by the surgeon. The scaffold must also have a maximum elastic modulus so that it can be stretched by the surgeon to be properly positioned over the UCL during the procedure.

Controlled release of biological additives: To promote healing of the UCL, the scaffold must be able to be seeded with a form of biological additive. The chosen additive will be one that has been found to stimulate one or a combination of fibroblast production, collagen deposition or angiogenesis in environments similar to the UCL. This additive will be essential for promoting healing so if the scaffold cannot be seeded with growth factors it will not be able to fulfill the previously described needs of the product. If the additives cannot be eluted in a controlled way the UCL may be over or under dosed with the additive, both of which will not promote the desired rate of healing. An overdose of many biological additives can result in decrease healing, the opposite of the desired effect.

4.1.2 Design Wants

Degradation rate: For the first 2-6 weeks after device implantation, the patient will be instructed to avoid moving their elbow unless necessary. After this time the patient may be allowed to begin physical therapy, depending on the state of the UCL. If the scaffold can degrade within this time frame, there will be no concern over the scaffold degradation lengthening the healing process. If the scaffold does not elicit an adverse immune response or fibrotic encapsulation, it may not be necessary for the scaffold to degrade in this time frame or at all. It is believed that electrospinning the scaffold would allow for a non-degradable scaffold to be used.

Compatible with current surgical practices: If the scaffold implantation process can line up with surgical practices that currently exist for UCL surgeries, surgeons would not be required to learn a new technique to implant our scaffold. Having an implantation procedure that is similar to current practices is not necessary since surgeons would likely be willing to learn a new technique if they felt it would lead to improved healing for their patient. A known surgical procedure would eliminate one obstacle for translation to the clinical field.

Short return to play time: A short return-to-play time is desirable for the proposed device, as it would set the device apart from current treatment methods. The most relevant treatment option on the market is Tommy John surgery. This surgery can sideline a patient for at least 9-12 months depending on the rigor of physical therapy. For our product to be a competitive alternative, the ideal return-to-play time would be 9 months at the most.

Low cost: Keeping the price of this treatment option in an affordable range will make the product more desirable. The main patient pool in the market for an alternative treatment option to UCL repairs are usually athletes. Many patients who suffer from these injuries are not high-profile and do not have the resources to spend thousands of dollars on invasive surgery. By keeping the cost of the implant low, the surgeon will be more likely to refer the implant to a wider range of patients that are looking for a reliable procedure at a lower cost to them.

4.1.3 Needs and Wants Design Matrix

A design matrix detailing how each "Need" and "Want" of the project affected the device characteristics is shown below. Needs and wants are listed along the top of the matrix and

scaffold characteristics are listed along the left-hand side. Not all needs or wants effected the decision-making process regarding all characteristics of the scaffold.

Scaffold Characteristics	Wants	Degradation Rate	Surgical Compatability	Short Return to Play Time	Low Cost	Needs	Biocompatibility	Healing Promotion	Does Not Impede Throwing Mechanics	Manipulatable By Surgeons	Controlled Release of Additives
Material		X		X	X		X	X		X	X
Shape			X	X					X	X	X
Manufacturing Process		X		X	X		X	X	X	X	X
Biological Additive				X			X	X			X
Size			X	X					X	X	

Table 11: Needs and Wants Matrix

4.2 Updated Functions and Specifications

Featured below in Table 12 is a matrix containing the functions and specifications for the proposed device. The functions of the device predominantly fall in line with the secondary objectives of the device. These include the ability of the device to promote cell ingrowth, allow for a controlled release of a biological additive, increase cell proliferation, increase fibroblast proliferation and migration, decrease recovery time, withstand manipulation by a surgeon and withstand suturing to the UCL. The specifications of the device align closely with the tertiary objectives of our scaffold and include the volume of biological additives the scaffold must be loaded with, the rate of release of the biological additive, the length of recovery time for a patient post implantation, and the length of degradation of the scaffold in vivo. All the sources of the specifications, and the reasoning for their exact values will be expanded upon later.

Table 12: Functions and Specifications

Functions	Specifications
Promotes Cell Ingrowth	10% Increase in Cell Proliferation Compared to Control
Stores Biological Additive	Can be Loaded with 3 mL of PRP
Controlled Release of Biological Additive	Releases PRP at a Rate Between 0.7 to 0.21 mL/day
Increases Cell Proliferation and Migration	10% Increase in Cell Proliferation Compared to Control
Increases Fibroblast Proliferation and Migration	10% Increase in Fibroblast Proliferation Compared to Control
Manipulatable by Surgeon	Ultimate Tensile Strength does not alter with multiple cycles of manipulation
Withstand Suturing	Can Withstand 10 N/mm of Thickness per Suture
Decrease Recovery Time	Restore Native Elbow Biomechanics within 9 Months

4.3 Analysis of Conceptual Designs and Materials

4.3.1 Brainstorming Session

To begin the design process, the team planned a brainstorming session with their advisors, Professor Pins and Dr. Magit, to theorize all possible designs. The team prepared topics of discussion to ensure that if the conversation lost momentum the group could quickly switch to a new idea. The topics discussed were the material of the scaffold, the manufacturing method of the scaffold, the overall design of the scaffold, the anchoring method of the scaffold, and a controlled release method for possible growth factors. With these topics, the group met and was able to brainstorm plenty of possible designs for the device that needed to be synthesized to determine which were best to move forward with.

To do this, the team created a document with their ranked objectives, specifications, and client statement to review each idea to ensure that it was viable and realistic for the scope of the project. After this initial review was completed, the team had a sizable group of ideas for each of

the five topics they brainstormed. All these results were synthesized into lists, and then each list was ranked using pairwise analyses to determine the best possible option for the final design.

4.3.2 Conceptual Design Analysis

After the team's brainstorming session, all the ideas for each part of the design were combined and compared against each other with a pairwise analyses to determine the best possible idea for the final design. The parts of the device that were brainstormed were the material of the scaffold, the manufacturing method of the scaffold, the design and shape of the scaffold, the anchoring method of the scaffold, and the controlled release method for possible growth factors. Each of the brainstormed ideas and their ranks compared to each other will be explained in this section. The topic of the pairwise analysis can be found in the top left cell of each table.

Anchoring Method	Cleat (Barbed Needles)	Parafilm	Ace Bandage Hooks	Biostaples	Adhesives	Suture	Total
Cleat (Barbed Needles)	X	1	0.5	1	0	0	2.5
Parafilm	0	X	0	0	0	0	0
Ace Bandage Hooks	0.5	1	X	0.5	0	0	2
Biostaples	0	1	0.5	X	0	0	1.5
Adhesives	1	1	1	1	X	0	4
Suture	1	1	1	1	1	X	5

Table 13: Anchoring Method Pairwise Analysis

There were six possibilities for the anchoring method for the device. These were the cleat method, an adapted form of parafilm, ace bandage like hooks, biostaples, adhesives, and sutures. The pairwise analysis used to analyze the anchoring method options can be found in Table 13. The lowest ranked method was the parafilm method. It was an extremely theoretical idea, and the

team could not formulate any method to create a design that would function inside of the body. Next were biostaples which were ranked low due to the restriction they would place on the UCL and their invasiveness compared to other methods. The ace bandage hooks were a design theorized by the team, and a drawing of the design can be found at Figure 7. This design entails attaching hooks, like ace bandage hooks, to the edges of the scaffold which can then hold the scaffold on top of the UCL. This design seemed like a promising idea, but it could have issues when it comes to being able to hold the scaffold firmly in place for a prolonged period of time. This led the team to abandon the idea for the main design due to the team's time constraints, but it could be a good idea to look back at in case of IP issues later in the project. The next design was the cleat or barbed needle design. It entails building a scaffold with microneedles spread across one of its sides. This side will then be pressed onto the UCL to hold the scaffold in place, see Section 4.5.2 for more information. The final two designs, sutures and adhesives, were ranked the highest since they are the most widely used currently in the market, and the team believed they would be effective and consistent. Dr. Magit informed the team that the anchoring method should not be the focus of their time, so the team decided that the most used designs should be adapted before novel designs. Suturing was only ranked higher because of its increased reliability compared to adhesives, and therefore the team decided to move forward with sutures.

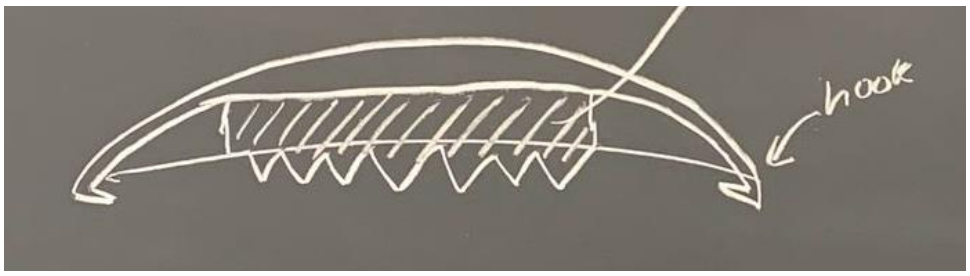

Figure 8: Ace Bandage Hook Design Preliminary Drawing

Manufacturing Method	Electrospinning	Cast Film	3D Printing	Additive Manufacturing	Total
Electrospinning	**X**	**1**	**1**	**1**	**3**
Cast Film	**0**	**X**	**1**	**1**	**2**
3D Printing	**0**	**0**	**X**	**0**	**0**
Additive Manufacturing	**0**	**0**	**1**	**X**	**1**

Table 14: Manufacturing Method Pairwise Analysis

There were four manufacturing methods that the team compared for the final possible option. These were electrospinning, cast film, 3D printing, and additive manufacturing. The pairwise analysis used to analyze them can be found in Table 14. The team rated additive manufacturing and 3D printing the lowest since they did not believe that they would be able to create refined scaffolds with the flexibility required to stay consistent with the movement of the UCL. Cast film was highly considered due to the large-scale manufacturing capability it has for the projects' purposes, but the team believed the design would be most capable of delivering a healing substance to the UCL if it had pores for the substance to seep out. Cast film would require these pores to be added to the cast films after their creations whereas the electrospinning method could allow for the pores to be added during the creation process. Electrospinning would also allow for many different materials to be used, and it is a quick process which would help the prototyping phase move quickly for the team which is important due to their time constraints. Therefore, electrospinning was decided upon on the manufacturing method for the scaffold.

Scaffold Design	Putty/ Gel	Multilayer Scaffold	Ravioli	Ridged Ravioli	Cleat	Hernia Mesh	Total
Putty/ Gel	**X**	**0**	**0**	**0**	**0**	**0**	**0**
Multilayer Scaffold	**1**	**X**	**0**	**0**	**0**	**1**	**2**
Ravioli	**1**	**1**	**X**	**0**	**0.5**	**1**	**3.5**
Ridged Ravioli	**1**	**1**	**1**	**X**	**0.5**	**1**	**4.5**
Cleat	**1**	**1**	**0.5**	**0.5**	**X**	**1**	**4**
Hernia Mesh	**1**	**0**	**0**	**0**	**0**	**X**	**1**

Table 15: Scaffold Design Pairwise Analysis

Six different designs were generated in the team's brainstorming process. Each design was presented in a post brainstorm discussion to determine the advantages and disadvantages of each design. This helped the team determine which one was best to move forward with. The team used a pairwise comparison chart to rank the designs against one another which can be found in Table 15. The putty/gel design entailed placing a soft gel onto the UCL as a soft malleable substance, but after interacting with the UCL, it would harden and cement itself in place. The gel design was ranked low due to its inability to deliver any form of growth factor to the UCL and since the design seemed more complicated for the surgeon compared to a single, rigid scaffold that simply needed to be attached to the UCL. The hernia mesh design would be a thin scaffold that would wrap around the edges of the UCL. The team ranked it low since it could not elute any form of growth factor overtime and because the team felt the design would be difficult to insert into the body. The multilayer scaffold design, which entailed using different layers of scaffolds which had different properties, was ranked low. Although the design had potential, the team felt other designs which were also multilayer scaffolds, such as the ravioli design, had clear advantages over this design. The ridged ravioli and cleat were ranked the

highest for their healing potential and ease of use. Additives can easily be incorporated into these designs to aid in the healing process of the UCL, and both designs simply needed to be attached to the UCL and either sutured or glued into place. The cleat design is also highly ranked due to the benefit that microneedles could give to the scaffold compared to the other designs. The microneedles attached to this design would allow for additives to be added into the ligament directly which the team thought was extremely interesting. They would also help the device stay in place ensuring that it does not slip away from the injured area. Finally, the ridged ravioli was given the highest score for a few reasons. The first being its ability to guide cell growth in the healing process. Ideally the ridges on the scaffold, see Section 4.5.3 for a visualization of the ridges, would guide cell growth towards the native orientation of the ligament itself. Also, the ravioli has an inner pocket that can be filled with a hydrogel seeded with healing additives or PRP which can elute out of the scaffold overtime. Lastly, the ridged ravioli can be designed in a way that allows for suturable material to be added along the edges, allowing for the device to be secured into place using current surgical techniques. Moving forward, the team decided to further inspect the viability of the top three designs, and this analysis can be found in Section 4.5.

Controlled Release Method	Dual Release	Multilayer w/o hydrogel	Hydrogel w/ nanoparticles	Multistage release w/ different g.f.	Total
Dual Release	**x**	**1**	**1**	**0**	**2**
Multilayer	**0**	**x**	**1**	**0**	**1**
Hydrogel w/ nanoparticles	**0**	**0**	**x**	**0**	**0**
Multistage release w/ different growth factors (g.f.)	**1**	**1**	**1**	**x**	**3**

Table 16: Controlled Release Method Pairwise Analysis

The brainstorming session gave the team four possible options for a controlled release method. The pairwise analysis for the controlled release method options can be found in Table 16. The hydrogel with nanoparticles was rated the lowest since the team believed that it would be difficult to consistently elute the nanoparticles out of the scaffold and believed the cost of the hydrogel could end up becoming too expensive for their budget. The multilayer method was next

which entailed using multiple layers of scaffolds which would have healing substances in between them. These substances would elute out as each layer degraded. The team believed this would be a good method of release but thought the healing effects of only a single growth factor between the two scaffolds may limit the healing capacity of the device. Therefore, the team came up with both the dual release and multistage release methods both of which include releasing multiple growth factors from a single scaffold. The dual release method was a multilayer scaffold which had two layers of growth factors to allow for more growth factors to be eluted from the scaffold over a longer period. Finally, the team rated multistage release with different growth factors the highest and plan to move forward with this release method. This method was better than the alternatives since it allowed for different growth factors to be applied to the UCL not only by eluding out of the scaffold, but through the outside of the scaffold simply contacting the UCL. This would allow the team to tailor the growth factor that the UCL is interacting with at each stage of the healing process. The team felt it would be the most effective and consistent method of controlled release, so the team moved forward with this design.

4.3.3 Material Analysis

To determine the best material or materials to use for our scaffold, we conducted a thorough analysis of many possible materials. The team examined both natural biomaterials and synthetic polymers as possibilities for the scaffold.

Collagen

Collagen is a natural polymer commonly found in connective tissue of mammals. There are 29 different types of collagen fibers and molecules that can be extracted from various animal donors. The most common places for collagen to be harvested are in bovine tendon and rat tail (Parenteau et al., 2010). Being that collagen is harvested from mammals, the material does well in vivo due to its familiarity with the extracellular matrix and regenerative cells. Type I collagen is mostly commonly used in implants because most patients do not suffer from allergic reactions towards it. Degradation rate for collagen depends on how it is processed. Degradation rate can be extended using methods such as chemical or physical crosslinking. While collagen is a commonly used and well tested material for biological scaffolds, upon communicating with BioSurfaces, a company with a commercialized electrospinning process, it was learned that collagen can prove difficult to electrospin compared to other biodegradable materials.

Chitosan

Chitosan is a natural biological material derived from chitin, an important material in fungi cell walls and crustacean and insect exoskeletons. It has a wide range of uses in biomedical applications including tissue engineering and drug delivery (Gond, 2020). It has high biocompatibility and is biodegradable. Chitosan and derivatives of it have played an important role in tendon engineering and tissue regeneration. It has been found to promote cell proliferation and integration while inhibiting fibroblast growth and prevent adhesion after tendon surgery. Chitosan derived scaffolds currently have poor mechanical function and require multiple additives to achieve the desired structural integrity and degradation rates. Advances in tissue engineering are required to improve chitosan enough to be usable as a scaffold material in tendon regeneration (Yan, 2017).

Gelatin

Gelatin is a naturally occurring protein derived from collagen, which is found in all mammals. It has many applications in tissue engineering and drug deliver as it can be used to create scaffolds and hydrogels with controlled drug and bioactive molecule release, different degradation rates, and different mechanical properties depending on the composite used. Using synthetic polymers with gelatin can improve its mechanical properties, leading to more applications for wound healing and tissue engineering. Gelatin hydrogels are useful for delayed drug delivery applications. Growth factors or drugs can be suspended in the hydrogel and as it degrades, they can slowly be released. Gelatin is a commonly used material with many applications in tissue engineering (Echave, et. al. 2017).

Elastin

Elastin is a structural protein found in the extracellular matrix of all mammals. Elastin is found in elastic tissue and is resilient and elastic. It is used in current biomedical research for tissue applications. It is important to develop an extracellular matrix that mimics those naturally found in the body. The structure of the ECM dictates both the mechanical and biological performance of the material (Sallach, Chaikof, 2008). Having the ability to mimic physical and biological properties of scaffolding materials allows for optimal regeneration of the human body. Elastin is found in extensible areas of the body such as the lungs, aorta, and skin. The flexibility

of elastin could have detrimental effects on the ligament as it heals. Elasticity is not good for ligaments since an elastic ligament cannot effectively transfer loads. It is possible that the ligament would contain some of the elastin from the scaffold after healing, leading to a more elastic ligament.

A combination of collagen and elastin is can be used in many biomaterial applications (Miranda-Nieves, 2017). Collagen provides strength, adding resistance to rupture while elastin provides the necessary elasticity to the material. Combining the two materials prevents deformation due to standard body function such as blood flow through vessels. Elastin and collagen have been combined in the past for the creation of tissue engineered blood vessels. Soluble collagen and soluble elastin can be electrospun to create a scaffold with high porosity and surface area.

Silk

Silk is a polymer naturally formed by silk moths, *Bombyx mori*. It is commonly used in biological applications due to its biocompatibility and mechanical properties. Silk has an ultimate tensile strength of up to 690 MPa and an elastic modulus of up to 17 GPa. These properties allow silk to be used for a greater range of applications than most natural polymers. Silk has been shown to slowly dissolve when implanted in vivo. Silk contains a glue-like protein call sericin that can lead to an adverse immune response. When this protein is removed however, silk has similar biocompatibility to other natural polymers (Altman 2003). Electrospinning silk has been studied for a variety of applications and intellectual property space regarding electrospinning silk is very limited (Zhou 2009).

PLGA

Polylactic-glycolic acid is a biocompatible synthetic polymer in the family of polyesters. PLGA is made by the combination of glycolic and lactic acid. This material is affordable, easy to work with as it can be molded or used in 3D printing applications, and is FDA approved (Kapoor, Bhatia, et al., 2015). PLGA is a biodegradable material whose degradation rate and crystallinity are controlled by the ratio of glycolic and lactic acid. The main drawbacks of this material are the acidic degradation products. The acidic byproducts produced by the degradation of the material can have adverse effects on surrounding tissue.

PLA

Polylactic acid (PLA) is a biocompatible synthetic polymer in the family of polyesters. PLA can exhibit various properties all based on the molecular weight and the copolymerization with different polymers (Tyler, Gullotti, et al., 2016). PLA is most used in 3D printing applications making the material not only easy to work with but also quite affordable. Being that PLA is so common, the material is FDA approved. PLA is a biodegradable material that can be tailored to any degradation rate based on the degree of crystallinity and copolymerization. The main drawback of this material is its acidic degradation byproducts. When PLA degrades lactic acid is released which can negatively affect surrounding tissue if implanted.

PLLA

The benefits of poly-L-lactic-acid (PLLA) were that it is 3D printing compatible, its degradation rate could be controlled, and it could be extruded in extremely fine varieties. PLLA can have extremely specific degradation rates when combined with other materials. The team specifically found an article stating that a mixture of 50% PLGA and 50% PLLA was able to create a scaffold that would degrade around approximately 4 to 6 weeks (Saito, Liao, Hu, et al., 2013). As for its negatives, PLLA leaves acidic degradation products in the body, and it alone has a long degradation time meaning it will almost certainly need to be combined with another material to meet our design specifications.

PCL

Polycaprolactone (PCL) was considered since it was 3D printing compatible, mechanically biodegradable, and modifiable by copolymerization. PCL is a very interesting material that the team thought could be very beneficial for the project. The possibility of degrading from a mechanical response from the body could be beneficial since it could allow the degradation time to be arbitrary if it would simply degrade once physical therapy began (Abedalwafa, Fujun, Wang, et al., 2012). There is also plenty of literature on the effects of blending the polymer with other materials which is very beneficial as it will allow the team to determine the best possible mixture of their specifications. The only issue they found was that the material does have a long degradation time on its own, so if the mechanical forces of the body were unable to degrade it, it may need to be removed through surgery.

PU

Polyurethane (PU) is a synthetic polymer with a microphase separated structure that gives it greater biocompatibility than other synthetic polymers. Polyurethane also has high mechanical strength compared to similar polymers. PU has poor cell affinity and is hydrophobic which decreases its use as a biological material. To compensate for these properties, PU is often combined with another polymer such as PEG or PET (Wang, 2012). PU has commonly been electrospun for use in biological scaffolds.

Zein

In recent years zein has gained significant traction in its use for biomedical applications. Zein based composites have been studied for tissue and bone regeneration, drug delivery, and wound healing. Zein is a beneficial material for the body as is has been found to be both biocompatible and biodegradable with its main limitation being its mechanical strength. Zein is a renewable natural source, as it is derived from corn, making it economically feasible as well. Zein itself is a major storage protein located in corn endosperm (Fereydouni, Movaffagh, et al., 2021). It can be extracted and processed in numerous different ways such as mechanical elongation, antisolvent precipitation and electrospinning. Each processing technique has very different outcomes, giving zein a wide range of applications (Demir, Ramos-Rivera, et al., 2017).

Specifically for this project, electrospinning of zein fibers was considered. When electrospinning zein, numerous different parameters can be altered that impact properties such as the density of the material. Also, by using electrospinning to process zein, drug and other biological additives can be spun directly into the final product as a means of creating a controlled drug delivery device. Zein has proven to be an effective drug carrier and has been studied in recent advancements of nano-therapeutics. When zein is placed into the body it provides the beneficial characteristics of being resistant to microbial attacks, as well as fostering cell attachment and proliferation (Demir, Ramos-Rivera, et al., 2017).

4.3.3 Final Material Choice

After discussing the various aspects of all the materials introduced in the brainstorming session and consulting our partners at BioSurfaces, the team decided on a PLGA scaffold with an internal Zein layer. Both options have been FDA approved and used in many drug delivery applications which were important requirements in the decision process. PLGA was selected due to its range of erosion times, biocompatibility, mechanical properties, and known ability to

deliver controlled release of small molecules. This gave the team a strong outer layer for the scaffold which could also be adjusted through the electrospinning process to whichever degradation properties or porosity that was required. A Zein layer was also added to the design due to Zein's biocompatibility, and its ability to absorb and hold material. The hope for the design is that the inner Zein layer will be able to hold and store PRP, and in doing so, increase the carrying capacity of the scaffold.

4.4 Preliminary Designs

From the brainstorming session, the team was able to determine three designs to further research to determine the best option for the final design. The preliminary designs that will be analyzed are the ravioli design, the cleat design, and the ridged ravioli design. All these preliminary designs came from the brainstorming session explained in Section 4.1 and to learn more about the other preliminary designs which were considered see section 4.1.1.

4.4.1 Ravioli

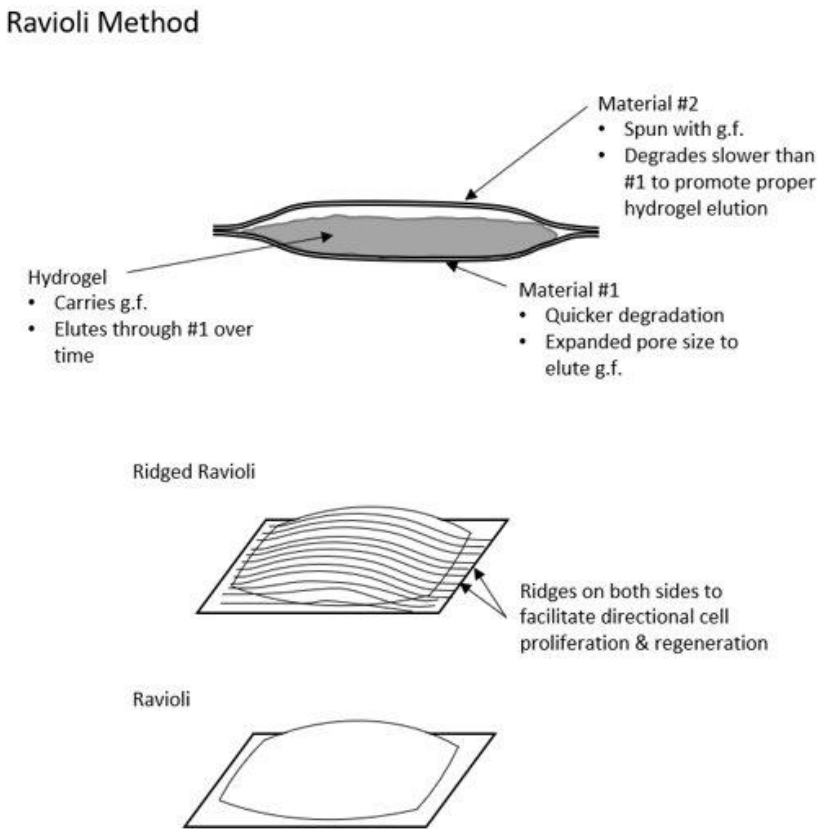

Figure 9: Ravioli Design Preliminary Drawing

The first preliminary design is the ravioli design, and an image of it can be seen in Figure 9. It entails creating a scaffold which contains two layers of electro spun sheets supersonically welded together along the perimeter of the two scaffolds. This will give the scaffold an open pocket in the middle of the two layers which can be filled with a growth factor induced hydrogel or PRP. The possible growth factor insertion methods will be reviewed in Section 4.5.4. The growth factor or PRP inside of the scaffold will gradually seep out of the scaffold overtime. This will allow the scaffold to heal the UCL injury throughout its entire life cycle. The scaffold will be anchored to the tissue surrounding the UCL using sutures which will attach to the welded perimeter of the scaffold to prevent the sutures from piercing the pocket in the scaffold holding the growth factor infused hydrogel. The purpose of this design is to create a scaffold which can surround the UCL and will gradually release a growth factor or PRP throughout its life cycle in hopes of promoting the most growth possible in the UCL.

4.4.2 Cleat

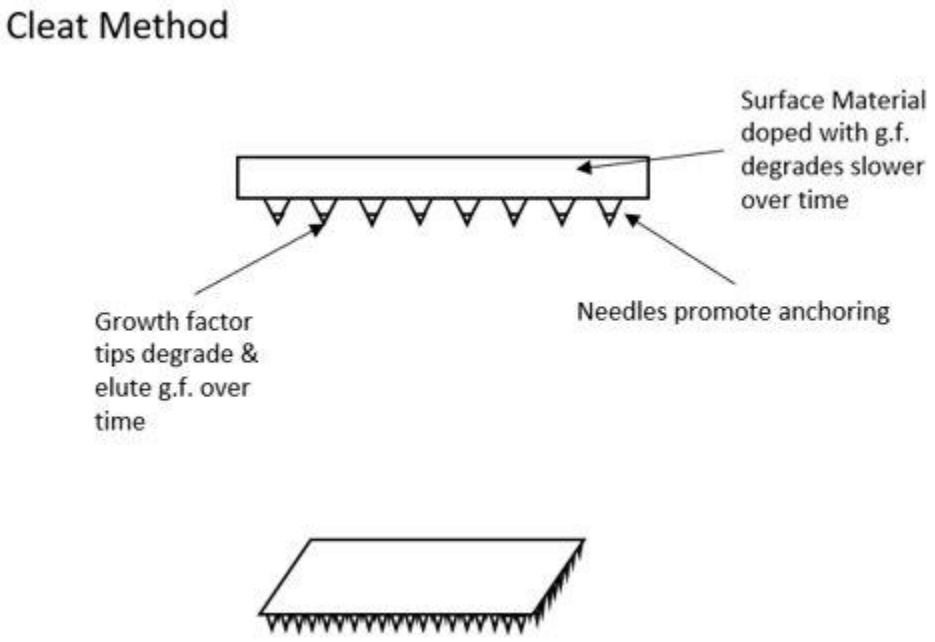

Figure 10: Cleat Design Preliminary Drawing

The cleat design uses ridged microneedles to attach the scaffold on the UCL. This entails first creating the scaffold and then molding the microneedles onto the bottom of the scaffold through a separate process. The scaffold in theory would be able to be pressed into the UCL along with an adhesive to ensure a secure fit. With the scaffold in place, the microneedles would elute a growth factor or PRP stored inside of the scaffold, inserted using insertion methods which will be explain in Section 4.5.4, directly into the UCL overtime. The team thought that a design like this could be very beneficial but through some initial research it was discovered that microneedles did not have nearly enough strength to survive the forces that could be applied on the scaffold (Tomono, 2019). Ultimately, the team determined that the weak nature of microneedles would make them too inconsistent for the scaffold, so the team decided to move forward without this design.

4.4.3 Ridged Ravioli

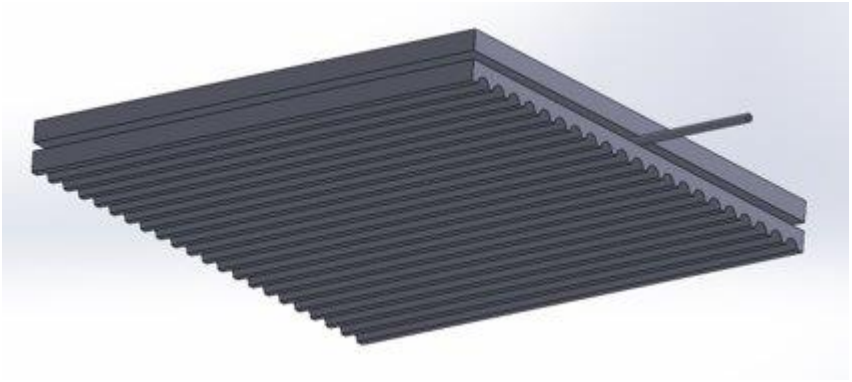

Figure 11: Ridged Ravioli Desi1gn Preliminary Drawing

The ridged ravioli design is in essence the same design as the ravioli design except it is altered to allow ridges to be formed on the bottom layer of the design, see Figure 11. These ridges will help guide the growth of the UCL towards the native orientation of the ligament. The design was thought of as an upgrade to the ravioli design as it has the same features, but it also attempts to align the direction of healing to hopefully make it more effective. To learn more about the design see Section 4.5.1. This design may entail a more complex and expensive manufacturing method due to the custom aspect of these ridges compared to the normal electrospinning process which was considering for the final design decision considering the limited amount of time that was available for the project.

4.4.4 Growth Factor Insertion Method Analysis

With the final design conceptualized, the team needed to determine the best method of inserting PRP into the scaffold. These insertion methods were created with PRP in mind as the growth factor that would be used. Three methods were considered: a plastic valve, a one-way patch of addition electro spun material, and adding a syringe-accepting needle or tube in between the two scaffolds prior to the welding process. All of these will be described in this section in order to explain the reasoning for the team's final decision.

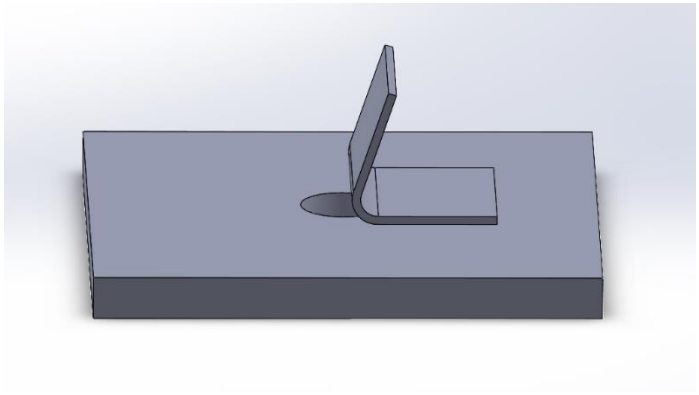

Figure 12: Plastic Valve Preliminary Solidworks Drawing

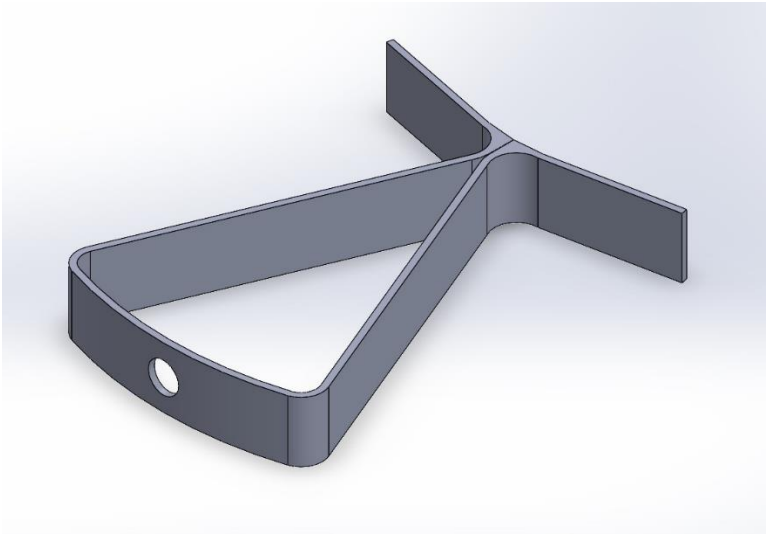

Figure 13: One-way Valve Preliminary Solidworks Drawing

The plastic valve, shown in Figure 12, was considered because the team believed the design would be extremely effective at allowing for the surgeon to easily insert PRP without disturbing the rest of the scaffold. The design is held closed through tension built up between the two arms of the device. However, these two arms could easily be spread apart by a syringe pressing in between them which would allow the doctor to inject a growth factor. The two arms would then close after the force applied by the syringe holding them apart was removed ensuring none of the growth factor This led the design to be abandoned.

Next is the one-way flap design, see Figure 13 for an example, which entailed attaching a smaller piece of scaffold material over a hole on the bottom layer of the scaffold. This thin piece of material would be placed inside of the chamber that would be holding the PRP, and it would be attached to the scaffold in three locations using the same welding method that would be used to attach each layer of the final scaffold together. To insert PRP into the scaffold, the surgeon would maneuver a syringe into this hole past the flap and inject the PRP. Once the PRP was inserted into the scaffold, it would be held in by the flap folding over itself, after the syringe exited the scaffold, effectively blocking the whole. This design did have some issues however. The team was afraid of this method would be too difficult since it may be difficult to insert a syringe into this small hole without puncturing the scaffold. We were also afraid that even if the surgeon correctly inserted into the syringe it may puncture the flap on insertion ruining its ability to hold the PRP inside of the scaffold. These limitations led the team to brainstorm a design that would work for the final device using the knowledge they had gained from the first two designs.

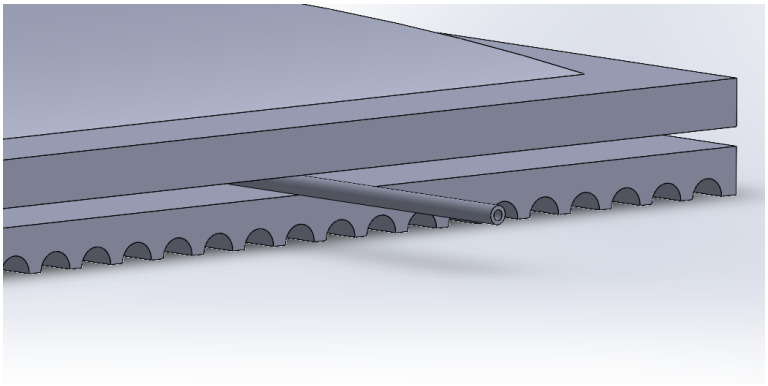

Figure 14: Insertion Tube Preliminary Solidworks Drawing

The final method the team considered, shown in Figure 14, was simply adding either a tube large enough to accept an 18-gauge syringe between the top and bottom layer of the ravioli design. An 18-gauge needle was decided upon because Dr. Magit explained that it was the smallest syringe that could be used to extrude PRP. The team realized that since the top and bottom layers already must be connected in some way that a tube could be placed between them. This was very beneficial since it would have minimum interference with the structures of each layers since it would not need to be added during the electrospinning process as some of the other designs needed to. It also allowed for the easiest insertion technique compared to all of the

other options the team felt. The method would be very consistent, and it would be extremely simple to close the hole created by the tube using biostaples.

5. Final Design and Verification

The final scaffold was generated from the Ravioli design that was outlined above. This design was chosen through our design matrix shown in Table 17 as it was believed to provide the best drug release profile and degrade over the desired time frame for recovery. Once the final design was decided upon, an agreement was created with Biosurfaces to use their electrospinning equipment to make prototypes of the scaffold. These prototypes were then tested using four different experiments which will be further explained in the next section.

Design Matrix	Provide Mechanical Strength	Low Cost	Short Return to Play Time	Easily Implantable	Reproducible	Promotes Healing of the UCL	Total
Putty/ Gel	1	2	5	2	2	5	17
Multilayer Scaffold	4	3	5	4	3	5	24
Ravioli	4	4	5	5	4	5	27
Cleat	2	3	5	3	1	5	19
Hernia Mesh	4	2	5	2	2	5	20

Table 17: Scaffold Design Matrix

5.1 Final Design

The scaffold, shown in Figure 15, was created with two electrospun PLGA sheets. In order to create these sheets PLGA was dissolved in an organic alcohol-based solvent. The solution was then electrospun onto a 167mm diameter mandril at a 15cm gap distance and 21kV for 60 minutes. The thickness of the sheets was measured to be 0.106mm with a fiber diameter ranging between 700 and 900nm. These sheets measured 2.0 x 1.0 cm each and were ultrasonically welded together across the entire perimeter at 1.0 mm from the edge of the scaffold leaving an open slot at the top to form the scaffold with the internal pocket. Zein, a 20kDa structural protein present in maize endosperm cells, was procured from Sigma-Aldrich. A 40% (w:v) Zein solution

was prepared in an organic alcohol solvent and electrospun onto a 167mm diameter mandrel at a 15cm gap distance and +21kV for 300 minutes. Material thickness ranged between 250 -350um. Porosity was not measured. Fiber diameters ranged between 700-900nm. In the slot, the electrospun Zein segment 1.5 x 0.5 cm was inserted will contain the growth factors, such as PRP or TGF-β, that are intended for the therapeutic effect of the scaffold. The slot end of the scaffold will be sealed using ultrasonic and tack welding in accordance with the rest of the scaffold. The therapeutic agent, PRP, will be inserted by puncturing the scaffold and administering the PRP through an 18-gauge needle as shown in Figure 16. The hole created by the needle will be sealed using a biologically compatible glue such as fibrin glue (Brennan, 1991).

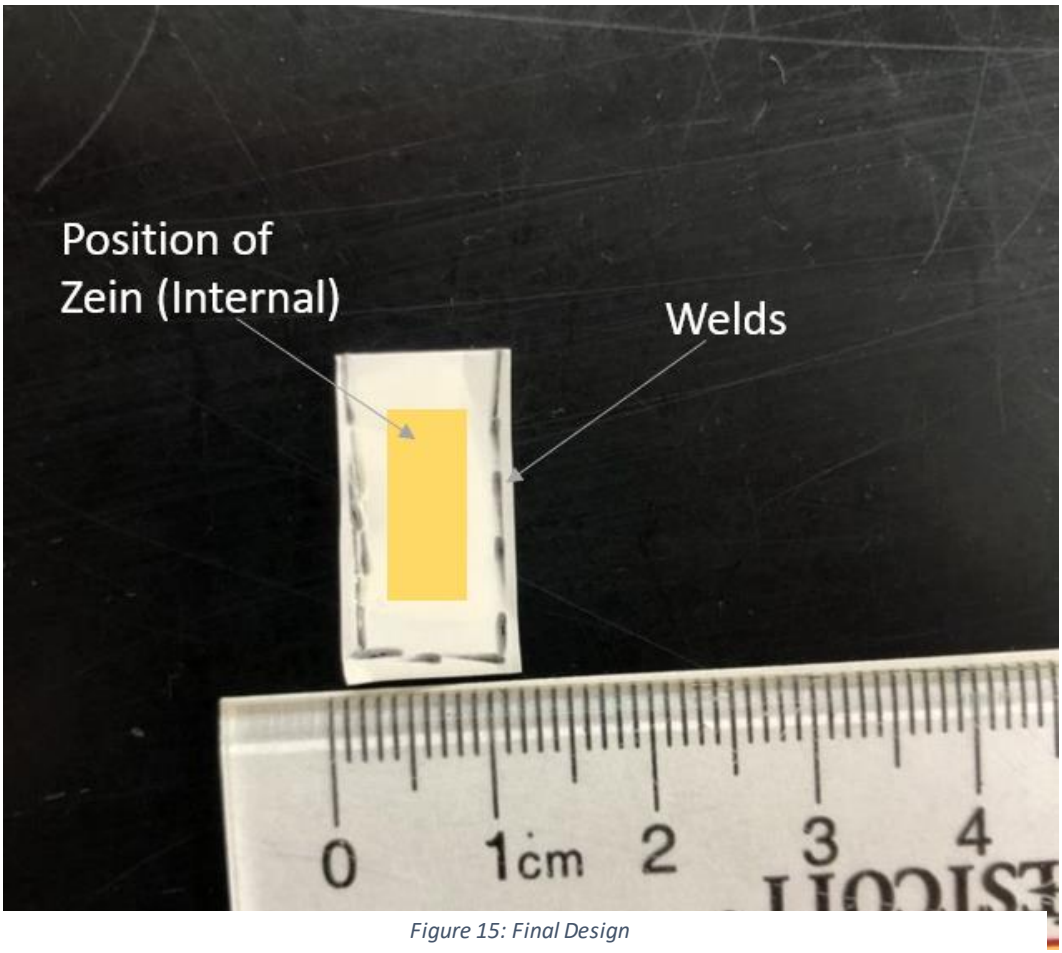

Figure 15: Final Design

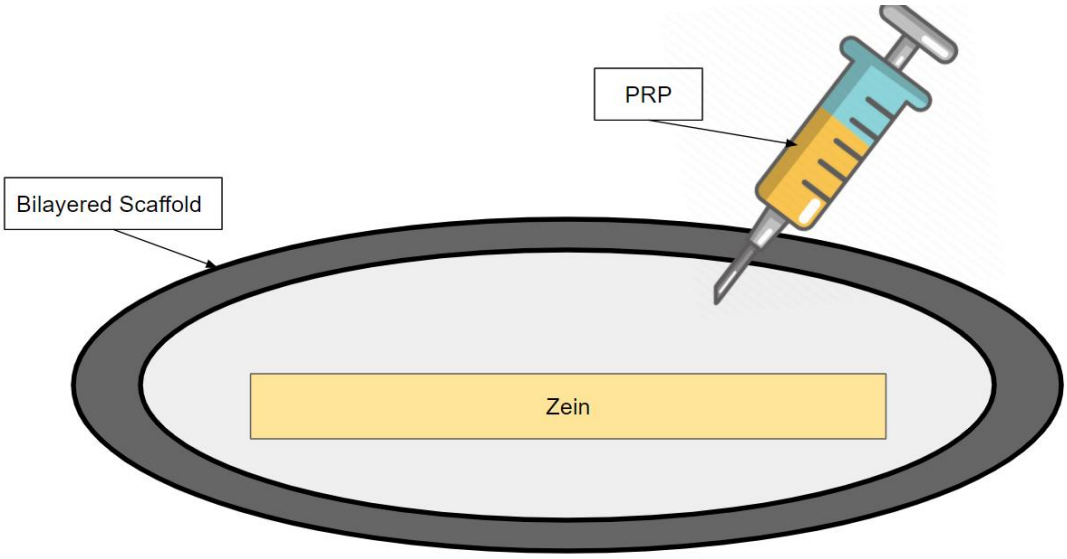

Figure 16: PRP Delivery Schematic

5.1.1 Implantation Procedure

The scaffold can be implanted during a minimally invasive surgical procedure on grade I and II ligament tears. The surgeon would need to only need to expose the UCL itself instead of the entire elbow joint as one would need to for Tommy John's Surgery. Once the UCL was exposed the scaffold will be implanted onto the UCL either through suturing, biological adhesives or biostaples. After proper fixation to the UCL the area used in the procedure would be closed and the patient would rest for 1-3 weeks. During this resting period is when the scaffold would elute the therapeutic agent. Due to the biological environment the scaffold will be subjected to, PRP will elute through the nanopores within the electrospun scaffold.

5.2 Validation Testing

For all experiments listed below, electrospun material provided by BioSurfaces was used. The scaffolds were composed of electrospun PLGA with half of the scaffolds used in the elution study filled with electrospun zein, a plant protein. It should be noted that prior to experimentation on electrospun material from Biosurfaces all the following tests were practiced on sample materials. This was done to confirm the test methods' accuracy, and to ensure none of the limited material from Biosurfaces was wasted due to issues with the test methods.

5.2.1 Mechanical Tests

The purpose of mechanical testing was to test the effectivity of the scaffold's anchoring method and confirm that the scaffold's properties would not alter with surgical manipulation. Therefore, two different Instron test methods were design and implemented to these attributes of the scaffold: a tensile test combined with a three-point bending test, and a suture pull-out test. The initial plan for the three-point bending test, the protocol for which can be found in Appendix C, as to record a loading and unloading force versus displacement curve and analyze the curves for permanent damage to the scaffold. This would have been performed by reviewing the differences between the integrals of loading and unloading curves to determine the amount of energy that was lost between the cycles and the variation between the maximum load of the initial cycle and the final cycle. However, it was determined that due to the scaffold's inability to consistently resist the force being applied, a consistent curve could not be recorded by the Instron. Therefore, it was decided to combine the three-point bending test with a tensile test. This was done by running half of the sample scaffolds through the three-bending test prior to the tensile test and compare their tensile test results with scaffolds that did not receive any form of bending load to evaluate differences in each scaffold tensile properties and ultimately the scaffold's ability to withstand bending. The scaffold's mechanical properties were also analyzed using the UTS values recorded from this test to confirm its ability to withstand the forces it could experience in the elbow. Finally, the anchoring method, or suture pull out strength, was tested by pulling a suture out of the scaffold at a consistent rate and recording the maximum force of the test to determine the maximum pullout force of the scaffold. All the tests will be expanded upon below.

The team created their three-point bending test method using ASTM Standard F2606 as a template (ASTM, 2014). It was chosen since it was a similar three-point bending test method, but it was conducted on heart stents meaning the method needed to be altered to function on our electrospun scaffold. Prior to beginning the test, the span length, or distance between supports, and the maximum deflection of the experiment were calculated using the length of the scaffold and equations found in the ASTM methodology. Using these equations, it was determined that the test's span length would need to be 15mm, and the maximum deflection would be 3.2mm. Once this was determined, new Instron fixtures were design and 3D printed by the team, see Figure 17, as the three-point bending fixture available in WPI's laboratory was not precise

enough for span length needed for this test. With the fixtures created a 50-cycle cyclic loading Instron method was created which deflected the scaffold 3.2mm each cycle at a rate of 0.25 cm/min. Due to the scaffold's low resistance to force, the same preload used in the ASTM test method could not be applied to this test, so instead visual confirmation of contact was used to ensure the Instron was contact the scaffold prior to beginning the test. This lack of resistance also led the scaffold to fall out of the test fixture during the cyclic loading, so a small amount of glue was attached to the top fixture to ensure the scaffold was consistently bending in the mid-point of the two bottom fixtures. After the three-point bending test was completed, the scaffolds that had undergone it were prepared for the tensile test.

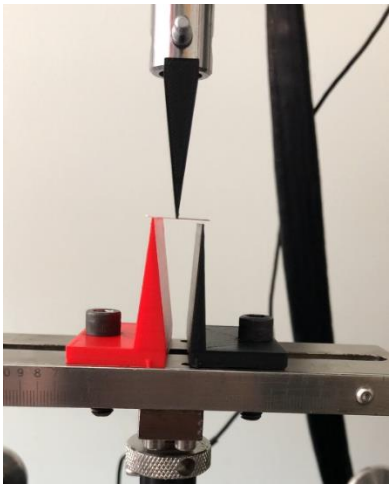

Figure 17: Three Point Bending Test setup with Custom Fixtures

The first step of the scaffold tensile test entailed attaching each side of a prototype scaffold to the Instron's load cells using the Instron's jaws that are then tightened using an Allen wrench, see Figure 18. Before any of the tests began, the dimensions of the scaffolds, width, length and height, were inputted into the Instron method created by the team to allow the Instron to calculate the stress and strain of the sample throughout the test. The scaffold was then pulled taught with a preload of 0.5 N, and the displacement was zeroed. After this was completed, the scaffold was stretched at a rate of 0.25 cm/min until the force being measured by the Instron drops by 60%, or the scaffold visibly breaks. This test method was then repeated on two control scaffolds, which had not been previously mechanically loaded, and two scaffolds that had undergone the previously mentioned bending test method for the team to get a baseline for the material properties. This gave the team the ability to compare the differences in properties

between scaffolds that had been heavily bent and those that had not been. This test method was informed by ASTM Standard D638 – 14 (ASTM, 2014).

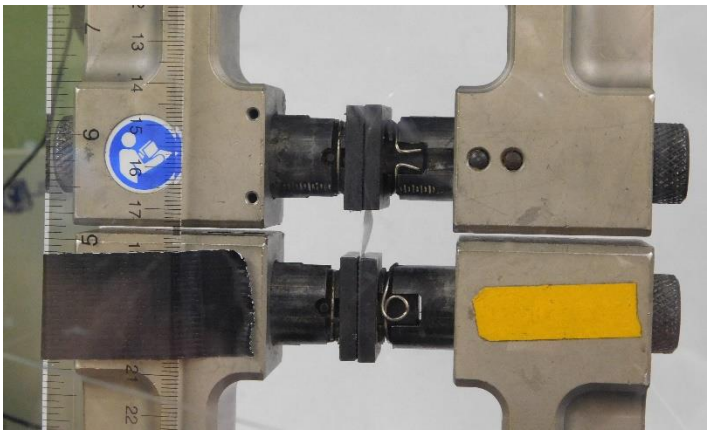

Figure 18: Tensile Strength Test Setup

The anchoring method was tested by suturing the scaffold, securing the scaffolds and the sutures to the Instron Jaws as seen in Figure 1, and finally performing a tensile test. To keep the suturing technique consistent, the team asked their advisor, Dr. David Magit, to perform the suturing for the samples that were tested to ensure there was no issue in the suturing technique and to ensure consistency between the samples. Before they were anchored into the Instron, the suture ends of the suture not attached to the scaffold were taped together and rotated 360 degrees five times, see Figure 19, to ensure the sutures were loaded consistently. Once the ends were secured, a preload of 0.3 N was applied, and a tensile test was run at a rate of 0.25 cm/min to find the max force it took to dislodge one of the suture's attachment points from the scaffold. The sutures were pulled out of the scaffold on both its vertical and horizontal axis to ensure there was no difference present between the two orientations: see Figure 20 for an example of each orientation. This will be used to verify the scaffold's ability to stay implanted in the body post insertion. This test method was informed by a similar experiment performed on Hernia Meshes to determine their suture pull out strength. (Ibrahim et. al, 2018).

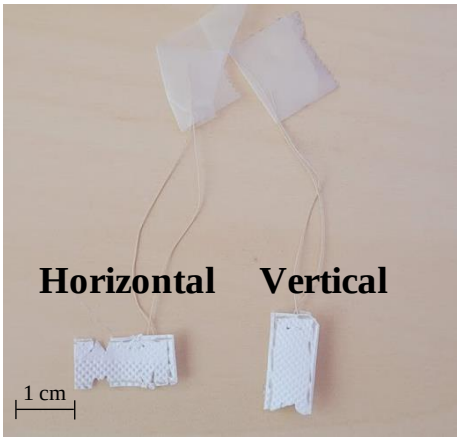

Figure 21:Horizontal and Vertical Examples

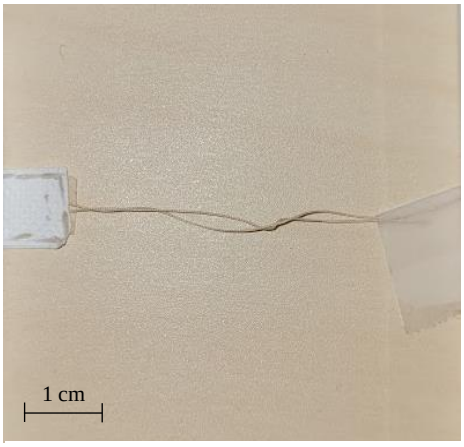

Figure 20: Suture Pullout Sample Example

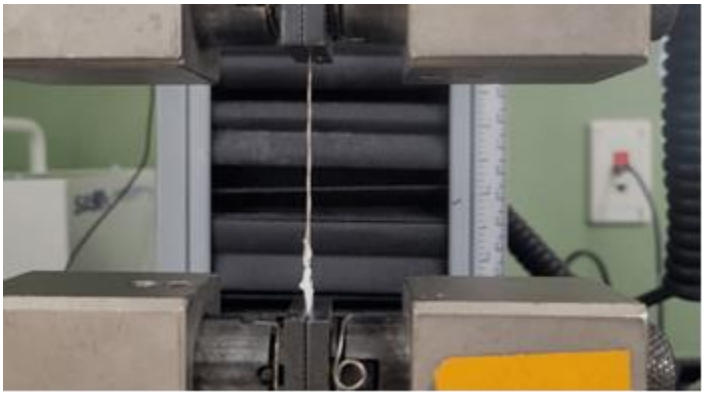

Figure 19: Suture Pullout Test Setup

5.2.1.1 Mechanical Testing Results

A custom MATLAB function was created to analyze the results of both the tensile tests and the suture pullout tests. The function required the type of test and the excel sheet of the data to generate a graph, and it used the max function to determine and record the max values of each curve. It then plotted these values as red circles onto to each respective plot. The graphs created by the function for each of the tests can be found in Figures 22-24, and the entire MATLAB script can be found at Appendix A. It should be noted that in Figure 22 samples 3 and 4 underwent the bending test method prior to the tensile test method whereas samples 1 and 2 only underwent the tensile test method.

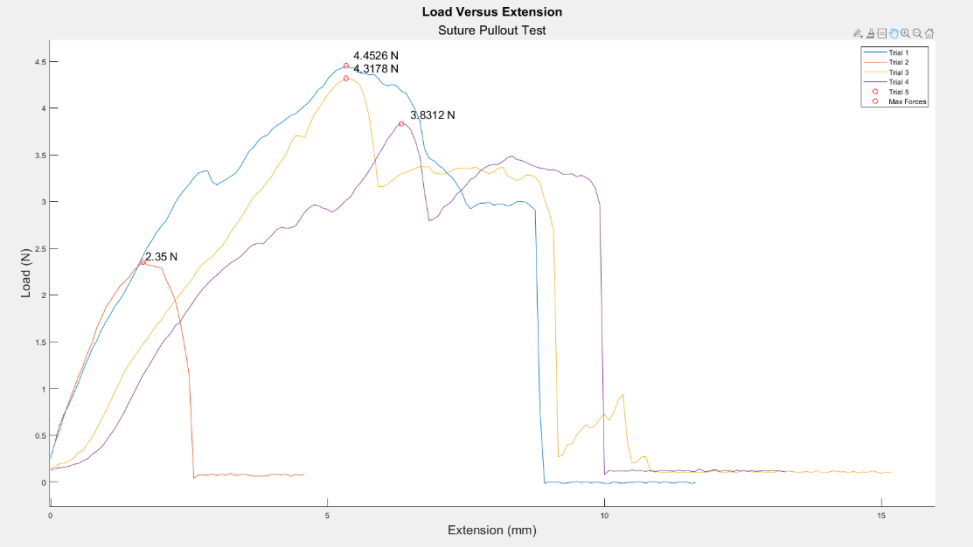

Figure 22: Tensile and Bending Test Results

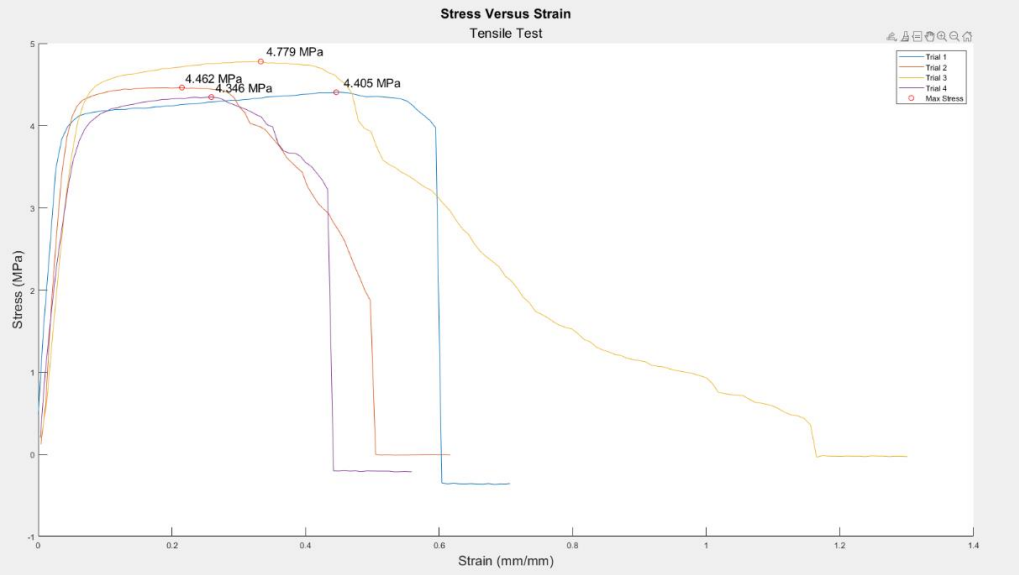

Figure 24: Vertical Suture Pullout Results

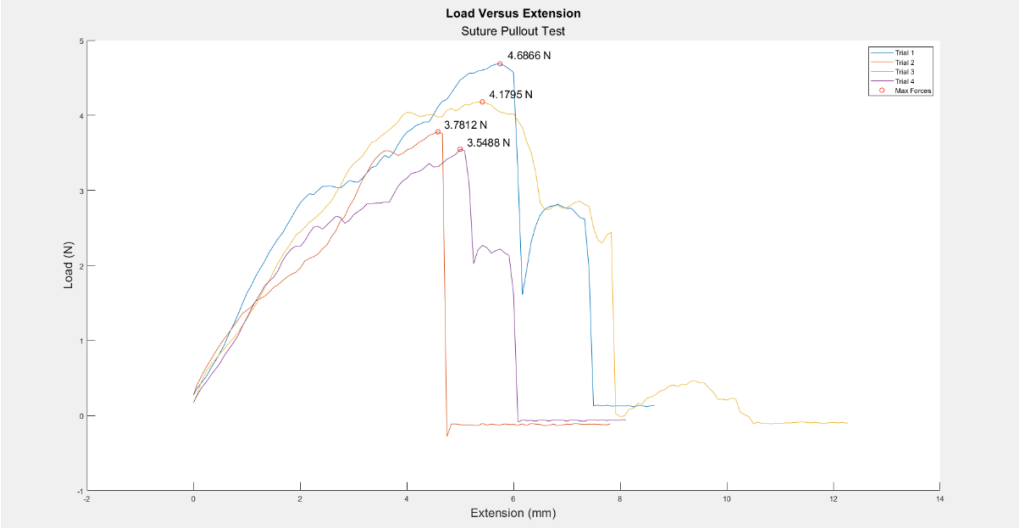

Figure 23: Horizontal Suture Pullout Results

Using the maximum values found by the MATLAB function, the following results were concluded. Ffor the combined tensile and bending test, the team found that the average maximum tensile stress, or UTS, of the non-mechanical loaded scaffolds was 4.434 MPa and the average UTS of the scaffolds that had undergone the bending test was 4.563. Dividing the average bending test UTS by the average UTS of the unbent scaffold showed that the UTS of the scaffolds that had undergone bending were on average 2.91% higher than the UTS of the scaffolds that did not undergo the bending test. For the suture pullout test, the team found that

the average suture pullout force was found to be 3.89N, which was converted to 7.78 N/mm for the 0.5mm length of the scaffold.

5.2.2 Elution Testing

The purpose of drug elution testing was to determine if the release of either PRP or growth factors from the scaffold could occur in a controlled manner. The main objective of the test was to ensure that the scaffold prototype could release growth factor sized particles at the desired rate to invoke a healing response at the site of the injury.

The scaffolds used for testing were split into two groups: scaffolds were filled with a hydrogel loaded with protein and scaffolds filled with zein soaked in water containing protein. An n of two was used for the scaffolds from each group. The hydrogel and pieces of zein were included in the scaffold to slow the release of growth factors from the scaffolds. The protein used for this experiment was soybean trypsin inhibitor due to its comparable size (20kDalton) to many common growth factors.

The soybean trypsin inhibitor was taken out of the refrigerator and brough to room temperature. 10 mg was weighed out and placed into a borosilicate test tube. 1 mL of PBS was added to the test tube and the solution was mixed gently. 500µl was removed from the solution and placed into a second test tube. 15.1µl of DyLight488 was added into the 500µl soybean trypsin inhibitor solution and mixed gently. The tubes were capped and wrapped in tin foil then allowed to sit for 1 hour at room temperature. While the dylight and protein were reacting, a ring stand and clamp was set up. A PD-10 column was secured to the ring stand. The tip of the column was cut off and the excess solution was drained into a plastic container and disposed of. 3mL of PBS was added to the top of the column in order to rinse it. This occurred 3 times.

After the protein and dylight had finished reacting, the solution was added to the top of the column. The solution was collected in 7 test tubes, with each test tube being used to collect 1mL of solution. 200 µl was removed from each test tube and placed into adjacent wells of a 96 well plate. The Spectramax M2 plate reader was used to read the plate at a wavelength of 275nm and again at a wavelength of 488nm. The samples with the highest absorbance at a wavelength of 275 contained the protein tagged with the dylight and were used for the rest of the experiment. The samples with high absorbance at a wavelength of 488nm but not at a wavelength of 488nm contained only free dylight and were disposed of. The remaining samples were pipetted into the

top of 15mL conical tube containing a 10k centrifugal filter unit. The conical tube was centrifuged for 3 hours at a speed of 3000 rpm.

Remove the cap from the top of a 10k centrifugal filter unit and pipette the combined solution into the upper reservoir. Place the cap back onto the unit once done. The solution remaining above the filter unit was extracted and placed into a microcentrifuge tube. The filter unit was rinsed with 150 µl of PBS which was also extracted and added to the microcentrifuge tube. The total volume in the microcentrifuge tube was around 200 µl.

A Lowry protein assay was run in order to determine the concentration of protein within the solution. Once the concentration of the solution was determined, the solution was diluted into 2.5 mL of PBS. The resulting solution had a protein concentration of 1017.24 µg/mL. 100 µl of this solution was added to each of the two scaffolds containing zein. 100 µl of the same solution was mixed with 100 µl of alginate and 100 µl of calcium chloride in order to make an alginate hydrogel. The solution was injected into the each of the two scaffolds not containing zein and allowed to sit at room temperature for 20 minutes to ensure that the aqueous solution had gelled. A control hydrogel formed using only 100 µl of alginate and 100 µl of calcium chloride was injected into a 5th scaffold. After the hydrogels had been given time to form, all 5 scaffold were placed into microcentrifuge tubes. 5mL of PBS was added to each tube and the tubes were wrapped in tinfoil. The tubes were then placed on a revolver and the revolver was inserted into an incubator set at 37 degrees Celsius.

At timepoints of 24 hours, 48 hours, 72 hours, 96 hours, 7 days, 10 days, and 14 days, .5mL of the PBS supernatant sample was removed and stored in a microcentrifuge tube in the fridge. .5mL of new PBS was added back into the microcentrifuge tubes containing the scaffolds. Once the trial was completed the supernatant samples were pipetted into a dark 96 well plate. The plate was run on the Spectramax M2 platereader at an wavelength of 488nm. A solution with a known conentration of protein was used to create a standard curve. The line of best fit obtained from the standard curve was used to determine the concentrations of the samples based of the respective absorbances obtained using the plate reader.

5.2.2.1 Elution Testing Results

After the fluorescence of the samples obtained from the drug elution study was measured, a standard curve was created to determine the corresponding concentration to each fluorescence value. The standard curve can be seen below in Figure 25.

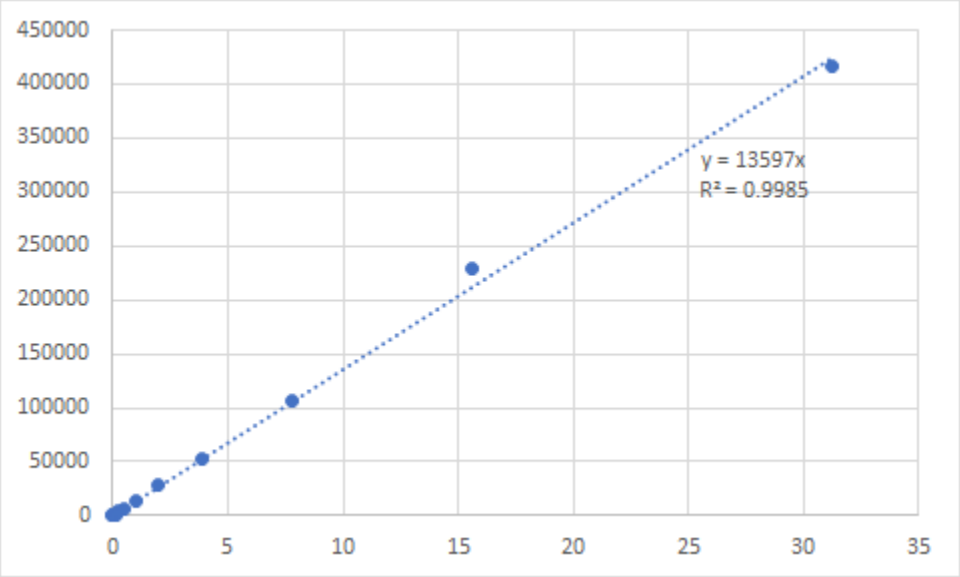

Figure 25: Fluorescence Standard Curve

The equation created by the standard curve was y = 13597x where y was the fluorescence of the sample and x was the concentration of the sample in micrograms. Using this equation, the concentrations of the samples was calculated as shown below in Table 17.

Hydrogel with protein 1			Hydrogel with protein 2			Zein pouch 1			Zein pouch 2		
Absorbance	Background	Concentration	Absorbance	Background	Concentration	Absorbance	Background	Concentration	Absorbance	Background	Concentration (ug/mL)
134912	134693	9.906	139362	139143	10.233	742207	741988	54.570	582799	582580	42.846
32114	31895	2.346	31130	30911	2.273	107245	107026	7.871	69683	69464	5.109
10525	10306	0.758	10190	9971	0.733	17285	17066	1.255	20169	19950	1.467
5015	4796	0.353	3979	3760	0.277	8222	8003	0.589	10411	10192	0.750
3653	3434	0.253	2378	2159	0.159	5862	5643	0.415	7902	7683	0.565
2185	1966	0.145	6202	5983	0.440	4697	4478	0.329	1448	1229	0.090
1927	1708	0.126	1088	869	0.064	4244	4025	0.296	5621	5402	0.397

Table 18: Drug Elution Results

Protein continued to elute out of the scaffold for all 7 days of the experiment. There was an initial bolus release of protein on the first day of the experiment followed by 6 days of decreasing protein elution. The release of protein was on average higher in the scaffolds containing zein than the scaffolds containing an alginate hydrogel on days 1-5 and again on day 7. The absorbance of one of the zein scaffolds on day 6 appeared to be an outlier which may be the cause of the drop in average elution from the zein filled scaffolds on day 6 of the experiment. The protein elution over time was graphed and can be seen below in Figure 25.

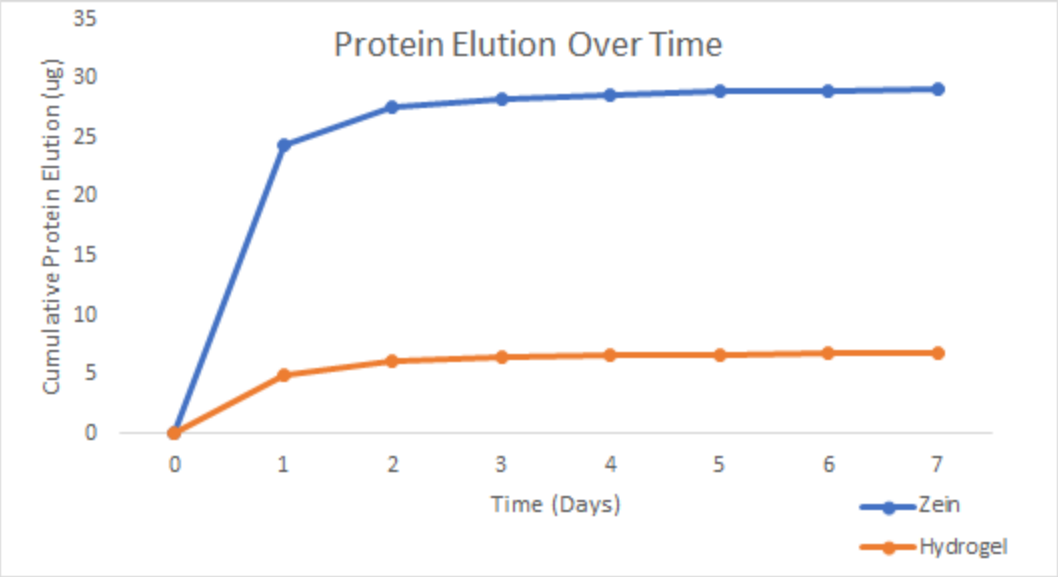

Figure 26: Cumulative Drug Elution

5.2.3 Cytotoxicity Testing

Cytotoxicity experiments were run on the chosen scaffold materials to validate the material biocompatibility, ensuring that there are no adverse reactions within the body. Cytotoxicity is often one of the first tests to be run in vitro to determine biocompatibility of a sample device. It is a fast, cheap, and standardized method of determining if a device has harmful extractables that will negatively impact cells in the body. To test cytotoxicity, a mouse fibroblastic cell line will be used instead of human cells. For this, the team utilized NIH-3T3 cells. The team followed the testing protocol outlined in ISO 10993-5.

Prior to working with the prototype scaffold's materials, a few practice trials were conducted to determine the best methodology and optimal seeding density for the experiments. Initially cytotoxicity testing was run using the fluid extractables methodology. For this the mouse fibroblastic cells were plated into six well plates and incubated for 24 hours to allow for cell attachment. In this initial trial, the cells were exposed to the test material through fluid extracts. To obtain these fluids, the test materials and control were placed in separate culture media and were left to incubate for 24 hours at 37°C. After incubation, the fluid extract was applied to the cultured monolayer of mouse fibroblastic cells, in place of the original culture media. The plate was then incubated at 37 ± 1ºC in 5 ± 1% CO2 for up to 3 days. Over this incubation period, the cells were periodically examined for any visible signs of toxicity. This experimental methodology was not used as after the 3 days in culture, the wells containing liquid extracts from

the latex were still healthy and proliferating at a standard rate. Latex is known to kill cells in culture, so it was clear that the methodology was not properly testing the cytotoxicity of our materials. During this time, the team also ran a few trials at different initial seeding densities. It was ultimately decided that an initial seeding density of 10,000 cells per well was ideal as the cells would reach the 75% confluency on day 3 when the experiment was ending. After initial testing the direct exposure methodology was chosen to run final experimentation.

To begin final experiments the NIH-3T3 cell line was grown in culture using proper cell culture techniques. These cells were then passaged and allocated into six well plates with an initial density of 10,000 cells per well. The six well plates were placed in the incubator at 37 ± 1ºC in 5 ± 1% CO2 for 24 hours to allow for adhesion to the bottom of the plate. During this incubation period the material samples were prepared. The two materials being evaluated in this experiment were PLGA and ZEIN as they were chosen for the final scaffold design. Latex (Fisher Scientific, cat# PMID148060) was used as a negative control as it is known to effectively kill all cells in culture. Sample wells were also run with no additional materials and 10% FBS media as a positive control, as cells were expected to grow as normal in these wells. Three samples of equal size were cut for each material. The samples were cut to cover approximately one tenth of the well area. The samples were cut using a hole punch with a diameter of 7mm, making circular samples with a total area of approximately 38mm^2. After being cut they were placed under UV light for 8 minutes per side inside a culture hood to sterilize them before being added to the cells.

After the initial 24-hour incubation period the cells were removed from the incubator and brought into a sterile hood. The media for each well was exchanged for fresh media and a material sample was laid gently in the center of each well. A piece of PDMS was then added on top of the material to weigh it down and prevent it from floating around in the culture media. The plate was then incubated again for 24-hours at 37 ± 1ºC in 5 ± 1% CO2. After incubation, the cells from each plate were imaged and evaluated under the microscope. Each well was imaged three times at 10x magnification using an Inverted phase contrast lab microscope. These images were later analyzed and averaged together to determine a daily cell count for each well. This incubation and imaging procedure was then repeated every 24 hours until the cells of the negative control reached approximately 75% confluency. On the final day, the cells were lifted from the plate and counted to obtain a final cell count for each well.

The images were analyzed using imageJ software to obtain cell counts for each day the plates were left in incubation. Daily cell counts allow for an understanding of cell proliferation and if the materials had any negative impacts on cell growth.

5.2.3.1 Cytotoxicity Testing Results

As described in the protocol, three images of each sample well were taken every 24 hours throughout the experiment, shown in Table 19 below. These images were used to analyze overall cell health and compare cellular proliferation rate between samples. Image J software and Excel were used to analyze the results from the cytotoxicity experiments. Examples of the cell images taken each day are shown below in table 18.

	Control	Latex	ZEIN	PLGA
24 Hours		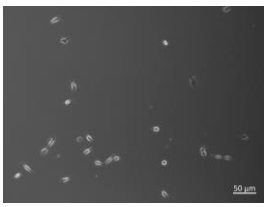	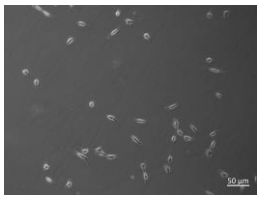	
48 Hours	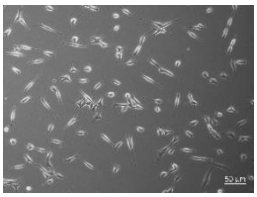	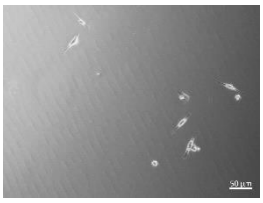	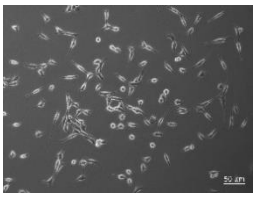	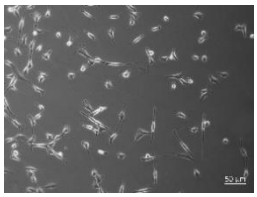
72 Hours	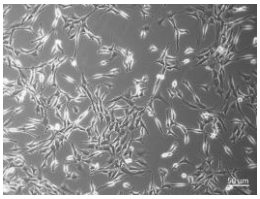	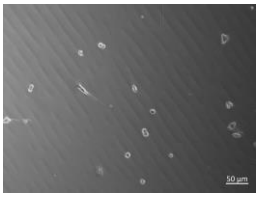	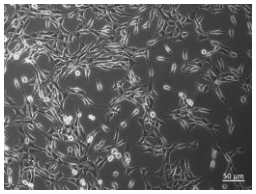	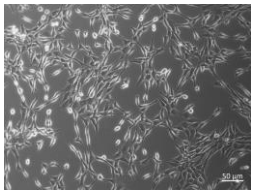

Table 19: Cytotoxicity Results

The number of cells in each image were counted using ImageJ software. To do this, each image was individually uploaded, and the multipoint tool was used to go through and count each cell. The total number of cells was recorded from each image and the three counts for each well were averaged together. This was done to get a total cell count for a well on each day. To get a total cell count for the well, the count found from the images was multiplied by the ratio of the well area to the area of the image. To do this, the area of the well itself was calculated by

measuring the diameter of the well and using the standard area of a circle equation. The area of each image was found using imageJ. The length of the scale bar seen in the image was measured in ImageJ and converted from pixels to micrometers. Once the scale on the image was set, the area of the image was found and a ratio of the size of the image to the size of the plate was calculated. The average cell count from each day was then multiplied by this ratio to find the total cell count per well. This was done for two trials of cytotoxicity testing. The cell counts from the two trials were averaged together and plotted to compare the cell counts between the different sample materials. The graph of this cell count is shown in Figure 27 below.

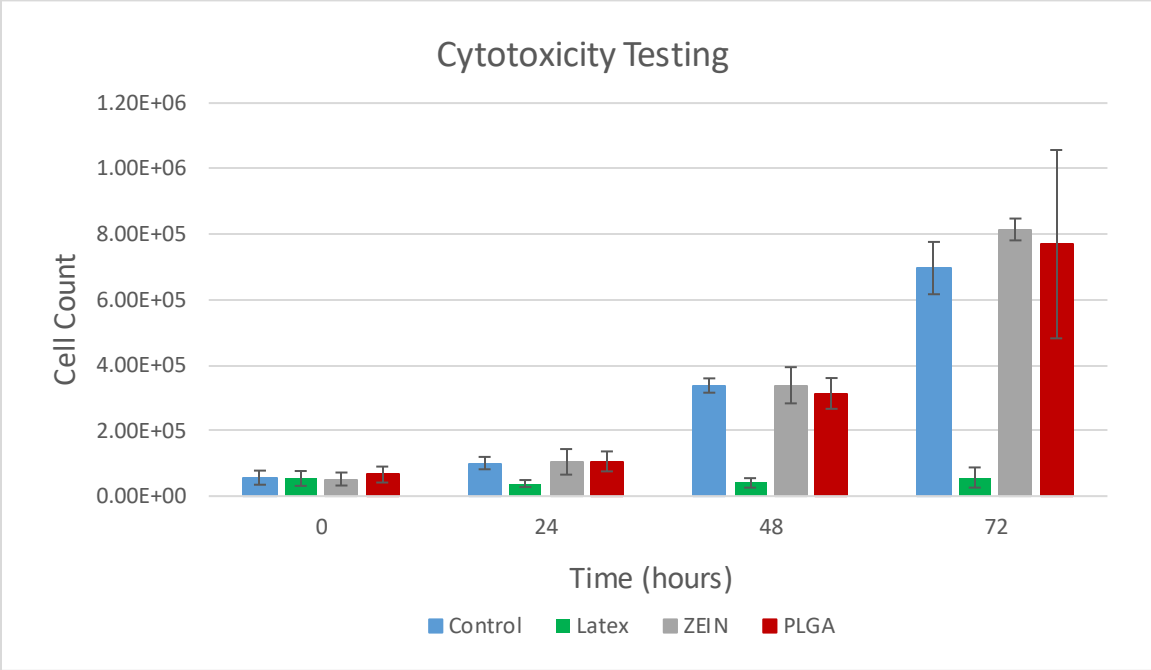

Figure 27: Cell count averages on each day of experimentation

An ANOVA single factor analysis was run on the data shown in the Figure 26 using Excel. No significant difference was seen between the sample materials. The only significant differences were seen when comparing the latex samples. This was expected as the latex was used as a negative control, as it is known to kill cells in culture. For this experiment, a p-value less then 0.05 indicated that there was a significant difference between the sample groups. If the p-value was larger than 0.05, it could not be concluded that a significant difference exists. One comparison was run between the positive control and the two sample materials. The p-value for this comparison was greater than 0.05, indicating no significant difference between the cell

growth in these samples. For this comparison the null hypothesis, that there's no difference between the means was accepted. Another comparison was run between the negative control and the sample materials. The p-value for this was less then 0.05, indicating a significant difference between the cell growth of the samples. For this comparison the null hypothesis was rejected as a significant difference between the means was identified.

5.2.4 PRP Validation Testing

To ensure that the PRP testing protocol works and produces relevant results, a validation test was run. Culture medium prepared with varying levels of fetal bovine serum (FBS) was used to culture NIH 3T3 cells derived from mice. FBS is a similar substance to PRP that is commonly used in cell culture. Normal culture medium was prepared with 1% Glutamax, 1% Penn/Strep, and brought to 10mL with DMEM. FBS was added to this basal medium at a concentration gradient as follows: 0%, 0.2%, 0.5%, 1%, 3%, 5%, 7%, 10% with 0% being the negative control and the 10% being the positive control. NIH 3T3 cells were seeded at 10,000 cells/well in a 24-well plate. Each concentration ran in triplicates and were imaged on days 1, 3, 5, 7. Cell proliferation was analyzed using ImageJ. By using this validation testing, the protocol for the bioactivity testing was confirmed and ready to implement.

5.2.5 PRP Bioactivity Testing

Once validation testing proved that the protocol works and there were no procedural changes to be made, a PRP bioactivity test was run to determine the effect of PRP on human fibroblastic cell proliferation. Approximately 30mL of whole blood was withdrawn from one healthy adult using two 15mL syringe and a butterfly needle provided in the Arthrex Angel PRP kit. These two syringes were then placed in a Hettich Zentrifugen Rotofix 32 A centrifuge and spun at 15g for 5 minutes to collect a total of 10mL of PRP. Once the PRP was obtained, a freeze/thaw cycle was used to process the sample for testing. This cycle lyses the platelets within the PRP that harbor growth factors such as PDGF, TGF-B, and VEGF. The lysing cycle started by placing the PRP in a -80C freezer for 24h. Then the sample was thawed in a 37C water bath for 1h. The freezing was repeated and then thawed to use the sample (Rubin, 2017). Sample was spun at 2000g for 10 minutes and filtered through a 0.22um syringe filter to filter out the lysed platelets. A concentration gradient of PRP was added to a 0.2% FBS culture media at the following concentrations: 0%, 0.2%, 0.5%, 1%, 3%, 5%, 7%, 10%. By keeping the concentration

of FBS at a small, consistent value, we were able to see the effects of PRP knowing that the cells will be in healthy environment. CRL 2097, human fibroblastic cells were cultured according to proper cell culturing techniques then seeded in triplicates on a 24-well plate at 200 cells/uL at 500uL of cell suspension per well and 1mL of each culture media was administered to these cells. Wells imaged on days 1, 2, and 4 and cell counts were taken on each day using ImageJ.

5.2.5.1 PRP Bioactivity Testing Results

As per the protocol, three images of each sample well were taken on days 0, 1, 2, and 4. These images were used to analyze cellular proliferation over time. ImageJ software and Excel were used to quantify the results. Cellular proliferation was analyzed much like the cytotoxicity data. Cell counts were taken of each image using ImageJ software. Each image was individually uploaded, and the multipoint tool was used to count each cell. Only full, visible cells were considered countable cells to standardize the procedure. The total number of cells was recorded from each image and the three counts for each well were averaged together. This was done to get a total cell count for a well at each time point. To get a total cell count for the well, the count found from the images was multiplied by the ratio of the well area to the area of the image. To do this, the area of the well itself was calculated by measuring the diameter of the well and using the standard area of a circle equation. The area of each image was found using ImageJ. The length of the scale bar seen in the image was measured in ImageJ and converted from pixels to micrometers. Once the scale on the image was set, the area of the image was found, and a ratio of the size of the image to the size of the plate was calculated. The average cell count from each day was then multiplied by this ratio to find the total cell count per well. The graph of this cell count is shown in Figure 28 below.

An ANOVA single factor analysis was run on the data shown in the Figure 27 using Excel. Two statistical tests were run on; one was run between the PRP samples and the other was run on the PRP samples versus the positive control. The null hypothesis for both of these tests was that there would be no statically meaningful differences in the data. For this experiment a p-value less than 0.05 indicated that there was a significant difference between the sample groups. If the p-value was larger than 0.05, it could not be concluded that a significant difference exists. The first comparison run was between all the PRP samples. This resulted in a p-value that was greater than 0.05, thereby failing to reject the null hypothesis. The next test was

run on the PRP samples against the positive control. Again, a p-value greater than 0.05 was recorded which fails to reject the null hypothesis that there would be no statistically meaningful differences in the data.

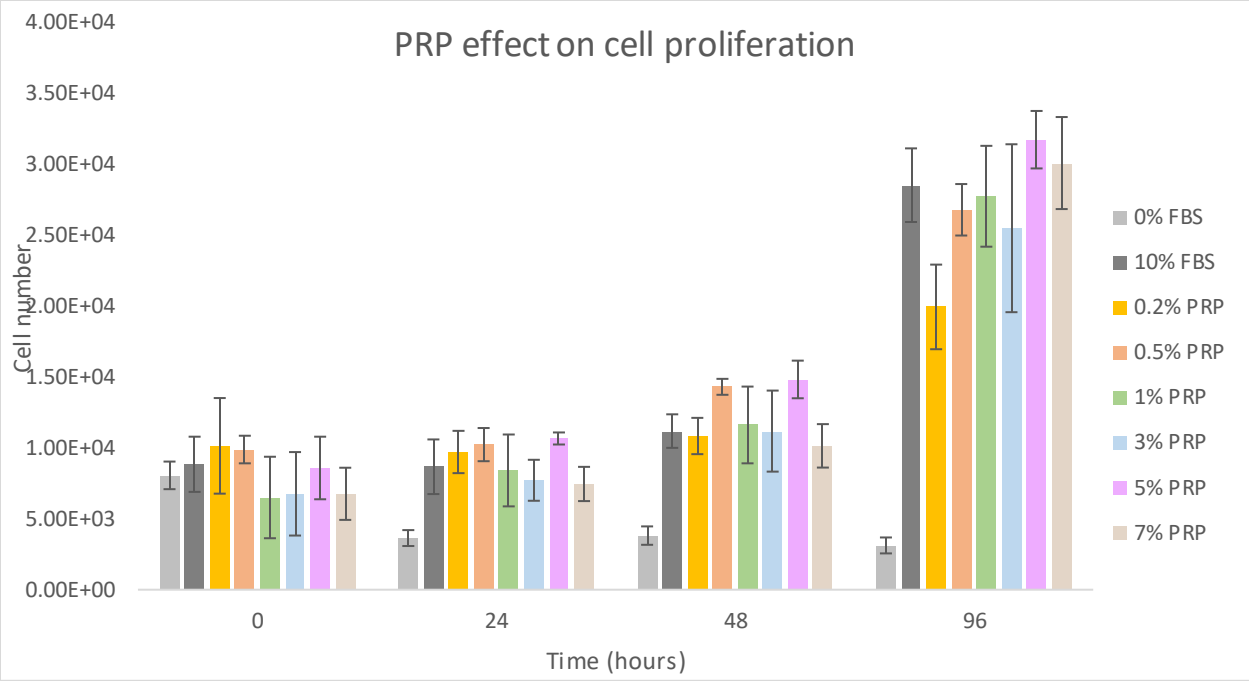

Figure 28: Cell counts over time

6. Discussion

6.1 Mechanical Testing Discussion

Through analysis of the combined three-point bending and tensile test results, the team found that the average maximum tensile stress, or UTS, of the non-mechanical loaded scaffolds was 4.434 MPa and the average UTS of the scaffolds that had undergone the bending test was 4.563. Both of these averages were nearly triple the control UTS for electrospun PGLA scaffolds: 1.438 MPa (Jiu, 2012). The large difference between our values and the control is either due to differences in the electrospinning processes between the scaffolds or due to issues in the stress calculations completed by the Instron Blue Hill Software. Either way the results still initially show that the scaffold's design does not hinder the material properties of the individual PLGA scaffolds, but it should be noted that the since the sample size for this test was so low that the results can only be viewed as initial trends, and not representative of the entire possible population of scaffold.

Since there was only a 2.91% difference in UTS between the scaffolds that underwent a bending test and those that had not, it can be initially concluded that bending, or surgical manipulation, will not impact the mechanical properties of the scaffold. Although it seems that the bending test is increasing the tensile strength of the scaffolds, it is more likely that the perceived increase in UTS is only due to the variability between the small number of samples. As seen in Figure 29, the small difference between the groups could be due to the small number of samples, 2, and may not be representative of the entire possible population of scaffold.

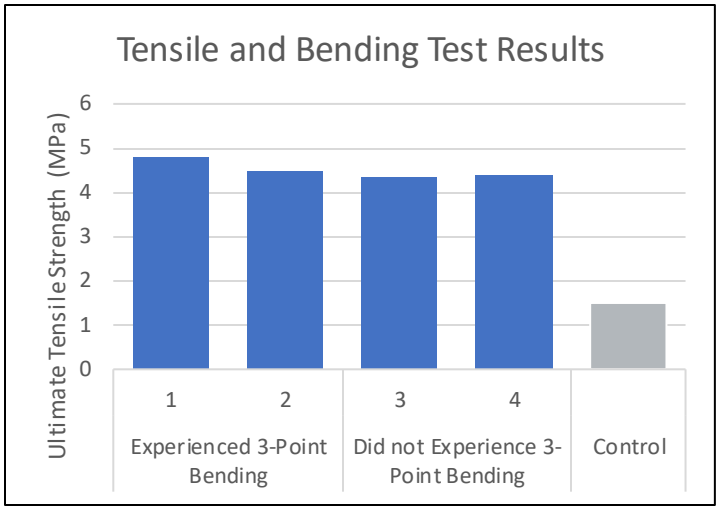

Figure 29: Tensile and Bending Results

The UTS was also compared to the forces the scaffold could experience in the body to confirm if it will fail under these forces. From Section 2.2 Biomechanics of the UCL, the UTS of the UCL itself is 13.77 MPa (Smith, 2018), and the UCL consistently must resist approximately 125 N (Dustin, 2015). For reference, the average load the scaffold was able to withstand was approximately 11N, and the UTS was approximately 4.5 MPa both of which are lower than the UCL's properties explained above. Although the scaffold's properties seem low, it is believed that whichever final anchoring method that is designed for the device will be able to absorb the excess forces which the scaffold cannot. Therefore, it is hypothesized that the scaffold will be able to withstand the forces being applied.

The average suture pullout force was compared against the desired suture pullout force of 10 N/mm for similar electrospun materials found in the literature (Norowski et al., 2012). This demonstrates that the scaffold's suture pullout force was approximately 20% lower than the desired suture pullout force of 10N/mm. The lower suture pullout force could possibly be the result of the two layers scaffold being welded together and not being consistent spun together throughout the total width. Either way, it is clear that in its current iteration, especially with the premature failure, that suturing will not be an effective anchoring method for the final device. Also, between the two orientations there was seemingly no real differences between the suture pullout forces, so it can be initially concluded that the force is consistent regardless of orientation. It should be noted however that one of the sutures in the vertical method failed

prematurely by exiting the scaffold through the connections between the sutures instead of being pulled until it breaks through the edge of the scaffold leading the suture pullout force to be far lower than the other samples, an image of which can be seen in Figure 30. Due thone of the sutures prematurely failed, suturing alone does not seem like an effective anchoring method for the final design.

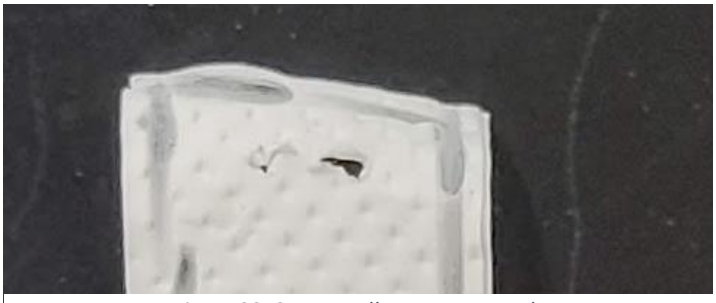

Figure 30: Suture Pullout Test Example

6.2 Drug Elution Testing Discussion

One of the main intentions of the drug elution assay was to ensure that the scaffold can release a biological additive in a controlled manner over time. The time frame highlighted by the team to monitor was the first 7 days after implantation as this coincides with the inflammatory and early proliferative stages. The results of the experiment showed that the scaffold was able to release a growth factor surrogate for at least 7 days after implantation into the body. One the last day of the study, there was still a noticeable amount of protein eluted from the scaffold. This indicates that the scaffold likely can continue to elute protein past the 7-day benchmark. The results indicate that zein may be a more suitable filling for the scaffold than an alginate hydrogel as more protein was released from the zein filled scaffolds on 6 out of the 7 days.

Additionally, the amount of protein eluted on all 7 days of the trial were above the amount of growth factors found to produce an increase in cellular proliferation *in vitro* (Scherping, 1997). If the soybean tryspin inhibitor used in the trial was replaced with growth factors it is believed they would elute at a similar rate, suggesting the scaffold could produce an increase in cellular proliferation in vivo. An important consideration is that overdosing of growth factors can have negative effects on healing and may increase risk of cancer cell formation. To

ensure that growth factor levels due not reach this level in the body, further testing will be necessary to narrow down the ideal amount of growth factors to inject into the scaffold.

For future testing, the same protocol can be used for a 21-day study rather than a 7-day study. This length would cover the inflammatory and proliferative stages of healing. A 21-day duration would likely also cover the large of protein elution from the scaffold, with any remaining protein eluting out as the scaffold degrades. Before the device can be used for clinical trials, animal testing will need to be conducted. Animal testing will give greater insight into how the biological additives added to the scaffold will affect in vivo cell proliferation. As there has been little literature published relating to the sustained release of therapeutic agents over time, the results may prove more informative than current studies performed *in vitro*.

6.3 Cytotoxicity Testing Discussion

The purpose of the cytotoxicity experiments was to determine if the materials selected for the device would negatively impact the growth of cells in culture. If the materials had a negative impact on the cells in culture, it would be expected that they also elicit a negative immune response within the body. From this initial device testing, the materials did not impact the growth of cells in culture compared to those grown in 10% FBS media.

The main limitation with this experiment was that the samples were difficult to keep on the plate. The device itself is thin so that it can be placed within the body. In terms of testing, the light weight of the materials made it so the samples would easily float in the media. This was recognized in preliminary testing and as a solution each sample was weighed done with a small piece of PDMS. This served as a temporary solution but in the future, it would be beneficial to find an alternative solution to this problem. Another limitation to this experiment was budgetary constraints. The protocol outlined in ISO-10993-5 included numerous different assays, such as an MTT assay that could be run to collect results. Due to budgetary constraints the team did not have the funds to obtain the materials to run more complex assays. Instead imaging and cell count was used for the experiment. This allowed the team to complete initial testing and gain a general idea of the materials toxicity but for further testing, the results can be collected in a different way. Another potential source of error was introduced with the sample materials. These materials were placed under UV light for sterilization but were not produced in a sterile environment so they could have potentially introduced some type of bacteria to the cell culture.

6.4 PRP Bioactivity Testing Discussion

PRP bioactivity testing was done to determine the effects of PRP on cellular proliferation in vitro and if PRP was a viable therapeutic agent for the device. If it was shown in this study that PRP would not induce cell proliferation, it is assumed that PRP would not work as a therapeutic in vivo. Overall, the results of the study show that all concentrations of PRP did have a positive effect that either rivaled or bested the 10% FBS positive control.

As mentioned in the results, a single factor ANOVA analysis was run on the PRP samples against themselves and against the 10% FBS positive control. Single factor ANOVA statistical analysis attempts to compare the means of multiple samples. After this test was run, it was clear that there were no significant differences between the samples in either test. The lack of meaningful significant differences in the data can likely be attributed to the high variation in the cell counting procedure used to analyze cell proliferation. Manual cell counting introduced human error as some images were not totally clear. The protocol tried to mitigate these differences by averaging out the cell counts of three separate images of each well. The high standard deviations and statistical analysis showed that to quantify this data more accurately, a fluorescent assay such as a BrdU ELISA would have been best suited to analyze cell proliferation. The reason why this assay was not run was due to time and budgetary constraints. Although the proper PRP concentration could not be statistically proven, an overall trend in the data suggests that the PRP did have a positive effect on cell proliferation.

6.5 Impact Analysis

For this project, the team performed an Impact Analysis to relate our project to prominent global concerns. It is important to look outside the scope of what our device directly affects, and attempt to analyze its reaching and indirect effects on global concerns. We address the impacts our device may have on economics, the environment, society, politics, as well as ethical concerns and potential issues our device could have in terms of health and safety, manufacturability, and sustainability.

6.5.1 Economics

It is important to consider the influence a new product will have on the current economy. Injuries are common in athletics, and UCL injuries are one of the most common (Gleiber, n.d.). The average cost of recovery from a UCL injury in the MLB between 2004 and 2014 was $1.9

million per player and in total amounting to $395 million (Meldau, 2020). This shows that a great deal of revenue is lost to injuries. If the average recovery time for an injury is reduced, this revenue loss can be minimized and athlete salaries can be increased, marketability of the device will be increased, and there will likely be an increase in jobs in the medical device industry.

At this point it is impossible to determine what exactly this device will cost, so it is difficult to define the economic impact of the device due to its cost directly. One of the goals set for the device is to lower the cost of a UCL repair surgery, which can cost between $10,000 and $26,000 (Magit, 2020). If this goal is achieved, it will be made more accessible to non-professional athletes who may need it, which could increase the overall revenue from UCL repair surgeries.

6.5.2 Environmental Impact

No large environmental impacts are expected. The device and the materials used in it and its packaging will not harm the environment more than other devices or materials used for similar applications if disposed of and handled properly. Very little waste should be produced by the product, mostly due to packaging materials. Proper disposal of waste from this product should be encouraged and clearly described on or in the packaging of the final product. Sterilization of the product could raise concerns about environmental impact, as certain methods, such as EO sterilization, can be harmful to the environment (Sharpless, 2019).

6.5.3 Societal Influence

Decreasing the cost of UCL repair procedures will increase accessibility of the treatment, allow more people who may not be able to afford the procedure to get it. The simplicity of our device will also decrease the invasiveness of surgeries and the time it takes to perform the surgery, enabling more procedures to be performed. In addition, this novel product has potential for applications in many other types of injuries, including rotator cuff repair, knee injuries, and other tendon or ligament damage.

6.5.4 Political Ramifications

The political ramifications of this product will likely be negligible. It is possible that this new product will affect biomedical research or global health through increased accessibility.

Major League Baseball is a large industry but changing how a specific injury related to the sport is handled will likely not affect the political impacts the sport currently has.

6.5.5 Ethical Concerns

Designing and testing our product may lead to ethical concerns rising from use of human cell lines and human blood samples, but because the device will rely on autologous blood samples to obtain the PRP, there is no ethical concern with the function of the device. The sourcing of some materials used may raise some ethical concerns since some are human and animal derived. Since our final product will not need to undergo the same type of testing, these ethical concerns will be nullified. However, our device must also be tested in both small and large animal models to fully determine efficacy, raising another ethical concern. It is important to be sure that the device is effective and safe before it is used in humans.

6.5.6 Health and Safety Issues

Health and safety concerns are inherent in tissue engineering. There are risks of contamination between manufacturing, delivery, and implantation. It is important that the device remain sterile through these phases. These processes will be designed to minimize the risk of contamination. This product was designed with the patient's health in mind. Our product will increase the health and safety of patients with UCL issues. We have no reason to believe that our device will pose any more health risks than current practices or products used in similar procedures.

6.5.7 Manufacturability

One of the main goals of this project was to produce a device that can easily be manufactured in high quantities. BioSurfaces has control over many variables surrounding the electrospinning process, giving them the ability to create electrospun materials within small windows of variability. The voltage used, gap distance between needle and mandril, mandril diameter, and time spent electrospinning can all be measured and kept at constant values, allowing for production of a product with the same characteristics for high volume scaffold production. By electrospinning large sheets of both PLGA and zein and cutting out the scaffolds from the sheets.

6.5.8 Sustainability

Plastics and other types of medical packaging waste are a contributor to declining global health. Our device will utilize sterile packaging for delivery which will be discarded upon use of the product. In addition, sterile syringes, needles, and sutures will be used for delivering PRP to the device and device insertion which will all have packaging materials that will be discarded as waste after opening. Our product will likely not change the amount of waste generated during a UCL procedure, so its impact on the environment will likely remain the same as it currently is. The zein portion of the scaffold is made from corn and is a highly sustainable material. However, the main component of the device, PLGA, is petroleum derived. In the future we hope a more renewable solution for medical device packaging will be discovered, as well as for petroleum derived materials.

7. Conclusions and Recommendations

A novel electrospun bilayer PLGA and zein implantable mesh with a flexible structure that allows us to control the release of therapeutic agents was developed and tested meeting required specifications. This successful project details a novel concept for ligament repair.

7.1 Recommendations

7.1.1 Further Mechanical Testing

As for the three-point bending and tensile test, the team suggests that further fatigue testing should be done in the future to confirm that the initial results are representative of the entire population of potential scaffold as for the suture pullout test, the team suggests that either new materials be researched and experimented with which have higher suture pullout forces or a new innovative anchoring solution be developed (Liu, 2012). The main idea the team has for a new anchoring method would attaching the scaffold to a larger electrospun sheet which would still fit in the incision dimensions of the surgery but allow for far more suture to attempt and account for the lower suture pullout force.

The team also highly suggests that for the project moving forward more in-depth studies are performed to determine the exact forces the scaffold may undergo inside of the body. The specifications used for the scaffold were concluded based on adapting similar tests, but none of them were specific to the scenario the scenario will truly be in as the idea of a scaffold that attaches directly over the UCL is such a novel idea that the real studies that must be completed to determine the force the scaffold may undergo have never been conducted. The team suggests that a model, such as the one used in the MQP "A Dynamic Elbow Flexion Simulator for Cadaveric Testing of UCL Injury and Reconstruction.", be created and used to test different possible loading scenarios for the scaffold. This would allow for a far greater understanding of the necessary specifications for the scaffold, and for the anchoring method.

7.1.2 Evaluate PLGA Degradation

To ensure the device will stay within specification as it degrades, it is recommended that all the tests completed in this project be repeated during different intervals of degradation of the device. These tests will ensure that not only does the device function before implantation, but that it will continue to function as it degrades after implantation.

7.1.3 Further Orthobiolgical Testing

Although the results of our orthobiological testing did produce relevant results, further testing should be done to accurately determine the correct concentration of PRP. Once the PRP is obtained, the number of platelets in the sample should be quantified using a fluorescence assay. This should give a better baseline as to how many platelets, and in turn, the level of growth factors presents within the sample. The second change would be to use a BrdU ELISA to quantify the cellular proliferation. Due to human error, cell counting was not the optimal method of determining cell proliferation. Using a fluorescence assay would help accurately quantify proliferation overtime.

7.1.4 Evaluate Internal Volume of Scaffold

The average internal volume of a sample scaffold must be evaluated. This must be completed to determine if the current scaffold design can store the necessary amount of PRP needed to heal the UCL or related injury. The ideal volume of PRP is approximately 2-3mL (Magit, 2020). Major design changes may have to occur if the carrying capacity is less than the required amount, so it is recommended the internal volume be evaluated before the project advances much further.

7.1.5 Advance to Animal Testing

Animal testing should be conducted to confirm that the properties of the scaffold which were tested throughout this project stay consistent inside of a living organism. Animal testing will additionally allow for the examination of the effects of biological additives released from the scaffolds in vivo. It is recommended that mice be used for initial animal testing as BioSurfaces has experience in testing with mice, and mice have shown to be effective tendon and ligament models (Mienaltowski, Brik, 2014). It should be noted however that the device will eventually require large animal testing as well. Sheep or pigs can have ligaments similar in structure to humans, providing an adequate analog in a larger animal (Proffen, 2012).

7.1.6 Further Testing of Zein

While zein was used in the drug elution testing and was found to aid in the controlled release of therapeutic agents, additional testing should be done to evaluate its absorbance and release characteristics. Further knowledge of these characteristics will help to determine what

volume of therapeutic agent should be added to the inner pocket of the scaffold in order to release from the scaffold at the desired concentration.

7.1.7 Expansion of Device Applications

Finally, it is recommended that the applications of the device be expanded upon. Initially the UCL was used as model for the scaffold, but the concept and design can be adapted to many more common injuries such as rotator cuff injuries. It is recommended that the design of this device be adapted using a brainstorming session that centers around the idea of treating the desired injury. This is to ensure that the team's resources do not become stretched thin, and to stay within the time constraints of the MQP project. This task would be a natural progression of the project for a future MQP team.

7.2 Conclusion

In conclusion, the project was a success as a novel prototype was design, created and through testing, showed to initial promise towards one day becoming an effective treatment for healing grade II UCL tears. The team completed four different types of tests on the scaffold initial prototype and were able to draw conclusions about the design current state and how it must improve moving forward. From the mechanical tests, the team found that the scaffold seemingly is able to withstand the manipulation, and therefore should be able to withstand the manipulation that may come with surgery. The team also found that the anchoring method they had chosen, suturing, would not be effective on its own as an anchoring method, and that a new one would need to be implemented. From the cytotoxicity test, the team found that the proposed materials of zein and PLGA did not have a toxic effect on cells in culture. There were no significant differences between the control and the sample materials. The scaffold was found to have the ability to release a controlled amount of therapeutic agent for at least 7 days. Platelet Rich Plasma, the intended therapeutic agent was found to increase fibroblast proliferation in vitro.

Although these tests gave good initial information about the scaffold and its properties. The project team believes that the design could be greatly improved by the recommendations explained above. It should also be emphasized that the scaffold designed in this project truly used the UCL as a model and should be adapted to different surgeries once the design is closer to its final stages. The world of UCL repairs is important, but this product can change the world of

ligament and tendon repair in a large way. The design created by the team aimed to meet the need for a product with a minimally invasive procedure to heal grade II UCL tears, but it truly can and should be expanded to heal any form of partial ligament tear.

References

Abedalwafa, M., Fujun, W., Wang, L., & Lu, C. (2012, December). BIODEGRADABLE POLY-EPSILON-CAPROLACTONE (PCL) FOR TISSUE ENGINEERING APPLICATIONS: A REVIEW. Retrieved November 16, 2020, from http://www.ipme.ru/e-journals/RAMS/no_23413/02_23413_abedalwafa.pdf

Altman, G., Diaz, F., Jakuba C., Calabro T., Horan R., Chen J., Lu H., Richmond J., Kaplan D., (2003). Silk-based biomaterials. *Biomaterials*, 24(3), 401-416. https://doi.org/10.1016/S0142-9612(02)00353-8.

Annabi, N., Mithieux, S. M., Camci-Unal, G., Dokmeci, M. R., Weiss, A. S., & Khademhosseini, A. (2013). Elastomeric Recombinant Protein-based Biomaterials. *Biochemical engineering journal*, *77*, 110–118. https://doi.org/10.1016/j.bej.2013.05.006

Antoine, E. E., Vlachos, P. P., Rylander, M. N. (2014). Review of collagen I hydrogels for bioengineered tissue microenvironments: characterization of mechanics, structure, and transport. *Tissue engineering. Part B, Reviews*, *20*(6), 683–696. https://doi.org/10.1089/ten.TEB.2014.0086

ASTM (2014, December 15). D638 − 14 Standard Test Method for Tensile Properties of Plastics1. Retrieved November 29, 2020, from https://compass-astm-org.ezpxy-web-p-u01.wpi.edu/download/D638.40573.pdf

ASTM (2014, December 15). F2606 Standard Guide for Three-Point Bending of Balloon Expandable Vascular Stents and Stent Systems. Retrieved November 29, 2020, from https://compass-astm-org.ezpxy-web-p-u01.wpi.edu/EDIT/html_annot.cgi?F2606+08(2014)

Apostolakos, J. M., Lin, K. M., Carr, J. B., 2nd, Bedi, A., Camp, C. L., & Dines, J. S. (2020). The Role of Biologic Agents in the Non-operative Management of Elbow Ulnar Collateral Ligament Injuries. *Current reviews in Musculoskeletal Medicine*, 13(4), 442–448. https://doi.org/10.1007/s12178-020-09637-9

Arthrex, UCL InternalBraceTM Ligament Augmentation Repair. (n.d.). Retrieved April 30, 2020, from https://www.arthrex.com/elbow/ucl-internalbrace-ligament-augmentation-repair

Bell, D. J., and Hapugoda, S., (n.d). Superior Ulnar Collateral Artery, *Radiopaedia*, Retrieved October 15, 2020 from https://radiopaedia.org/articles/superior-ulnar-collateral-artery?lang=us

Bhandari, M. (2011). Evidence-Based Medicine: Why Bother?, *Journal of Arthroscopy and Related Surgery*, 25(3), 296-297. https://doi.org/10.1016/j.arthro.2009.01.013

Bosworth, L. A., and Sandra. D., *Electrospinning for Tissue Regeneration*. Cambridge; Woodhead Pub., 2011. Print.

Boudriot, U., Dersch, R., Greiner, A. and Wendorff, J.H. (2006), Electrospinning Approaches Toward Scaffold Engineering—A Brief Overview. Artificial Organs, 30: 785-792. https://doi.org/10.1111/j.1525-1594.2006.00301.x

Brennan M. (1991). Fibrin glue. *Blood reviews*, *5*(4), 240–244. https://doi.org/10.1016/0268-960x(91)90015-5

Buckley, P. S., Morris, E. R., Robbins, C. M., Kemler, B. R., Frangiamore, S. J., Ciccotti, M. G., Huard, J., LaPrade, R. F., & Hackett, T. R. (2019). Variations in Blood Supply From Proximal to Distal in the Ulnar Collateral Ligament of the Elbow: A Qualitative Descriptive Cadaveric Study. *The American Journal of Sports Medicine*, 47(5), 1117–1123. https://doi.org/10.1177/0363546519831693

Buttafoco L, Kolkman NG, Engbers-Buijtenhuijs P, Poot AA, Dijkstra PJ, Vermes I, Feijen J. Electrospinning of collagen and elastin for tissue engineering applications. Biomaterials. 2006 Feb;27(5):724-34. doi: 10.1016/j.biomaterials.2005.06.024. Epub 2005 Aug 19. PMID: 16111744.

Caliari, S. R., Burdick, J. A., (2016). A Practical Guide to Hydrogels for Cell Culture. *Nature America*, 13(5), 405-414. https://doi.org/10.1038/nmeth.3839

Chahla, J., Kennedy, M. I., Aman, Z. S., & Laprade, R. F. (2019). Ortho-Biologics for Ligament Repair and Reconstruction. *Clinics in Sports Medicine*, *38*(1), 97–107. https://doi.org/10.1016/j.csm.2018.08.003

Chan, B. P., Fu, S.-C., Qin, L., Lee, K.-M., Rolf, C. G., & Chan, K.-M. (2000). Effects of basic fibroblast growth factor (bFGF) on early stages of tendon healing: A rat patellar tendon model. *Acta Orthopaedica Scandinavica*, *71*(5), 513–518.201 https://doi.org/10.1080/000164700317381234

Chang, J., Thunder, R., Most, D., Longaker, M. T., & Lineaweaver, W. C. (2000). Studies in Flexor Tendon Wound Healing: Neutralizing Antibody to TGF-β1 Increases Postoperative Range of Motion. *Plastic and Reconstructive Surgery*, *105*(1), 148–155. https://doi.org/10.1097/00006534-200001000-00025

Chauhan A, McQueen P, Chalmers PN, et al. (2019). Nonoperative treatment of elbow ulnar collateral ligament injuries with and without platelet-rich plasma in professional baseball players: a comparative and matched cohort analysis. *American Journal of Sports Medicine,* 47(13), 3107–3119. https://doi.org/10.1177%2F0363546519876305

Chen, X., Qi, Y., Wang, L., Yin, Z., Yin, G., Zou, X., & Ouyang, H. (2008). Ligament regeneration using a knitted silk scaffold combined with collagen matrix. *Biomaterials, 29*(27), 3683-3692. doi:10.1016/j.biomaterials.2008.05.017

Chrobak K. M., Potter D. R., Tien J., (2006). Formation of perfused, functional microvascular tubes *in vitro*. *Microvascular Research*. 71(3):185-96. https://doi.org/10.1016/j.mvr.2006.02.005

Clark, N., Desai, V., Dines, J., Morrey, M., & Camp, C. (2018), Nonreconstruction Options for Treating Medial Ulnar Collateral Ligament Injuries of the Elbow in Overhead Athletes. *Curr Rev Musculoskelet Med*, 11(1), 48–54. https://doi.org/10.1007/s12178-018-9458-3

Deal J. B., Smith E., Heard W., O'Brien M. J., Savoie F. H., (2017). Platelet-rich plasma for primary treatment of partial ulnar collateral ligament tears: MRI correlation with results. *Orthopaedic Journal of Sports Medicine*, 5(11). https://doi.org/10.1177%2F2325967117738238

Demir M, Ramos-Rivera L, Silva R, Nazhat SN, Boccaccini AR. Zein-based composites in biomedical applications. J Biomed Mater Res A. 2017 Jun;105(6):1656-1665. doi: 10.1002/jbm.a.36040. Epub 2017 Mar 27. PMID: 28205372.

Dines J. S., Williams P. N., Elattrache N., et al. (2016). Platelet-rich plasma can be used to successfully treat elbow ulnar collateral ligament insufficiency in high-level throwers. *American Journal of Orthopedics*, 45(5):296–300. Corpus ID: 3566262

Doran, N. (2015). Running down the velocity upswing. *Redleg Nation*, Retrieved from https://redlegnation.com/2015/02/19/running-down-the-velocity-upswing/

Doroski, D. M., Brink, K. S., & Temenoff, J. S. (2006). Techniques for biological characterization of tissue-engineered tendon and ligament. *Biomaterials*, 28(2), 187-202. https://doi.org/10.1016/j.biomaterials.2006.08.040

Dugas, J., Looze, C., Jones, C., Walters, B., Rothermich, M., Emblom, B., Fleisig G. S., Aune K., Cain, E. (2018). Ulnar Collateral Ligament Repair with Internal Brace Augmentation in Amateur Overhead Throwing Athletes. 6(7 suppl4), https://doi.org/10.1177%2F2325967118S00084

Dustin, A. D., Geer, E. A., & Hulburt, T. C. (2015). *A Dynamic Elbow Flexion Simulator for Cadaveric Testing of UCL Injury and Reconstruction*. (Undergraduate Major Qualifying Project No. E-project-043015-053558) Retrieved from Worcester Polytechnic Institute Electronic Projects Collection: https://web.wpi.edu/Pubs/E-project/Available/E-project-043015-053558/

Echave, M., Burgo, L., Pedraz, J., Gorka, O. (2017). Gelatin as a Biomaterial for Tissue Engineering. *Current Pharmaceutical*. 24(24):3567-3584. https://doi.org/10.2174/0929867324666170511123101

Eghbali, M., Tomek, R., Sukhatme, V. P., Woods, C., & Bhambi, B. (1991). Differential effects of transforming growth factor-beta 1 and phorbol myristate acetate on cardiac fibroblasts.

Regulation of fibrillar collagen mRNAs and expression of early transcription factors. *Circulation Research, 69*(2), 483-490. doi:10.1161/01.res.69.2.483

Fereydouni, N., Movaffagh, J., Amiri, N. *et al.* Synthesis of nano-fibers containing nano- curcumin in zein corn protein and its physicochemical and biological characteristics. *Sci Rep* **11,** 1902 (2021). https://doi.org/10.1038/s41598-020-73678-w

Fleisig, G. S., Andrews, J. R., (2012). Prevention of elbow injuries in youth baseball pitchers. Sports Health: A Multidisciplinary Approach, *Sports Health*, 4(5), 419-424. https://doi.org/10.1177%2F1941738112454828

Gentleman, E., Lay, A. N., Dickerson, D. A., Nauman, E. A., Livesay, G. A., & Dee, K. C. (2003). Mechanical characterization of collagen fibers and scaffolds for tissue engineering. *Biomaterials, 24*(21), 3805-3813. doi:10.1016/s0142-9612(03)00206-0

Gleiber, M. A. (n.d). Common Baseball Injuries. *Michael Gleiber, MD, PA, Concierge Spine Surgery*. Retrieved May 4, 2021, from https://www.michaelgleibermd.com/news/common-baseball-injuries/

Gomber, M. M. (n.d). Elbow Sprain and UCL Tear Treatments - Houston, Beaumont, Cypress TX. *Mufaddal Gomber, MD, Orthopedic Surgery & Sports Medicine*. Retrieved from https://www.gomberamd.com/ucl-sprain.html.

Gond, L., Pradhan, P., Bajpai, A. (2020). Preparation and application of biomimetic and bioinspired membranes based on chitosan. *Handbook of Chitin and Chitosan*. 3:307-339. https://doi.org/10.1016/B978-0-12-817966-6.00010-8

Haley, A. (2017). New Tommy John Surgery Alternative Has Potential to Cut Rehab Time in Half. *Andrews Sports Medicine and Orthopaedic* Center. Retrieved September 28, 2020, from https://www.stack.com/a/new-tommy-john-surgery-promises-to-cut-rehab-time-in-half

Ham, T. R., Lee, R. T., Han, S., Haque, S., Vodovotz, Y., Gu, J., . . . Saul, J. M. (2015). Tunable Keratin Hydrogels for Controlled Erosion and Growth Factor Delivery. *Biomacromolecules, 17*(1), 225-236. doi:10.1021/acs.biomac.5b01328

Hurwit D. J., Garcia G. H., Liu J., Altchek D. W., Romeo A., Dines J.. (2017). Management of ulnar collateral ligament injury in throwing athletes: a survey of the American Shoulder and Elbow Surgeons. *Journal of Shoulder and Elbow Surgery*. 26(11), 2023–2028. https://doi.org/10.1016/j.jse.2017.08.005

Hwang, J., Hammer, J., Schwartz, H., Malaviya, P. (2012). *U.S. Patent No. US8226715B2*. Washington, DC: U.S. Patent and Trademark Office.

Ibrahim, M., Poveromo, L., Glisson, R., Cornejo, A., Farjat, A., Gall, K., & Levinson, H. (2018, April 11). Modifying hernia mesh design to improve device mechanical performance and promote tension-free repair. Retrieved December 20, 2020, from https://www.ncbi.nlm.nih.gov/pmc/articles/PMC5878138/

ISO 10993-5 (2009) Biological Evaluation of Medical Devices. Part 5: Tests for *in vitro* Cytotoxicity. https://www.iso.org/standard/36406.html

John, T. (2018). Why Tommy John Is Against the Surgery Named for Him. *AARP*, Retrieved September 23, 2020, from https://www.aarp.org/health/conditions-treatments/info-2018/tommy-john-opposes-namesake-surgery.html

Johnson, J. A., Rath, D. A., Dunning, C. E., Roth, S. E., & King, G. J. W. (2000). Simulation of elbow and forearm motion *in vitro* using a load controlled testing apparatus. *Journal of Biomechanics*, 33(5), 635-639. https://doi.org/10.1016/S0021-9290(99)00204-3

Jones, C., Beason, D., & Dugas, J. (2018). Ulnar Collateral Ligament Reconstruction Versus Repair With Internal Bracing: Comparison of Cyclic Fatigue Mechanics. *Orthopaedic Journal of Sports* Medicine, 6(2), 2325967118755991. https://doi.org/10.1177%2F2325967118755991

Kaplan, D. J., Glait, S. A., Ryan, W. E., Jazrawi, L. M. (2016). Modified Jobe Approach With Docking Technique for Ulnar Collateral Ligament Reconstruction. *Arthroscopy Techniques*, 5(6), e1321–e1326. https://doi.org/10.1016/j.eats.2016.08.002

Kapoor, N. D., Bhatia, A., Kaur, R. (2015). PLGA: A unique polymer for drug delivery. *Therapeutic Delivery,* 6(1), 41-58. https://www.researchgate.net/publication/270765946_PLGA_A_unique_polymer_for_drug_delivery

Karaman, O., Şen, M., & Demirci, E. (2017). Electrospun scaffolds for vascular tissue engineering. *Science Direct,* 261-287. https://doi.org/10.1016/B978-0-08-101022-8.00006-5

Kim, J., Conway, A., & Chauhan, A. (2008). Extended delivery of ophthalmic drugs by silicone hydrogel contact lenses. *Biomaterials,* 29(14), 2259-2269. https://doi.org/10.1016/j.biomaterials.2008.01.030

Kobayashi, D., Kurosaka, M., Yoshiya, S., & Mizuno, K. (1997). Effect of basic fibroblast growth factor on the healing of defects in the canine anterior cruciate ligament. *Knee Surgery, Sports Traumatology, Arthroscopy*, *5*(3), 189–194. https://doi.org/10.1007/s001670050049

Koob, T., Davis, T., & Pringle, D. (2012). *U.S. Patent No. US8177839B2*. Washington, DC: U.S. Patent and Trademark Office.

Kreger S. T., Bell B. J., Bailey J., Stites E., Kuske J., Waisner B., Voytik-Harbin S. L., (2010) Polymerization and matrix physical properties as important design considerations for soluble collagen formulations. *Biopolymers*. 93(8):690-707. https://doi.org/10.1002/bip.21431

Kurtz, C. A., Loebig, T. G., Anderson, D. D., Demeo, P. J., & Campbell, P. G. (1999). Insulin-Like Growth Factor I Accelerates Functional Recovery from Achilles Tendon Injury in a Rat Model. *The American Journal of Sports Medicine*, *27*(3), 363–369. https://doi.org/10.1177/03635465990270031701

Labott, J. R., Aibinder, W. R., Dines, J. S., & Camp, C. L. (2018). Understanding the medial ulnar collateral ligament of the elbow: Review of native ligament anatomy and function. *World journal of orthopedics*, *9*(6), 78–84. https://doi.org/10.5312/wjo.v9.i6.78

Laksin, O., & Du, G. W. (2003). *U.S. Patent No. US20030100944A1*. Washington, DC: U.S. Patent and Trademark Office.

Laurencin, C. T., Ko, F. K., Cooper, J. A., Lu, H. H., Attawia, M. A. (2015). *U.S. Patent No. US8945218B2*. Washington, DC: U.S. Patent and Trademark Office.

Le X., Poinern G. E. J., Ali N., Berry C. M., Fawcett D., (2013). Engineering a Biocompatible Scaffold with Either Micrometre or Nanometre Scale Surface Topography for Promoting Protein Adsorption and Cellular Response, *International Journal of Biomaterials*, Article ID 782549. https://doi.org/10.1155/2013/782549

Lelkes, P. I., Li, M., Mondrinos, M., & Ko, F. (2011). *U.S. Patent No. US8048446B2*. Washington, DC: U.S. Patent and Trademark Office.

Letson, A. K., & Dahners, L. E. (1994). The Effect of Combinations of Growth Factors on Ligament Healing. *Clinical Orthopaedics and Related Research, &NA;*(308). https://doi.org/10.1097/00003086-199411000-00030

Liu, H., Wang, S. and Qi, N. (2012), Controllable structure, properties, and degradation of the electrospun PLGA/PLA-blended nanofibrous scaffolds. J. Appl. Polym. Sci., 125: E468-E476. https://doi.org/10.1002/app.36757

Lu, H. H., Spalazzi, J. (2009). *U.S. Patent No. US8753391B2*. Washington, DC: U.S. Patent and Trademark Office.

Magit, D. (2018) CORR LECTURE

Magit, D. (2020, September 29). Specifications Meeting [Personal communication].

Magit, D. (2020, October 2). Weekly MQP Meeting [Personal communication].

McCarthy, C. D., Cataldo, G. F., & Cannata, M. J. (2020). *Design of an Implantable Ulnar Collateral Ligament Repair System*. (Undergraduate Major Qualifying Project No. E-project-050307-071942). Retrieved from Worcester Polytechnic Institute Electronic Projects Collection: https://web.wpi.edu/Pubs/E-project/Available/E-project-051820-010049/

Meldau, J. E., Srivastava, K., Okoroha, K. R., Ahmad, C. S., Moutzouros, V., & Makhni, E. C. (2020). Cost analysis of Tommy John surgery for Major League Baseball teams. Journal of

shoulder and elbow surgery, *J Shoulder Elbow Surg*. 29(1), 121–125. https://doi.org/10.1016/j.jse.2019.07.019

Mienaltowski MJ, Birk DE. Mouse models in tendon and ligament research. Adv Exp Med Biol. 2014;802:201-30. doi: 10.1007/978-94-007-7893-1_13. PMID: 24443029.

Miranda-Nieves, D., Chaikof, E. L. (2017). Collagen and Elastin Biomaterials for the Fabrication of Engineered Living Tissues. *ACS Biomaterials Science & Engineering*. 3(5), 694-711. DOI: 10.1021/acsbiomaterials.6b00250

Murray, M. M., (2017). *U.S. Patent No. US9849213B2*. Washington, DC: U.S. Patent and Trademark Office.

Murray, M. M., (2020). *U.S. Patent No. US20200171203A1*. Washington, DC: U.S. Patent and Trademark Office.

Molloy, T., Wang, Y., & Murrell, G. A. C. (2003). The Roles of Growth Factors in Tendon and Ligament Healing. *Sports Medicine, 33*(5), 381–394. https://doi.org/10.2165/00007256-200333050-00004

Naciri, M., Kuystermans, D., Al-Rubeai, M. (2008). Monitoring pH and dissolved oxygen in mammalian cell culture using optical sensors. *Cytotechnology*, *57*(3), 245–250. https://doi.org/10.1007/s10616-008-9160-1

Norowski PA, Mishra S, Adatrow PC, Haggard WO, Bumgardner JD. 2012. Suture pullout strength and *in vitro* fibroblast and RAW 264.7 monocyte biocompatibility of genipin crosslinked nanofibrous chitosan mats for guided tissue regeneration. J Biomed Mater Res Part A 2012:100A:2890–2896.

O'Brien, Fergal J. (2011). Biomaterials & Scaffolds for Tissue Engineering. *Materials Today*, 14(3), 88-95. https://doi.org/10.1016/S1369-7021(11)70058-X

Oyama, S. (2012). Baseball pitching kinematics, joint loads, and injury prevention. *Journal of Sport and Health Science*, 1(2), 80-91. https://doi.org/10.1016/j.jshs.2012.06.004

Pagliari S., Romanazzo S., Mosqueira D., Pinto-do-Ó P., Aoyagi T., Forte G.. Adult stem cells and biocompatible scaffolds as smart drug delivery tools for cardiac tissue repair. *Current Medicinal Chemistry*. 20(28):3429-47. https://doi.org/10.2174/09298673113209990032

Papay, F. A., Byerman, B. P. (2001). *U.S. Patent No. US6517542B1*. Washington, DC: U.S. Patent and Trademark Office.

Parenteau-Bareil, R., Gauvin, R., & Berthod, F. (2010). Collagen-Based Biomaterials for Tissue Engineering Applications. *Materials*, *3*(3), 1863–1887. https://doi.org/10.3390/ma3031863

Parenteau-Bareil R., Gauvin R., Cliche S., Gariépy C., Germain L., Berthod F., (2011) Comparative study of bovine, porcine and avian collagens for the production of a tissue engineered dermis. *Acta Biomaterialia*.7(10):3757-65. https://doi.org/10.1016/j.actbio.2011.06.020

Pedowitz, R. A., Weichel, D. W., & Barber, A. (2016, June 19). Implant Choices: The Biomechanics of Anchors and Sutures. *Musculoskeletal Key*. Retrieved October 06, 2020, from https://musculoskeletalkey.com/implant-choices-the-biomechanics-of-anchors-and-sutures/

Podesta L., Crow S. A., Volkmer D., Bert T., Yocum L. A., (2013). Treatment of partial ulnar collateral ligament tears in the elbow with platelet-rich plasma. *American Journal of Sports Medicine*. 41(7):1689–1694. https://doi.org/10.1177%2F0363546513487979

Proffen, B. L., McElfresh, M., Fleming, B. C., & Murray, M. M. (2012). A comparative anatomical study of the human knee and six animal species. *The Knee*, 19(4), 493–499. https://doi.org/10.1016/j.knee.2011.07.005

Rebolledo, B. J., Dugas, J. R., Bedi, A., Ciccotti, M. G., Altchek, D. W., Dines, J. S. (2017). Avoiding Tommy John Surgery: What Are the Alternatives?. *The American Journal of Sports Medicine*, 45(13), 3143-3148. https://doi.org/10.1177%2F0363546517692548

Rettig, A. C., Sherrill, C., Snead, D. S., Mendler, J. C., Mieling, P. (2001). Nonoperative Treatment of Ulnar Collateral Ligament Injuries in Throwing Athletes. *The American Journal of Sports Medicine*, 29(1), 15-17. https://doi.org/10.1177%2F03635465010290010601

Rocco, K. A., Mohanraj, B., Ott, J., Bendigo, J., Komenda, J. E., Aronson, M. T., Carter, A. J. (2020). *U.S. Patent No. US20200337828A1*. Washington, DC: U.S. Patent and Trademark Office.

Rowley, JA, Madlambayan, G, Mooney, DJ (1999). Alginate hydrogels as synthetic extracellular matrix materials. *Biomaterials*, 20(1), 45-53. https://doi.org/10.1016/S0142-9612(98)00107-0.

Saito, E., Liao, E., Hu, W., Krebsbach, P., & Hollister, S. (2013, February). Effects of designed PLLA and 50:50 PLGA scaffold architectures on bone formation in vivo. Retrieved November 16, 2020, from https://www.ncbi.nlm.nih.gov/pmc/articles/PMC4367810/

Saltzman, C., & Schon, L. (2010). *U.S. Patent No. US20100179591A1*. Washington, DC: U.S. Patent and Trademark Office.

S. C. Scherping, C. C. Schmidt, H. I. Georgescu, C. K. Kwoh, C. H. Evans & S. L-Y. Woo (1997) Effect of Growth Factors on the Proliferation of Ligament Fibroblasts from Skeletally Mature Rabbits, Connective Tissue Research, 36:1, 1-8, DOI: 10.3109/03008209709160209

Sensini, A., Cristofolini, L. (2018). Biofabrication of Electrospun Scaffolds for the Regeneration of Tendons and Ligaments. *Materials*, 11(10), 1963. https://doi.org/10.3390/ma11101963

Setayesh, K., Villarreal, A., Gottschalk, A., Tokish, J. M., & Choate, W. S. (2018). Treatment of Muscle Injuries with Platelet-Rich Plasma: a Review of the Literature. *Current reviews in musculoskeletal medicine*, *11*(4), 635–642. https://doi.org/10.1007/s12178-018-9526-8

Sharma, L., Song, J., Dunlop, D., Felson, D., Lewis, C. E., Segal, N., Torner, J., Cooke, T. D., Hietpas, J., Lynch, J., Nevitt, M. (2010). Varus and valgus alignment and incident and progressive knee osteoarthritis. *Annals of the rheumatic diseases*, 69(11), 1940–1945. https://doi.org/10.1136/ard.2010.129742

Sharpless, N. E. (2019). Statement on concerns with medical device availability due to certain sterilization facility closures. *FDA Statement*. Retrieved May 4, 2021, from https://www.fda.gov/news-events/press-announcements/statement-concerns-medical-device-availability-due-certain-sterilization-facility-closures

Sigg, D., Hiniduma-Lokuge, P., Sharma, V., & Sommer, J. (2007). *U.S. Patent No. US20070087033A1*. Washington, DC: U.S. Patent and Trademark Office.

Smith, M. V., Castile, R. M., Brophy, R. H., Dewan, A., Bernholt, D., Lake, S. P. (2019). Mechanical Properties and Microstructural Collagen Alignment of the Ulnar Collateral Ligament During Dynamic Loading. *The American Journal of Sports Medicine*, *47*(1), 151–157. https://doi.org/10.1177/0363546518812416

Statcast. (2019). *Baseball Savant.* Retrieved September 16, 2020, from http://m.mlb.com/statcast/leaderboard

The Pricer. (n.d.) Tommy John Surgery Cost. ThePricer. Retrieved March 21, 2021 from https://www.thepricer.org/tommy-john-surgery-cost/

Thompson, N. W., Mockford, B. J., Cran, G. W. (2001). Absence of the palmaris longus muscle: A population study. *The Ulster Medical Journal*, 70(1), 22–24. PMCID: PMC2449224

Tomono, T. (2019, April 24). A new way to control the internal structure of microneedles: A case of chitosan lactate. Retrieved December 06, 2020, from https://www-sciencedirect-com.ezpxy-web-p-u01.wpi.edu/science/article/pii/S246851941930031X

Trofa, D., Lombardi, J., Noticewala, M., Ahmad, C. (2017). Ulnar Collateral Ligament Repair With Suture Augmentation. *Arthroscopy Techniques.* 7(1), e53-e56. https://doi.org/10.1016/j.eats.2017.08.052

Tyler, B., Gullotti, D., Mangraviti, A., Utsuki, T., Brem, H. (2016). Polylactic acid (PLA) controlled delivery carriers for biomedical applications. *Advanced Drug Delivery Reviews*, 107, 163-175. https://doi.org/10.1016/j.addr.2016.06.018

UCL Injuries of the Elbow. (n.d.) John Hopkins Medicine.*Beacon Orthopedics and Sports Medicine.* Retrieved September 9 2020 from https://www.beaconortho.com/blog/ucl-injuries-elbow/

Walden, M., (2019). Sprained Ankle—Treatment, Rehabilitation & Exercises. *Sports Injury Clinic.* Retrieved 29 September 2020 from https://www.sportsinjuryclinic.net/sport-injuries/ankle-pain/acute-ankle-injuries/sprained-ankle

Wang H., Feng Y., Fang Z., Yuan W., Khan M., (2012). Co-electrospun blends of PU and PEG as potential biocompatible scaffolds for small-diameter vascular tissue engineering. *Materials Science and Engineering: C*. 32(8), 2306-2315. https://doi.org/10.1016/j.msec.2012.07.001.

Wang, X., Jin, J., Hou, R., Zhou, M., Mou, X., Xu, K., Zhu, Y., Shen, Z., Shang, X. (2019). Differentiation of BMSCs on Biocompatible, Biodegradable, and Biomimetic Scaffolds for Largely Defected Tissue Repair. *ACS Applied Bio Materials*, 3(1), 735-746. https://doi.org/10.1021/acsabm.9b01063

Watson, J. N., McQueen, P., Hutchinson, M. R. (2014). A systematic review of ulnar collateral ligament reconstruction techniques. *The American Journal of Sports Medicine*, 42(10), 2510– 2516. https://doi.org/10.1177/0363546513509051

Wenger, M., Bozec, L., Horton, M., Mesquida, P. (2007). Mechanical properties of collagen fibrils. *Biophysical Journal*, 93(4), 1255-1263. https://doi.org/10.1529/biophysj.106.103192

Wiedrich, T., Davis, T., Koob, T. (2017). *U.S. Patent No. US9681869B2*. Washington, DC: U.S. Patent and Trademark Office.

Wolf, K., Alexander, S., Schacht, V., Coussens, L. M., von Andrian, U. H., van Rheenen, J., Deryugina, E., & Friedl, P. (2009). Collagen-based cell migration models in vitro and in vivo. *Seminars in cell & developmental biology*, *20*(8), 931–941. https://doi.org/10.1016/j.semcdb.2009.08.005

Yan, X. (2017). Chitosan for tendon engineering and regeneration. *Chitosan Based Biomaterials Volume 2*. 2:73-87. https://doi.org/10.1016/B978-0-08-100228-5.00003-1

Zaremski, Jason L., et al. (2017). "Trends in Sports-Related Elbow Ulnar Collateral Ligament Injuries." *Orthopaedic Journal of Sports Medicine*, Oct. 2017, doi:10.1177/2325967117731296.

Zhou J., Cao C., Ma X., (2009). A novel three-dimensional tubular scaffold prepared from silk fibroin by electrospinning. International Journal of Biological Macromolecules. 45,(5), 504-510. https://doi.org/10.1016/j.ijbiomac.2009.09.006.

Zreiqat, H., Roohaniesfahani, S. I., Ramaswamy, Y., No, Y. J. (2017). *U.S. Patent No. US20190343985A1*. Washington, DC: U.S. Patent and Trademark Office.

Appendix

Appendix A: Custom Instron Fixture 3D Drawings

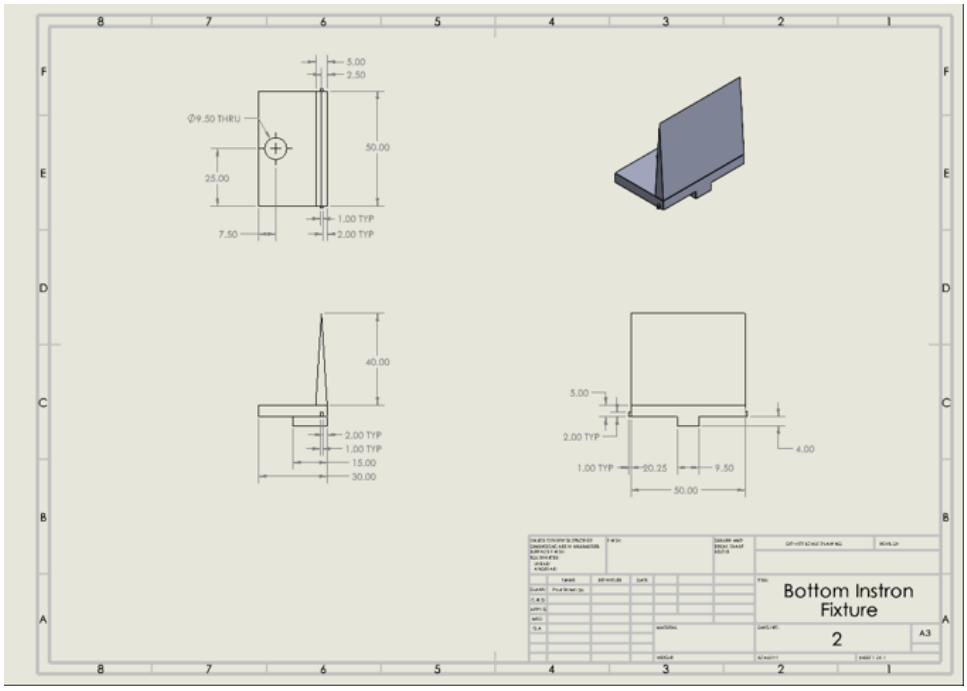

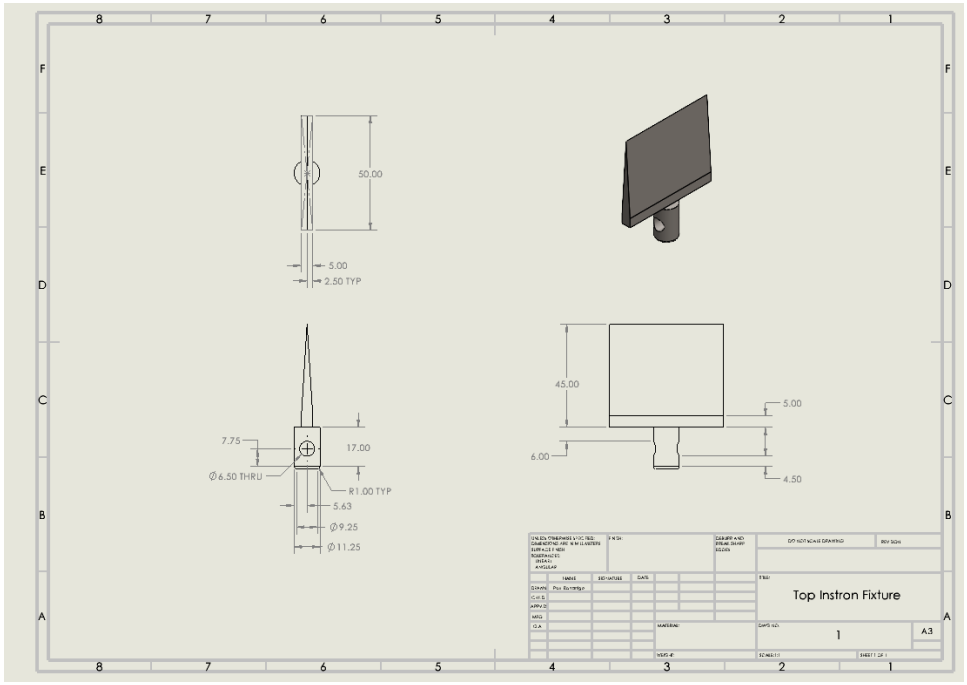

Appendix B: Mechanical Testing MATLAB Function

```
function answer = MQPUCL(TestType)
Analysis = 0;
if TestType == 'b'
    TestType = 'Bending Test';
    Analysis = 1;
elseif TestType == 't'
    TestType = 'Tensile Test';
    Analysis = 2;
elseif TestType == 's'
    TestType = 'Suture Pullout Test';
    Analysis = 1;
end
maxloads = [];
if Analysis == 1
    fig1 = figure(); hold on
    for trial = 1:2
        trialstr = num2str(trial);
        fname = append('Specimen_RawData_',trialstr,'.csv');
        datafile = readtable(fname, 'HeaderLines', 2);%Import the data
        Extension = datafile(:,2);
        ExtensionAr = table2array(Extension);
        Load = datafile(:,3);
        LoadAr = table2array(Load);
        maxload = (max(LoadAr));
        maxloads(trial) = maxload;
        plot(ExtensionAr, LoadAr);
        title('Load Versus Extension', TestType, 'Fontsize',16);
        xlabel('Extension (mm)', 'Fontsize',16);
        ylabel('Load (N)',  'Fontsize',16);
    end
    for trial = 1:2
        trial = num2str(trial);
        fname = append('Specimen_RawData_',trial,'.csv');
        datafile = readtable(fname, 'HeaderLines', 2);%Import the data
        Extension = datafile(:,2);
        ExtensionAr = table2array(Extension);
        Load = datafile(:,3);
        LoadAr = table2array(Load);
        maxload = (max(LoadAr));
        index = find(LoadAr == maxload);
        string = append(num2str(maxload), ' N');
        text(1.025*ExtensionAr(index),1.025*LoadAr(index), string, 'Fontsize',14);
        index = find(LoadAr == maxload);
        plot1 = plot(ExtensionAr(index),LoadAr(index), 'ro');
    end
    legend('Trial 1', 'Trial 2', 'Trial 3', 'Trial 4', 'Trial 5', 'Max Forces');
    hold off
    fig2 = figure(); hold on
    for trial = 1:5
        trial = num2str(trial);
        fname = append('Specimen_RawData_',trial,'.csv');
        datafile = readtable(fname, 'HeaderLines', 2);%Import the data
        Time = datafile(:,1);
        TimeAr = table2array(Time);
        Load = datafile(:,3);
        LoadAr = table2array(Load);
        plot(TimeAr, LoadAr);
        title('Load Versus Time', TestType, 'Fontsize',16)
        xlabel('Time (s)', 'Fontsize',16)
        ylabel('Load (N)', 'Fontsize',16)
    end
    legend('Trial 1', 'Trial 2', 'Trial 3', 'Trial 4', 'Trial 5')
    hold off
```

```
elseif Analysis == 2
    fig3 = figure(); hold on
    for trial = 1:5
        trial = num2str(trial)
        fname = append('Specimen_RawData_',trial,'.csv')
        datafile = readtable(fname, 'HeaderLines', 8);%Import the data
        Strain  = datafile(:,4);
        StrainAr = table2array(Strain)
        Stress = datafile(:,5);
        StressAr = table2array(Stress)
        plot(StrainAr, StressAr)
        title('Stress Versus Strain', TestType, 'Fontsize',16)
        xlabel('Strain (mm/mm)', 'Fontsize',16)
        ylabel('Stress (MPa)', 'Fontsize',16)
    end
    for trial = 1:5;
        trial = num2str(trial);
        fname = append('Specimen_RawData_',trial,'.csv');
        datafile = readtable(fname, 'HeaderLines', 2);%Import the data
        Strain  = datafile(:,4);
        StrainAr = table2array(Strain)
        Stress = datafile(:,5);
        StressAr = table2array(Stress)
        maxstress = (max(StressAr));
        index = find(StressAr == maxstress);
        string = append(num2str(maxstress), ' N');
        text(1.025*StrainAr(index),1.025*StressAr(index), string, 'Fontsize',14);
        plot1 = plot(StrainAr(index),StressAr(index), 'ro');
    end
    legend('Trial 1', 'Trial 2', 'Trial 3', 'Trial 4', 'Trial 5', 'Max Forces');
    hold off

    fig4 = figure(); hold on
    for trial = 1:5
        trial = num2str(trial)
        fname = append('Specimen_RawData_',trial,'.csv')
        datafile = readtable(fname, 'HeaderLines', 8);%Import the data
        Time = datafile(:,1);
        TimeAr = table2array(Time)
        Extension = datafile(:,2);
        ExtensionAr = table2array(Extension)
        Strain  = datafile(:,4);
        StrainAr = table2array(Strain)
        Stress = datafile(:,5);
        StressAr = table2array(Stress)
        Load = datafile(:,3);
        LoadAr = table2array(Load)
        maxstress = (max(StressAr))
        index = find(StressAr == maxstress)
        figure
        plot(ExtensionAr, LoadAr)
        title('Load Versus Extension', TestType)
        xlabel('Extension (mm)', 'Fontsize',16)
        ylabel('Load (N)', 'Fontsize',16)
        hold on
        maxload = (max(LoadAr))
        index = find(LoadAr == maxload)
        plot1 = plot(ExtensionAr(index),LoadAr(index), 'ro')
        legend(plot1, 'Max Force', 'Fontsize',14)
    end
    legend('Trial 1', 'Trial 2', 'Trial 3', 'Trial 4', 'Trial 5')
    hold off
end
```

Appendix C: Three-point Bending and Tensile Test Methodology

Materials:

- 4 sample scaffolds
- Custom three-point bending fixtures
- Instron
- Instron adjustable jaws
- Instron three-point bending fixture
- Glue
- Calipers
- Allen Wrench

Procedure:

1. Select two scaffolds to undergo the three-point bending test.
2. Measure the length of these two scaffolds using calipers.
3. Use Table 1 of ASTM F2606, found below, and the scaffold measurements to determine the span length and maximum deflection of each sample.
4. Create a custom Instron tensile test method.
5. Edit the pre cycling information with the maximum deflection found from Table 1, a testing rate of 0.25 cm/min, and a cycle count of 50.
6. Swap the bases of the Instron three-point bending fixture with the custom fixtures.
7. Attach the three-point bending fixture to the Instron.
8. Using the ruler on the fixture confirm that the distance between the fixtures is equal to the span length found from Table 1.
9. Glue the tip of the custom top Instron fixture, and attach one of the samples, at the midpoint, to the fixture.
10. Run the scaffold through the bending test ensuring to balance force and displacement prior to starting the test.
11. Repeat the previous two steps for the second scaffold selected to undergo the bending test.
12. With the bending test completed, detach the bending fixtures from the Instron, and attach the Instron adjustable jaws to the Instron.
13. Create a new Instron tensile method with a testing rate of 0.25 cm/min which also intakes the length and width of each sample and calculates the stress and strain of each sample with this information.
14. Insert a scaffold in between the clamps of the top Instron adjustable jaw and tighten it in place using an Allen wrench ensuring that it is as straight as possible.
15. Use the Instron control panel to move the top jaw to a location where the scaffold can be tightened into the bottom jaw.
16. Tighten the scaffold into the bottom jaw.
17. Use calipers determine the width, length, and thickness of the scaffold. It should be noted that the length is the distance between the two Instron jaws.
18. Input this information into the Instron test method.
19. Balance all of the forces and displacements and apply a preload of 0.5 N prior to beginning the test method.
20. Run the test method on the scaffold.

21. Remove the sample scaffold and repeat the previous 7 steps on next 3 scaffolds ensuring to keep track of which scaffolds had undergone the bending tests and which ones had not.
22. Ensure to power off the Instron correctly prior to concluding testing.

TABLE 1 Recommended Span Length and Maximum Deflection for the Variable Span Length Method

Stent Length (mm)[A]	Span Length (mm)[B]	Maximum Deflection[C]
10—14	6[D]	1.2
15—19	11	2.2
20—24	16	3.2
25—35	21	4.2
>35	(stent length/1.093) — 2	0.2 × (span length)

Appendix D: Suture Pullout Test

Materials:

- 3 sample scaffolds
- 8 4-0 Securopro Sutures
- Instron
- Instron adjustable jaws
- Scotch Tape
- Allen wrench

Procedure:

1. Select two scaffolds to be sutured vertically.
2. Suture these scaffolds on each side along their length simply by inserting the suture through one end and creating a loop around the scaffold.
3. Suture the remaining scaffold 4 times along its with width with the same method as explained earlier.
4. Once the suturing is completed, the excess suture should be rotated 360° 5 times and then taped together.
5. Attach the Instron adjustable jaws to the Instron.
6. Create a new Instron tensile method with a testing rate of 0.25 cm/min.
7. For the vertically sutured samples.
    1. Load a scaffold into the bottom Instron clamp and tighten it using an Allen wrench.
    2. Next move the top Instron jaw down until the tape used to hold the suture together can be tightened into the Instron jaw. Attempt to keep the suture as straight as possible for the most consistent results.
    3. Apply a preload of 0.5 N and run the Instron method.
    4. Repeat the previous three methods for all 4 sutures in the 2 sample scaffolds.
8. For the horizontally sutured samples.
    1. Load the scaffold into the bottom Instron clamp and tighten it using an Allen wrench.
    2. Next move the top Instron jaw down until the tape used to hold the suture together can be tightened into the Instron jaw. Attempt to keep the suture as straight as possible for the most consistent results.
    3. Apply a preload of 0.5 N and run the Instron method. Repeat the previous three methods for all 4 sutures in the sample scaffolds.
9. Ensure to power off the Instron correctly prior to concluding testing.

Appendix E: Cytotoxicity Testing

Media Preparation

Combine all materials listed below and place in refrigerator until needed for cell culture.

10% FBS Media – 100mL batches

- DMEM - 88mL
- Penn Strep - 1.0mL
- L-Glutamine/Glutamax - 1.0mL
- FBS – 10mL

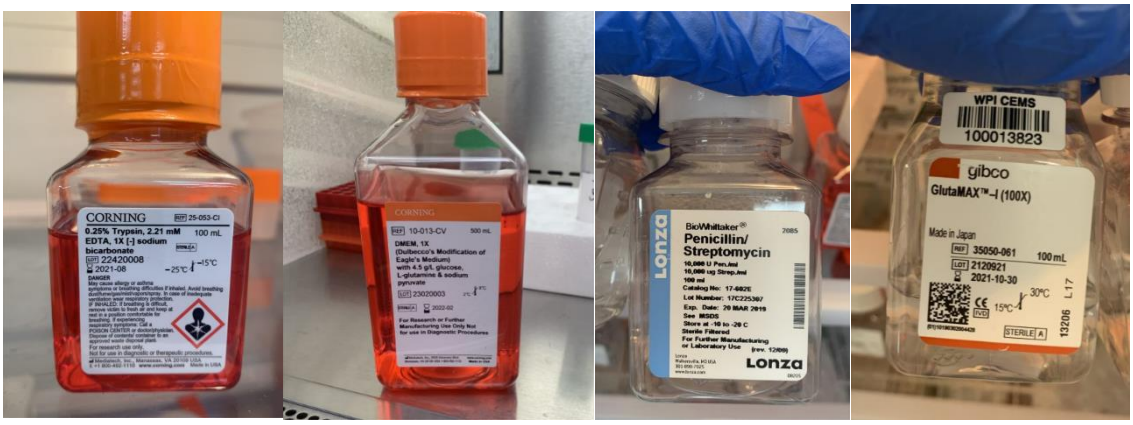

Sample Preparation

This is done to prepare and sterilize the materials needed to run the experiment.

1. Collect all sample materials, ZEIN, PLGA and Latex Glove
2. Using a hole-punch with approximately 7mm diameter cut 3 samples for each material.
3. Clean a cell culture hood using proper sterile technique.
4. Place the samples into 3 dishes and bring them into the hood.
5. Close the hood and turn on the UV light for 8 minutes.
6. After this, open the hood, flip the samples using sterile forceps and repeat step 5 for an additional 8 minutes.
7. When done cover the sample dishes to maintain sterilization of the materials

Test by direct contact (-Written procedure modified from ISO-10993-5)

This test can be used for both qualitative and quantitative evaluation of cytotoxicity

1. Obtain the materials needed for this experiment.
    - 10% FBS Media
    - NIH 3T3 cells
    - Sample materials – ZEIN, PLGA, Latex
    - PDMS squares
    - 2 – 6-well plates

2. Pipette 2mL of 10% FBS media into 2, 6-well plates. Then pipette a known aliquot of the continuously stirred cell suspension into each of the 12 sample wells. For this experiment 10,000 NIH 3T3 cells were aliquoted into each well and distributed evenly by gently rotating the plate in a horizontal motion.

3. Incubate the culture at (37 ± 1) °C and 5% CO_2 in an incubator for 24 hours. Or until the cells have adhered to the bottom of the plate.
4. Verify and Image the confluency and the morphology of the cultures with a microscope before starting the test.
5 Remove and discard the culture medium. Then add 2 mL of fresh culture medium to each vessel.
6. Carefully place individual specimens of the test sample on the cell layer in the center of each of the replicate vessels. Ensure that the specimen covers approximately one tenth of the cell layer surface. Exercise care to prevent unnecessary movement of the specimens, as this could cause physical trauma to the cells. Add a small piece of PDMS to the top of the specimen to weigh it down and prevent it from shifting in the well.
7. Prepare replicate vessels for both the negative control and positive control material.
8. Incubate the vessels under the same conditions as described in step 2.
9. Remove the plates from the incubator and image all wells under the microscope every 24 hours until the cells reach a confluency of approximately 75%.
10. For imaging take 3 images per well to obtain a proper cell count.
11. Discard the supernatant culture medium and discard the plate into a biohazard bin.

Appendix F: PRP Bioactivity Testing

Media preparation procedure:
This procedure details the procedure for making the cell culture media necessary for the PRP preliminary and validation testing. 10% FBS cell culture media was made in 50mL batches, all other FBS and PRP cell culture media were made in 10mL batches.

1. Gather all essential materials and bring to a sterile fume hood.

DMEM
Penn Strep
L-Glutamine/Glutamax
FBS or processed PRP

2. Mix contents at the denoted concentrations
    a. 1% Penn/Strep
    b. 1% L-Glutamine/Glutamax
    c. X% FBS or processed PRP
    d. Fill to desired batch amount with DMEM

Preliminary Testing: Proof of Concept testing
The purpose of this test was to determine the validity of the protocol. If successful, this protocol would be adapted to run with PRP sample.

Procedure:

1. Formulate 10% FBS cell culture media
2. Make a mastermix of known cell concentration (200 cells/uL) using NIH 3T3 mouse fibroblastic cells .
3. Dispense 500mL of the mastermix solution into 24-well plate and add 1 mL of 10% FBS cell culture media bring total volume in the well to 1.5mL
4. Incubate the plate for 24h in an incubator at 37ºC and 5% CO2.
5. Remove 24-well plate from incubation, check for health of the cells, and image wells.
6. Aspirate media in the wells and add 1mL of each concentration of FBS media in triplicates.
7. Incubate the plate for 24h at 37ºC and 5% CO2.
8. Image cells on days 1, 2, and 4 after FBS exposure.
9. Data is analyzed qualitatively

PRP Extraction procedure:
This procedure is run to obtain the growth factors stored inside the platelets after the PRP extraction process has successfully been completed.

1. Withdraw 30mL of whole blood using a butterfly needle with two 15mL syringe attached provided in the Arthrex Angel PRP kit.
2. Spin whole blood in Hettich Zentrifugen Rotofix 32A centrifuge at 15g for 5 minutes.
3. Collect supernatant and store in a 15mL conical tube in 4ºC refrigerator.
4. Transfer sample into 1.5mL cryovials and place in a -80ºC freezer for 24h.

5. Remove sample and thaw in a water bath at 37ºC for 1h.
6. Refreeze sample in -80ºC fridge for 24h.
7. Thaw sample again for 1h then pipette into 1.5mL microcentrifuge tubes.
8. Spin sample tubes at 2000g for 10mins.
9. Draw sample into a 3mL Leur-lock syringe and attach a 0.22um syringe filter.
10. Extract the PRP sample through the filter and dispense sample in 1.5mL microcentrifuge tubes for storage in 4ºC refridgeratior.

Validation Testing: PRP Bioactivity testing

The purpose of this test was to determine the effects of PRP on the proliferation of CRL 2097 human fibroblastic cells. The main goal was to determine the optimal concentration of PRP that would excite the most proliferation and determine whether it has the same effect as the positive control, 10% FBS cell culture media.

Procedure

1. Gather materials for the test and set up in a sterile fume hood:
    a. 0%,10% FBS media, 0.2%,0.5%,1%,3%,5%,7% PRP media
    b. CRL 2097 human fibroblastic cells
    c. 2 – 24-well plates
2. Mark one 24-well plate as a control plate and one as the PRP plate
3. Pipettte 500mL of CRL 2097 cell mastermix at known concentration (2000 cells/uL) in two rows of triplicates onto the control plate.
4. Complete the same process in step three to the PRP plate expect now with triplicates for every PRP concentration.
5. Add 1mL of 10% FBS media into all wells with cells in them and incubate for 24h at 37ºC and 5% CO2.
6. Check for health of cells and image each well three times.
7. Aspritate media in wells and add 1mL of respective media to each well.
8. Incubate 24-well plates for 24h at 37ºC and 5% CO2.
9. Image each well three times on days 1, 2, and 4 after media exposure.
10. Use ImageJ software to count cells in cell images.

Appendix G: Drug Elution Testing Protocol

BioSurfaces Fluorescent Tagging Protocol:

1. Turn on Beckman spectrophotometer using the power switch located in the back right portion of the unit. Put on the monitor using the button located on the bottom right portion of the screen. After the machine goes through its diagnostic check, click "quit" on the screen to exit to the main screen. To turn on the UV and VIS light, use the mouse to click on "UV light" and "VIS light" located in the lower left task bar on the screen. Font color will change once light source is on. Note – Allow the lights to warm up for at least 10 minutes prior to use.
2. Remove the BSA from the refrigerator and allow to come to room temperature (approximately 10 minutes). Weigh out 10 mg (0.0100g reading on the scale) of BSA and place into a borosilicate test tube. Dissolve BSA by adding 1 mL of PBS into the test tube and mix gently but thoroughly. For the final reaction volume for DyLight and BSA; you want to be less than 1mL)
3. Remove 500µl from the BSA solution and place in another test tube. Cap both test tubes with polyethylene Flange caps, keep the starting BSA solution (evaluated for protein concentration via Lowry Protein assay)
4. Based on the calculation above, combine 15.1µl DyLight488 into the 500µl BSA solution. Mix gently and then cap the solution with a 12X75mm stopper plug. Enclose the tube with tin foil to reduce light exposure. Let the **solution sit for 1 hour at room temperature**, gently mixing the solution in the tube every 15 minutes.
5. As the DyLight and protein are reacting in step 4, set up a ring stand and clamp on benchtop. Remove PD-10 column from box along with column plug. Using a razor blade, cut the tip off from the bottom of the column (approximately 3mm). Secure column to ring stand using the clamp. Place the plastic collecting cup underneath the PD-10 column and remove the cover, which will let the storage elute out.
6. Equilibrate (rinse) the column by filling the upper chamber of the PD-10 column (area above the filter) with approximately 3mL of PBS using a transfer pipette. When the PBS is entirely filtered out (i.e. there is no more liquid between the top of the column and filter), repeat 2 more times. Right before the solution gets to the filter level on the last rinse, place the bottom cap onto the PD-10 column followed by the top cap.
7. Retrieve 7 borosilicate test tubes, label them "1" through "7" and place them in a row in a test tube rack.
8. Right before the 1 hour reaction is complete (approximately 2 minutes), remove the caps from the PD-10 column and allow the remaining solution to drain into the plastic collection cup.
9. Using a pipette, remove the DyLight-BSA solution form the tube and add it into the PD-10 column. Allow the solution to drain into the cup. After the last drop, place the 1st test tube labeled "1" underneath the PD-10 column tip.
10. Fill the area above the filter in the PD-10 column with PBS using a transfer pipette. Collect approximately 15 drops (1mL) into the first tube prior to moving the test tube rack to align with tube marked "2." Add PBS as needed in order to collect 1mL in all 7 tubes. Note - If the dripping is slow, adding more PBS into the top of the chamber will fasten the pace. When protein-Dylight is eluting out from the column, drip speed will also

decrease. After collecting 1mL in all 7 tubes, place the lower and the upper caps onto the PD-10 column and discard the column.

11. Select the "**Fixed Wavelength"** setting on the main screen. In the upper right corner, under method name, click on whatever file is on the screen. In folder, select "**DY-488**" file and exit.
12. Using a pipette, transfer 1mL of PBS into a cuvette. Open the lid located on the top right of the spectrophotometer. Place cuvette with V side facing left into the spectrophotometer (furthest slot from the user). Press "blank" located on the lower portion of the screen using the mouse cursor. Once you have blanked the unit, the absorbance reading on the lower bar in the screen should be close to 0.0000.
13. When the number of the sample appears, left click on it to change the name to "blank." Right click on the mouse to obtain an absorbance reading for the "blank" sample. This value should be close to 0.0000 (± 0.0002).
14. Open the door once the value read appears on the screen and remove the cuvette from the spectrometer.
15. Pipette 1mL from the tube labeled "1" into a new cuvette and repeat the procedure, left clicking on the next indicator on the screen to label the sample (e.g. BSA-DyL 1). Continue this process until the last test tube ("7") has been read.
16. Look at the absorbances of the samples. The samples that have the highest absorbance at 275nm in the earliest peak fractions (typically in samples 2-5) are mixed together. The second peak fractions are unbound DyLight and should not be pooled with the first group.
17. Remove the cap from the top of a 10k centrifugal filter unit and pipette the combined solution into the upper reservoir. Place the cap back onto the unit once done.
18. Turn on the power to the Hermle centrifuge (bottom right green button). Open the lid by pressing the clear button next to the power followed by pushing the lever located on the front top right portion of the unit. If the door is not closed right, the unit will make a loud sound. Gently put outward pressure between the lid and the unit and repeat the opening process.
19. Remove the internal centrifuge tube cartridge from each chamber holder from the centrifuge and place the 10k centrifugal filter unit inside the cartridge. Weigh the cartridge with 10K unit using the scale and note the weight. To the contralateral centrifuge cartridge, add a 15mL Falcon tube, open the cap and place the unit including the cap onto the scale. Add distilled water into the Falcon tube using a squirt bottle until the weight of this tube is equivalent to the weight of the cartridge containing the 10k unit.
20. Place both cartridges back into the centrifuge, making sure they sit opposite of each other. For the 10k unit, make sure the "v" shape of the 10k unit is facing the center of the centrifuge to allow faster concentration (see image). Close the lid.

BioSurfaces Lowry Assay:

1. Set up Standard curve to a total of 200 ul per tube (in duplicate, see assay sheet):

    a.) Thaw one vial of (1 mg/ml) Protein Stock (BSA). Mix 100 ul of (1 mg/ml) Stock + 900 ul dH_2O to generate a **100 ug/ml Working Protein Standard.**
        a. Add appropriate volume of dH_2O to each assay tube.
        b. Add Standard to each tube: 10ul (=1ug), 20ul (=2ug), 50 ul (=5ug), 100 ul (=10 ug) and 200 ul (=20 ug). Use dH_2O for "0 ug".

2. Set up Samples ("Unknowns") in duplicate (if you have enough sample): Add up to 200 ul sample per tube. For samples with anticipated high protein levels, use a smaller sample volume and bring total volume to 200 ul with dH_2O. Record amounts of each used on assay sheet.

3. Prepare Lowry reagent after Std. curve and Sample tubes have been set up. Make enough Lowry reagent to add 800 ul/assay tube:
    a. Per 25 ml in graduated cylinder: 25 ml of Sol'n A + 0.25 ml Sol'n B_1 + 0.25 ml Sol'n B_2
    b. Parafilm and invert to mix.

4. Add 800 ul Lowry reagent to each 200 ul Std. and sample tube. Vortex and let stand 10 min at room temp.

5. Add 100 ul Folin reagent (1N) to each tube. Vortex and let stand 30 min. at room temp.

6. Set up the **Spectrophotometer (Beckman DU 640)** ***at least 15 minutes*** prior to use for VIS light warmup:
    a. Turn on Spec (on/off in back), monitor (bottom), and printer (side).
    b. After initial diagnostics finished, hit "**Quit**".
    c. Click on "**VIS**" (at bottom of screen) to turn on visible light.
    d. Select "**Protein**" in Applications box at top of screen.
    e. Click "**Method**" and select "**Lowry**" as assay type.

The following should appear on the screen:
Method in use: A:\Lowry
Assay type: LowryHS
Analytical wl: 750.0 nm
Note: This is an example of user note *(You can enter info here)*
Curve fit parameters: Linear, non-zero intercept
Number of standards: 6
Number of standard replicates: 2
Standards' concentrations: VIEW (if you click on **VIEW**, the following should appear):
Std Conc
1 0.0000
2 1.0000
3 2.0000
4 5.0000
5 10.0000
6 20.0000
Units: ug/ml
Component name: *(You can enter info here)*
Number of sample replicates: (*Enter # here, Program will average values of assay replicates for you*)
Flag standards and samples over: 1.000% CV
Dilution correction: **[No]**

Read average time: **0.50 sec**
Sampling device: **None**

7. **Blank the Spec** with 1 ml dH_2O in clean cuvette.
    a. ****For this and all readings**, place cuvette in back position in Spec's cuvette holder with "VEE" shape on cuvette facing to the right.
    b. Click **"Blank"** (at lower left) to read this as zero.

8. **Read Standard curve** tubes in duplicate from lowest to highest [conc] according to program. In this order you can use the same transfer/bulb pipette and cuvette to do measurement of all Stds.

    a. Transfer the standard from its assay tube to the cuvette using a bulb pipette and place in Spec.
    b. Click **"Read"** for that Std.; the mean of replicates is automatically calculated. Repeat for all Stds.
    c. After reading all Stds, click "**Display Std Curve**" at top of screen. "**Print"** Std curve, then "**EXIT**".
    d. Returns to Std. curve data page. "**Print"** data page.

9. **Read Unknown samples:**
    a. Click "**Samples**" at top left of screen.
    b. Use a separate bulb pipette and cuvette for each sample. As above, place cuvette in Spec.
    c. Click on **(sample number)**--> type in identifiers, i.e., "Sample A" (You *cannot go back to do this later*). Hit **"OK".**
    d. Click "**Read Sample**" or right click to read the sample.
    e. Repeat for each sample in order.
    f. "**Print"** results when finished.
    g. Hit **"Quit".**
    h. It will ask if you want to save Changes to Method, Save Standards file, and Save Results before clearing. **Answer "No" by clicking any filled-in boxes**- this will de-highlight them. Then click **"OK".**

10. To Shut Down: Turn off lamp by clicking **[VIS ON]--> [VIS OFF]**. Turn off Spec, monitor and printer.

**Note: Results read as "ug/ml" because the assay tubes (before Folin reagent) have 1 ml total volume. Consider the result (in ug) to be *the total amount of protein in the volume of sample you added* when setting up the assay tube. For example, if you used 100 ul of your Unknown sample to set up the assay and the assay tube read as 10 ug/ml, it means there was 10 ug of protein in that original 100 ul. So the actual protein concentration of your Unknown solution would be 100 ug/ml.